

AL/CF-SR-1994-0032



**DEVELOPMENT OF AN OPERATIONAL ALTITUDE
DECOMPRESSION SICKNESS COMPUTER MODEL:
FEASIBILITY STUDY RESULTS**

**Zahid M. Sulaiman, First Lieutenant, USAF, BSC
Terrel E. Scoggins, Captain, USAF, BSC
Andrew A. Pilmanis**

**Crew Technology Division
Brooks Air Force Base, Texas 78235-5104**

**Payson E. Ripley
Amy Melkonian**

**Krug Life Sciences, Inc.
San Antonio, Texas**

Yun Wang

**Rothe Development, Inc.
4614 Sinclair Road
San Antonio, Texas 78222**



**Crew Systems Directorate
Crew Technology Division
2504 Gillingham Drive, Suite 1
Brooks Air Force Base, Texas 78235-5104**

August 1995

Interim Technical Report for Period August 1989 - May 1994

Approved for public release; distribution is unlimited.

DTIC QUALITY INSPECTED 5

**AIR FORCE MATERIEL COMMAND
BROOKS AIR FORCE BASE, TEXAS**

**A
R
M
S
T
R
O
N
G**

**L
A
B
O
R
A
T
O
R
Y**

19950911 059

NOTICES

When Government drawings, specifications, or other data are used for any purpose other than in connection with a definitely Government-related procurement, the United States Government incurs no responsibility or any obligation whatsoever. The fact that the Government may have formulated or in any way supplied the said drawings, specifications, or other data, is not to be regarded by implication, or otherwise in any manner construed, as licensing the holder or any other person or corporation; or as conveying any rights or permission to manufacture, use, or sell any patented invention that may in any way be related thereto.

The Office of Public Affairs has reviewed this report, and it is releasable to the National Technical Information Service, where it will be available to the general public, including foreign nationals.

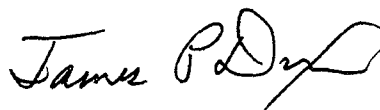
This report has been reviewed and is approved for publication.

Government agencies and their contractors registered with Defense Technical Information Center (DTIC) should direct requests for copies to: DTIC, Building #5, Cameron Station, 5010 Duke Street, Alexandria, VA 22304-6145.

Non-Government agencies may purchase copies of this report from: National Technical Information Services (NTIS), 5285 Port Royal Road, Springfield, VA 22161-2103.



ZAHD M. SULAIMAN, 1Lt, USAF BSC
Project Scientist



JAMES P. DIXON, Colonel, USAF, BSC
Chief, Crew Technology Division

REPORT DOCUMENTATION PAGE			Form Approved OMB No. 0704-0188	
Public reporting burden for this collection of information is estimated to average 1 hour per response, including the time for reviewing instructions, searching existing data sources, gathering and maintaining the data needed, and completing and reviewing the collection of information. Send comments regarding this burden estimate or any other aspect of this collection of information, including suggestions for reducing this burden, to Washington Headquarters Services, Directorate for Information Operations and Reports, 1215 Jefferson Davis Highway, Suite 1204, Arlington, VA 22202-4302, and to the Office of Management and Budget, Paperwork Reduction Project (0704-0188), Washington, DC 20503.				
1. AGENCY USE ONLY (Leave blank)	2. REPORT DATE August 1995	3. REPORT TYPE AND DATES COVERED Interim - August 1989 - May 1994		
4. TITLE AND SUBTITLE Development of an Operational Altitude Decompression Sickness Computer Model: Feasibility Study Results		5. FUNDING NUMBERS PE - 62202F PR - 7930 TA - 18 WU - 01		
6. AUTHOR(S) Sulaiman, Z.M. (Mil) Scoggins T.E. (Mil) Pilmanis, A.A. (Civ) Ripley P.E. (Contr) Melkonian A. (Contr) Wang Y. (Contr)				
7. PERFORMING ORGANIZATION NAME(S) AND ADDRESS(ES) KRUG Life Sciences, Inc. 11923 Radium San Antonio, Tx 78216		8. PERFORMING ORGANIZATION REPORT NUMBER		
9. SPONSORING/MONITORING AGENCY NAME(S) AND ADDRESS(ES) Armstrong Laboratory (AFMC) Crews Systems Directorate Crew Technology Division 2504 Gillingham Drive Ste 1 Brooks Air Force Base, TX 78235-5104		10. SPONSORING/MONITORING AGENCY REPORT NUMBER AL/CF-SR-1994-0032		
11. SUPPLEMENTARY NOTES Armstrong Laboratory Technical Monitor: F.W. Baumgardner, (210)536-3361				
12a. DISTRIBUTION/AVAILABILITY STATEMENT Approved for public release; distribution is unlimited.		12b. DISTRIBUTION CODE		
13. ABSTRACT (Maximum 200 words) In response to the need for a standardized methodology for altitude decompression sickness risk assessment across the wide range of exposures encountered in USAF flight operations, the Armstrong Laboratory's Crew Technology Division initiated a research program in this area in late 1989. The focus of work has been on determining whether development of an operational altitude decompression computer for both predictive and real-time DCS risk assessment is feasible, given the current level of understanding about altitude decompression sickness, the amount of available experimental data, and the inherent variability in individual susceptibility to altitude DCS. The results of this feasibility study indicate that although some technical risk is involved, development of the proposed altitude decompression computer is feasible. This was demonstrated through the implementation of a simplified, preliminary model for altitude DCS risk assessment. This technical report documents the work accomplished during this research effort and provides a road map for development of the desired operational altitude decompression computer.				
14. SUBJECT TERMS Altitude Decompression Sickness Computers Bubble growth Altitude Decompression Sickness DCS rick Assessment Model		15. NUMBER OF PAGES 90		
		16. PRICE CODE		
17. SECURITY CLASSIFICATION OF REPORT UNCLASSIFIED	18. SECURITY CLASSIFICATION OF THIS PAGE UNCLASSIFIED	19. SECURITY CLASSIFICATION OF ABSTRACT UNCLASSIFIED	20. LIMITATION OF ABSTRACT UL	

TABLE OF CONTENTS

1. INTRODUCTION	1
2. OBJECTIVES OF THIS STUDY	2
3. APPROACH	3
4. BACKGROUND	3
4.A. Basics of Decompression Sickness.....	4
4.B. Problems Inherent in Modeling Decompression Sickness	5
4.C. Important Differences between Hyperbaric and Hypobaric DCS	6
5. REVIEW OF THE LITERATURE ON DCS MODELING.....	10
5.A. Hyperbaric Decompression Models.....	11
5.B. Hypobaric Decompression Model	18
6. ALTITUDE DECOMPRESSION COMPUTER CONCEPT DEFINITION	26
6.A. Requirements for an Operational Altitude Decompression Computer.....	26
7. ALTITUDE DCS MODEL DEVELOPMENT GUIDELINES	27
8. STRUCTURE OF THE CONCEPTUAL ALTITUDE DCS MODEL	28
9. PRELIMINARY DCS MODEL DEVELOPMENT EFFORTS	30
9.A. Overview of DCS Model Development	31
9.B. Theoretical Development of the Underlying Mathematical Models	34
B.1. Perfusion.....	34
B.2. Bubble Diffusion.....	36
B.3. Gas Exchange between Tissue and Bubbles.....	40
B.4. Correlation with database	41
9.C. Development, Evaluation and Documentation of the Preliminary Mathematical Altitude DCS Model and Its Corresponding Computer Implementation	41
C.1. Mathematical Model Structure.....	42
C.2. Parameter Identification Techniques	43
9.D. Computer Implementation of the Model.....	44
D.1. Program.....	45
D.2. Integration with Database	47
10. RESEARCH NEEDS	47
10.A. Verification of the Basic Physical and Physiological Concepts	47
A.1. Bubble Growth	48
A.2. Factors Affecting Bubble Formation	48
A.3. DCS Latency Period	49
10.B. Elucidation and Quantification through in Vivo Human Studies	50
B.1. Exercise at Altitude	50
B.2. DCS and intravascular gas emboli above 30,000 ft and the impact of PPB on N ₂ elimination at these high altitudes	51
11. AREAS REQUIRING FURTHER RESEARCH	52
11.A. Research Requirements in Support of the Model Development.....	52
A.1. Process governing bubble formation and growth.....	52
A.2. DCS above 30,000 feet and the effect of PPB on denitrogenation	52
A.3. Exercise at altitude as a predisposing factor.....	53
A.4. The effects of repetitive altitude exposures on DCS risk.....	53
12. ROAD MAP FOR ALTITUDE DECOMPRESSION COMPUTER DEVELOPMENT.....	54
12.A. Verification with DCS Databases	54
12.B. Experimental Trials.....	55
12.C. Goals and Approach.....	55
C.1. First-year goals	56
12.D. Outyear goals.....	58
D.1. Continuation of year 1 objectives.....	58
D.2. Incorporate predisposing factors and individual variability (biases)	58
D.3. Develop "read-out" configuration.....	58
D.4. Human subject validation trials	60
D.5. Final software package for transition development of operational device.....	60
13. CONCLUSIONS.....	60
14. REFERENCES	61
15. APPENDIX A: Derivation of Bubble Growth Equation.....	73

List of Figures

Figure 1.	Relative nitrogen content in bubble vs ambient pressure.....	7
Figure 2.	Showing gas tension-vs-volume.....	8
Figure 3.	Unsaturation vs Pressure and Oxygen Concentration.	9
Figure 4.	Uptake of nitrogen in tissues as predicted by the Haldane model.	12
Figure 5.	Nitrogen Uptake and Elimination in Tissue.	13
Figure 6.	Illustration of Inert gas partial pressures in various tissue compartments as a function of time during a staged decompression. Arrows indicate which tissue is the rate-limiting factor for different phases of the decompression.	14
Figure 7.	Diffusion of inert gas into tissue slab.	16
Figure 8.	Diffusion of inert gas out of tissue slab.	16
Figure 9.	Change in Bubble Radius vs Volume.	21
Figure 10.	Conceptual Altitude DCS Risk Assessment Model.....	29
Figure 11.	Gross component of working model.....	30
Figure 12.	Armstrong Laboratory Altitude DCS Model.	33
Figure 13.	Perfusion.....	35
Figure 14.	Bubble Diffusion.....	37
Figure 15.	Implementation.....	45
Figure 16.	Program Flow Diagram.....	46
Figure 17.	Altitude DCS Model Development Milestones.	57
Figure 18.	Flight Profile of DCS Risk.....	59

List of Tables

Table 1.	Pressure differential of O ₂ diffusion into the tissue.	9
Table 2.	Models reviewed for applicability to development of an altitude decompression computer.	11

Accession For		
NTIS	CRA&I	<input checked="" type="checkbox"/>
DTIC	TAB	<input type="checkbox"/>
Unannounced		<input type="checkbox"/>
Justification		
By		
Distribution /		
Availability Codes		
Dist	Avail and / or Special	
A-1		

1. INTRODUCTION

Formal reports of decompression sickness (DCS) from the field are indeed rare. However, recent research conducted by the Armstrong Laboratory has shown that: 1) the incidence of DCS in high-altitude missions is actually quite high, but reports are suppressed for fear of being grounded (122); and 2) accurate evaluation of DCS incidence is significantly hindered by inconsistent classification of symptoms (90). When coupled with the extensive data from altitude chamber studies showing high rates of DCS incidence for simulated operational flight profiles, these findings indicate that DCS is a problem that must be addressed. Future operations at higher altitudes will only increase the risk unless improved protective measures can be developed.

Fortunately, with proper procedures, the risk of altitude DCS can be effectively controlled. Prebreathing 100% oxygen for denitrogenation prior to the exposure, the primary DCS countermeasure—aside from pressurized cabins and/or pressure suits, is effective; but no scientifically validated methodology for determining the amount of prebreathing required exists. This problem is compounded by use of: 1) dilution breathing systems which typically provide less than 100% oxygen during routine flight; and 2) positive pressure breathing for altitude and acceleration protection. Future DCS countermeasures, such as cabin pressurization at higher differentials and use of partially inflated full-pressure suits, could further reduce risk. Effective countermeasures for preventing DCS are thus not the problem. Rather, the problem facing aircrews today is how to quantify the risk of DCS and then select an appropriate combination of available countermeasures compatible with the constraints of the given mission.

The need for a standardized approach for DCS risk management will become even more important for the Air Force in the future, especially as newer aircraft, such as the F-22 expand the operational envelope to higher and higher altitudes. The same problem will have to be addressed when designing and selecting protective equipment for future high-altitude surveillance and transatmospheric vehicles. Current high-altitude surveillance operations will also be impacted if future strategies require longer missions due to Continental United States (CONUS) basing. In addition, rapid sortie generation requirements may reduce the time available for prebreathing prior to take-off. Although inflight denitrogenation can provide an effective alternative in this situation (122), the technology for determining what pressure and time schedule to use to minimize DCS risks within the constraints of the mission is lacking.

Currently, DCS risk assessment in the USAF is not standardized. In response to an inquiry concerning the DCS risk for a new or unusual altitude exposure, one of three approaches is used. A literature search can be initiated to find data, in a "scattergram" of over 50 years of DCS research, that either match the desired flight profile or are close enough to allow reasonably confident interpolation or extrapolation of the old data to the new exposure conditions. This is time consuming and, most often, unsuccessful. If the question is of high priority, a new research study specific to the particular issue in question can be initiated. This is a lengthy and resource-intensive undertaking, but will most likely provide a valid answer. In most cases however, the inquiry is answered by giving a "best guess" estimate of risk based on the memory and experience of the available experts. The situation is even worse for the flying pilot who, upon sudden loss of cabin pressure, may be fatally short of the information necessary to make contingency decisions in real time. A more rational approach would be to take the wealth of information accumulated during the last 50 years of altitude DCS research and use it as the basis for the development of a hypobaric decompression model to serve as the operational "standard" for the altitude field.

In the hyperbaric field, this approach has resulted in the development of countless decompression tables, and, more recently, small diving computers carried by the diver that provide continuously updated limits to guide the decompression. Unfortunately, as demonstrated by Conkin and Van Liew (32), direct extrapolation of the algorithms used to compute decompression procedures for ascent from a dive cannot be reliably used to assess the hypobaric exposures encountered in flight.

Despite these limitations, numerous attempts to model altitude decompression sickness have been made (3,31,54,96,125,147). Much of the work in this area has been sponsored by the National Aeronautics and Space Administration (NASA) and Johnson Space Center (JSC) to support definition of decompression procedures for extravehicular activity (EVA) during Shuttle and Space Station operations. Although NASA has achieved some success with these models, their utility is limited to the narrow range of exposures associated with current EVA operations. Also, these models have focused on a single independent variable, namely, degree of nitrogen supersaturation in tissue, to assess the risk of DCS. Other variables known or suspected to affect DCS risk and susceptibility, e.g., exposure duration, bubble dynamics, exercise, age, gender, body composition, hydration state, etc., have not been incorporated into the NASA models.

In response to the need for a standardized methodology for altitude decompression sickness risk assessment across the wide range of exposures encountered in USAF flight operations, the Armstrong Laboratory's Crew Technology Division (formerly part of the USAF School of Aerospace Medicine) initiated a research program in this area in late 1989. An overview of this effort was presented by Dr. Andrew Pilmanis at the 1990 Hypobaric Decompression Sickness Workshop at Brooks AFB (121). The focus of work to date has been on determining whether development of an operational altitude decompression computer for both predictive and real-time DCS risk assessment is feasible, given the current level of understanding about altitude decompression sickness, the amount of available experimental data, and the inherent variability in individual susceptibility to altitude DCS.

The results of this feasibility study indicate that although some technical risk is involved, development of the proposed altitude decompression computer is feasible. This was demonstrated through the implementation of a simplified, preliminary model for altitude DCS risk assessment. This technical report documents the work accomplished during this research effort and provides a road map for development of the desired operational altitude decompression computer.

2. OBJECTIVES OF THIS STUDY

As stated above, the purpose of the Altitude Decompression Sickness Computer Development Feasibility Study was to determine whether there was reasonable probability of success for developing the desired model/computer. In today's climate of rapidly declining resources, this feasibility assessment was needed before initiation of a comprehensive research program in this area could be justified. The specific objectives to be accomplished during the study are listed below.

1. Define the requirements for an operational altitude decompression computer.
2. Review the research literature to determine what data and which, if any, previously proposed models could be used in development of the altitude decompression computer.
3. Develop a set of guidelines and a conceptual framework for development of the altitude decompression computer and its associated model of DCS risk prediction.
4. Identify promising concepts and algorithms and implement them in a prototype computer model.
5. Evaluate the prototype model by comparing model predictions with previously reported experimental data on DCS incidence.
6. Identify and prioritize areas/issues requiring further research.
7. Develop a comprehensive research program plan that will provide a realistic road map for successful development of an operational altitude decompression computer.

3. APPROACH

This research has been conducted as an in-house effort under the direction of the High Altitude Protection Function within the Systems Research Branch of the Armstrong Laboratory (AL/CFTS). Extensive scientific and technical support for this effort was provided by KRUG Life Sciences, Inc., under Contract # F33615-89-C-0603. Rothe Development, Inc., also provided scientific and technical support for certain portions of the project under Contract # F33615-89-D-0604. Continuation of this research has been somewhat difficult due to the limited availability of dedicated personnel. Over the three-year period from late 1989 to late 1993 four different people have had primary responsibility for the technical work. As a result of these personnel changes and other research priorities within the Crew Technology Division, the project has progressed rather slowly.

Due to the above constraints, this feasibility study was conducted using a broad, top-down approach. The initial work focused on developing the concept for the altitude DCS computer and defining the general requirements for the underlying mathematical model. During this early period an extensive review of the literature concerning DCS modeling was carried out. Based on the results of these efforts, several promising concepts were selected for further evaluation.

The next phase of the study centered on implementation and evaluation of the leading concepts into a "working" DCS model. The primary goal was to get a prototype model that would demonstrate the concept of an operational altitude DCS computer. This goal often conflicted with the desire to develop a more detailed (and presumably more accurate) model. The trade-offs between these two goals were resolved in favor of completeness rather than absolute accuracy. Detailed investigation of several important aspects of the DCS model was postponed until additional resources become available.

Likewise, as of the writing of this report, a thorough analysis of the validity and limitations of the preliminary model developed during this study has not yet been accomplished. The results reported here represent a snap shot of the current status of the model development effort. These results should therefore be evaluated in the context of a "proof-of-concept" demonstration rather than interpreted as "real" model predictions for operational use.

This top-down approach has facilitated the identification of numerous areas where further research is needed. This information has been used to put together a suggested road map for the actual development and validation of an operational decompression computer. The definition of the proposed research program represents the culmination of the Feasibility Study. Further development of the DCS model/computer is dependent upon availability of adequate resources.

4. BACKGROUND

The effects of exposure to changes in environmental pressure and methods to counter these effects have been studied extensively. A complete bibliography of the literature on decompression sickness alone would fill a book. The literature database covering this subject maintained by the High Altitude Protection Function at the Armstrong Laboratory, although far from completely covering the topic, contains over 1000 articles focused primarily on altitude decompression sickness (172). The literature on hyperbaric DCS is even more prolific. Despite this wealth of research, the underlying physiological and pathological mechanisms that give rise to the multitude of symptoms that can result from decompression are not yet well understood. Nonetheless, to determine the feasibility of developing an altitude decompression sickness risk assessment model that meets the above objectives, one must first begin by developing a thorough understanding of the literature on this subject.

Due to the volume of material involved, a review of the physiology of DCS is outside the scope of this report. A comprehensive and well-written treatment of the subject has been presented by Vann in the latest edition of Bennett's Diving Medicine. Both the physiology and operational aspects of altitude

decompression sickness were also thoroughly reviewed at the Hypobaric DCS Workshop held at Brooks AFB, TX in October 1990 (121). The proceedings of this workshop, which was jointly sponsored by the USAF School of Aerospace Medicine, NASA/Johnson Space Center, and the Air Force Office of Scientific Research, are an invaluable reference on the topic.

For the reader who may be unfamiliar with decompression sickness, a short summary of the key concepts relevant to the etiology of DCS is included below. Following that, the remaining material in this section identifies several problems that must be considered in trying to model DCS. Several issues important for assessing altitude DCS but often ignored in analyzing hyperbaric exposures are also discussed. Having thus laid the proper groundwork, the significant developments of earlier work in decompression sickness modeling will be reviewed.

4.A. Basics of Decompression Sickness

Decompression sickness, often referred to as the bends, is a disease thought to be caused by evolved gas phenomena that occur when living tissue is exposed to a reduction in environmental pressure. Such decompressions are encountered during ascent from a dive, flying at altitude, or through intentionally induced pressure changes in either hyperbaric or hypobaric chambers. As a result of the pressure change, the natural balances between concentrations of the dissolved gases in tissues and blood and between the blood and gas concentrations in the inspired air present at the alveoli are disturbed. In response to the specific concentration gradients for each component of the gas, the concentration in the supersaturated tissue is reduced by diffusion of gas from tissue to blood. The gas-rich blood is then carried away from the tissue to the lungs where the gas is exchanged with the inspired air. When the magnitude of the pressure change is large enough and rapid enough, the processes involved in tissue gas exchange can't keep up and the tissue becomes supersaturated.

The various clinical symptoms of DCS are thought to be due to pathology associated with the separation of excess amounts of inert gases (primarily nitrogen) into a gas phase whenever the tissue becomes sufficiently supersaturated. The gas that comes out of solution is thought to collect in "bubbles" in the tissue that may interact with free nerve endings, cause biochemical changes at the cellular level, block the microcirculation and cause localized ischemia, etc. In addition to joint pain, DCS symptoms may include: paraesthesia, skin symptoms such as mottling, CNS effects such as visual deficits, pulmonary distress or "chokes," etc. Both the size and location of the gas phase are thought to be important determinants in the resulting clinical symptoms.

Since the body's homeostatic mechanisms normally keep the tensions of the metabolic gases dissolved in the blood and tissue stable over time, the metabolic gases are usually ignored when considering the effects of decompression on tissue gas exchange. The remaining gas tensions are assumed to be due to the inert gases present in the tissue. Since nitrogen is by far the most predominant gas in air, the effects of trace amounts of other inert gases on the gas exchange processes are also usually ignored.

Three important issues concerning the above processes are worth mentioning here. The first is that the formation of a gas phase and subsequent onset of symptoms takes some finite amount of time. The magnitude of the delay or latency in symptom onset depends on the magnitude of the pressure change. The second important issue is that the severity of the symptoms may also be related to the size of the pressure differential. Larger, more provocative decompressions generally result in more severe symptoms that occur more rapidly. However, these trends must be interpreted in the context of the third issue—that is, a large degree of variability is involved in determining what, if any, DCS symptoms will be observed in a given individual for a given pressure change. This variability is compounded by numerous factors such as hydration state, temperature, recent exercise, etc., which may change an individual's susceptibility from one exposure to the next. These factors, when combined with the lack of

understanding of the intermediate processes through which the evolved gas actually affects the resulting symptoms, make attempts at modeling decompression sickness quite challenging.

4.B. Problems Inherent in Modeling Decompression Sickness

Before diving into the literature on DCS modeling it is helpful to understand some of the problems involved in modeling this disease. The most difficult problem is the diverse nature of the symptoms. Severe cases may exhibit serious cardiopulmonary and/or neurological deficits that, if not properly treated, may be fatal. Fortunately, with proper use of operational procedures designed to control DCS risks, severe cases of DCS occur infrequently in both hyper/hypobaric decompressions. The mild-to-moderate symptoms that do occur with greater frequency cover a wide spectrum of clinical conditions. The partial list given above is only representative.

This variability presents great difficulty in accurately modeling DCS for two reasons. First, from a pathological viewpoint, it is difficult, if not impossible, to postulate any single mechanism that will adequately explain all possible symptoms. Any model must therefore try to incorporate a variety of physical and physiological processes that may contribute to DCS. Numerous mechanisms have been suggested including physiological, pathological, and biochemical. Despite countless human and animal experiments, efforts to identify the underlying causes of DCS are severely limited by our inability to monitor the appropriate processes *in vivo*. *In vitro* studies have contributed a great deal of basic knowledge on gas exchange, gas phase separation and bubble growth. However, extrapolation of these data to living systems is difficult due to the highly complex nature of the processes involved. Despite these difficulties, considerable progress has been made in recent years through application of state-of-the-art ultrasound imaging and Doppler technology (117,118,125). Further efforts in this area show great promise for providing the much needed insight into this critical area of the problem.

The second reason that the large variation in DCS symptomatology makes modeling difficult is that no standardized classification scheme yet exists with which to describe DCS cases (49,90,136). This lack has resulted in numerous scales of severity that make comparison of experimental data from different researchers very difficult. The classification dilemma is not limited to the research setting. In a survey of USAF and other physicians involved in the treatment of DCS, Kemper et al (90) found very little consistency of diagnosis on ten different case histories. In addition to non-standard classification taxonomies, data on the incidence of DCS in the operational Air Force are further confounded by lack of reporting among aircrew—whose only current incentive is, at best, a hassle with the flight "doc," and at worst, the end of their flying career.

Another problem that must be dealt with in developing models of decompression sickness is the typically low-incidence rates that occur on the milder exposures. To obtain sufficient statistical power in the data analysis, a large number of subjects is required for each study. The cost of doing such large studies today is prohibitive. This requires that all available data be consolidated into a common framework that will give more statistical power than relying only on data obtained at any one research center.

Several large databases on altitude DCS do exist. Both the USAF and NASA have extensive computerized data on DCS and venous gas emboli obtained from many years of research. Within the last several years Conkin has successfully organized a large percentage of all the experimental altitude DCS data available in the common literature in a computerized database (28). Also, considerable data on altitude DCS was recorded during and immediately after World War II (51,52). Most of these early studies were part of various aircrew screening programs, so large numbers of individuals were used. Unfortunately, much of the detailed data from the individual flight records have not been properly organized and are in serious danger of being lost forever. Although the different endpoints for terminating the exposure and symptom classification systems used in these early studies varied significantly, it should be possible to correlate these variables by carefully reviewing and comparing the detailed records based

on symptomatology rather than classification of DCS. This would provide a critical volume of data that, due to stricter limitations on human experimentation, could never be repeated today.

Yet another problem encountered in modeling DCS is the nature of the model's output. Traditionally, decompression models developed for hyperbaric exposures have expressed the output as a binary prediction of whether DCS was likely to occur or not. This simple, yes/no answer was computed based on whether or not a given parameter, such as tissue supersaturation or perhaps bubble size, exceeded a specified limit or threshold. The limiting values of the various parameters were determined on a priority based on the level of risk deemed acceptable for the planned mission. These models were then used to compute sets of tables that were used to guide the decompression. These models do not have the capability to adjust the DCS outcome prediction for different levels of acceptable risk. In certain scenarios, such as flying over areas with enemy anti-aircraft weapons, a large risk of DCS may be acceptable, given the available alternatives. For these situations a simple yes/no answer does not provide enough information for effective trade-off analyses. Therefore, it is important to know both what the relative risk is and how severe the resulting DCS might be. To date, few models have attempted to account for differences in the severity of possible DCS symptoms. The simple binary output models of the past have also failed to incorporate another important feature: the delayed onset or latency period associated with most cases of DCS.

Having a model that could reliably predict DCS latency would provide the advantage of safely permitting a more hazardous exposure to a larger pressure differential, as long as recompression occurred before the processes causing symptom development had progressed too far. In operational terms, this could be translated into higher aircraft altitudes and/or reduced operating pressures for full-pressure suits. The first would expand the envelope of operations and could provide a substantial combat advantage. The latter would reduce the mobility/dexterity limitations and fatigue associated with fully inflated pressure suits.

4.C. Important Differences between Hyperbaric and Hypobaric DCS

Many models have been created to delineate the boundaries of safe decompression procedures for hyperbaric exposures. While these models provide a basis from which to develop a model for flight, some important issues are not addressed and must be taken into consideration to develop an altitude decompression computer.

Perhaps the most important difference is in the type of information that is needed to properly assess DCS risk and to develop acceptable decompression procedures. If we were to consider an expedition, whether at depth or in flight, as composed of two stages, the initial stage would be the "action" phase. During this time the individual would complete the objectives of the mission. The second stage could be referred to as the "return" stage. This would involve transferring the individual from the altered environment back to sea level and common air. For a diver, decompression is not a factor until after the action phase. Therefore, given enough time and an adequate air supply, a diver can make his decompression as conservative as necessary without interfering with the work of the dive. Complete avoidance of even minimal DCS symptoms is the goal; therefore, prediction can be quantified as a binary output, with any stress above a certain level defined as bends-producing.

In flight, pressure reduction is coupled with the action phase. The aircrew may be willing to risk developing DCS to complete the mission. For this reason, a risk analysis would be desirable, since DCS may be difficult to avoid entirely. Often, the risk will be so high as to require a preparation stage, during which denitrogenation is accomplished.

In other types of missions, such as high-altitude parachute insertion, the mission has more than two phases. Unlike the diver who can decompress after the work is done, or the aircrew at risk while doing their job, special forces troops must endure the DCS risk just to get to the job. The problem is often

compounded by the remote nature of these types of operations: treatment for DCS, should it occur, is simply not available. In the case of flying after diving, the route to and from work is even more hazardous because of the increased inert gas loading that occurs during the dive portion of the mission.

Although the above differences in the nature of the missions don't necessarily change the underlying processes which give rise to DCS symptoms, they are important considerations when defining the types of risk assessment information required. It is clear that a simple yes/no prediction of DCS will not be adequate for flight or special operations. These situations require a prediction of relative risk which can be evaluated in the context of other risks and constraints associated with the particular mission in question.

We would also expect the composition of gases in a bubble at altitude to be different from that at depth (1). In both applications, the tensions of metabolic gases in a bubble are assumed to be the same as their tensions in the tissue. For O_2 , CO_2 , and H_2O , the tissue values will normally be constant at approximately 40, 46, and 47 mmHg, respectively, at all pressures. If, as explained above, nitrogen is assumed to make up the difference between the sum of the partial pressures of the metabolic gases plus water vapor and the total pressure in the bubble, then at sea level nitrogen would compose roughly 83% $\{ (760-40-46-47) / 760 \}$ of the gas volume in a bubble. At an arbitrary depth of 33 fsw, the pressure would be 1520 mmHg, and nitrogen would compose about 92% $\{ (1520-40-46-47) / 1520 \}$ of the bubble's gas volume. Similarly, at an arbitrary altitude of 30,000 feet, the pressure would be 226 mmHg, and nitrogen would compose 44% of the volume of the bubble. Figure 1 gives a plot of the relative nitrogen content in the bubble as a function of ambient pressure.

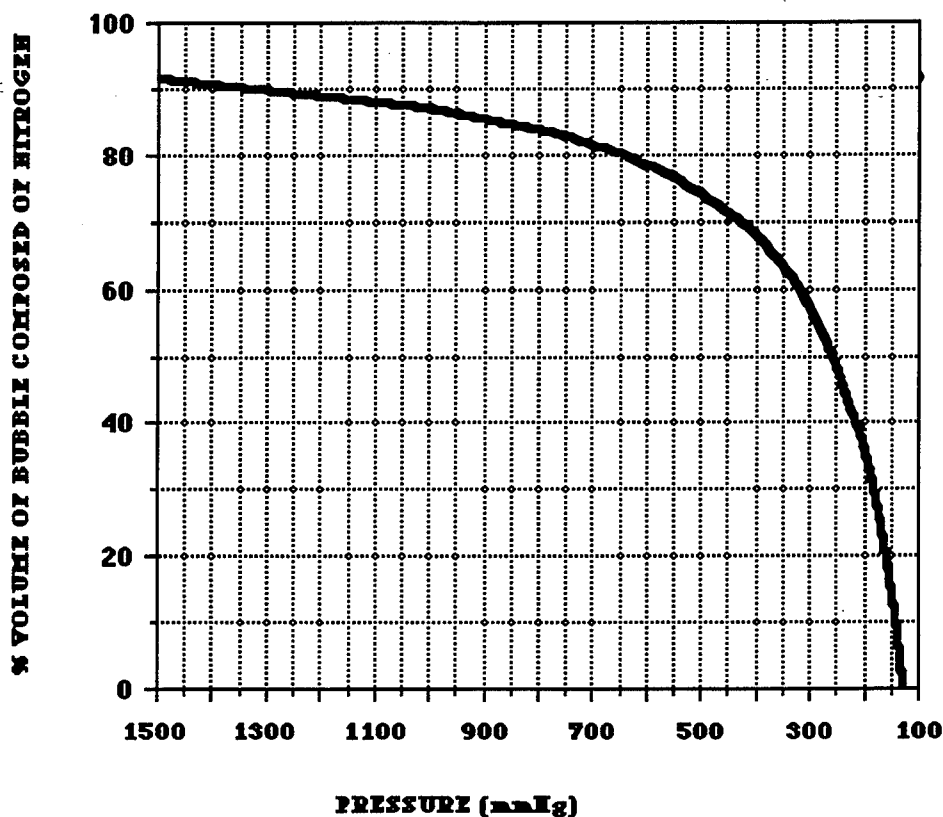


Figure 1. Relative nitrogen content in bubble vs ambient pressure.

The reader will immediately observe that this graph shows no nitrogen for altitudes above roughly 42,000 ft. At slightly more than 42,000, the ambient pressure would be 127 mmHg, which exactly equals the sum of the partial pressures of the metabolic gases and water vapor. Based on the above reasoning, there should be no nitrogen in the bubble whatsoever. Of course, this does not make sense intuitively, as it would imply that the tissues could withstand infinite supersaturation of nitrogen above 42,000 feet. However, it does raise some interesting questions about the composition of gases in the bubble at altitude and the effect that this would have on diffusion of gases into and out of the bubble.

A few points that make inert gas exchange in the tissues are a subject of special interest. Carbon dioxide is much more soluble in body fluids than oxygen. Thus an equal volume of carbon dioxide will exert less pressure in solution than oxygen (159). For example, from Figure 2 below, it is evident that three volumes of oxygen would have a partial pressure of 100 mmHg in solution, while the same quantity of carbon dioxide would exert only 4.9 mmHg.

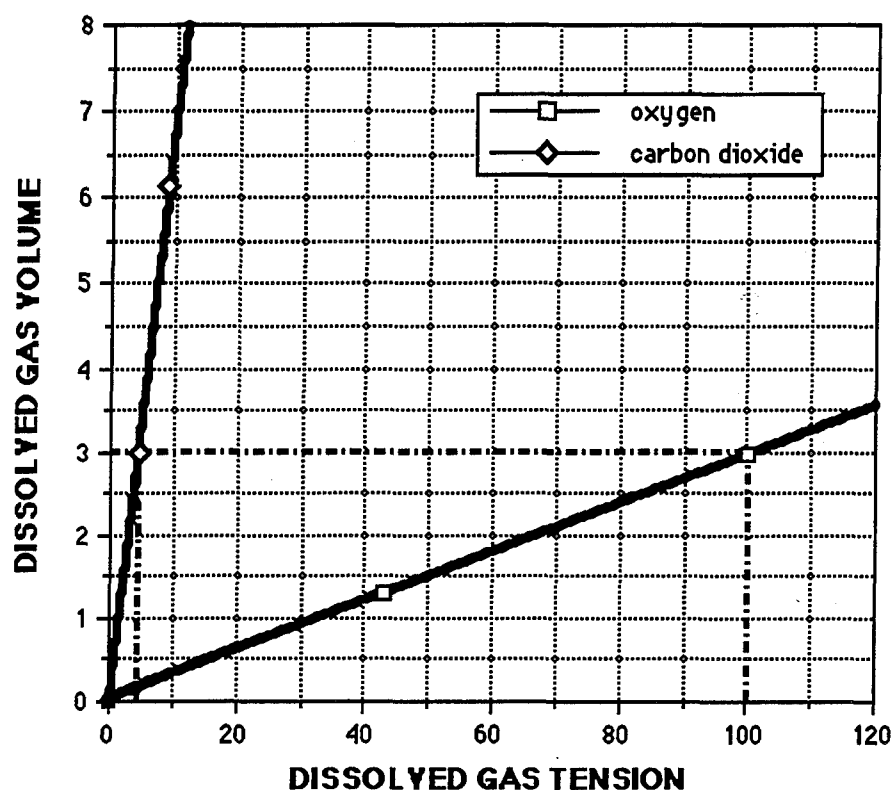


Figure 2. Showing gas tension-vs-volume, Bove (1990) (18).

Therefore, when oxygen is metabolized and replaced with the same molar volume of carbon dioxide, the sum of the partial pressures of gases dissolved in the tissues is inherently less than the sum of the partial pressures of the inspired gases. This phenomenon is referred to as the "oxygen window" or "inherent unsaturation" (15,77). This pressure gradient provides the driving force for diffusion of oxygen into the blood and tissues and diffusion of carbon dioxide from the blood to the tissues and from blood into the expired air.

Because high levels of dissolved oxygen are toxic, the body's regulatory processes try to prevent its accumulation in the tissues (96). Unless the partial pressure of oxygen in the inspired air is especially high, the partial pressure of oxygen in the tissues is then a relative constant at 46 mmHg (24,151,152). The oxygen window would therefore be expected to increase with increasing partial pressures of O_2 . This has been demonstrated experimentally by several researchers (77,101,148). The table below gives the

magnitude of the pressure differential favoring diffusion of oxygen into the tissues for various concentrations of nitrogen in the inspired air at different inhalation pressures.

Table 1. Pressure differential of O₂ diffusion into the tissue (77).

<u>Inhalation pressure</u>	<u>% Nitrogen</u>	<u>Magnitude of the Oxygen Window (mm Hg)</u>
480	80	18
760	0	628
760	18.3	507
760	42	322
760	62	209
760	80	79
1116	80	166
1349	80	236
1761	80	314

If it weren't for the toxicity of oxygen at higher pressures, DCS could be prevented in diving by eliminating inert gas from the breathing mix. With this in mind, the relationship between the driving force for inherent unsaturation and the ambient pressure for air and oxygen breathing could be described by the following graph (Figure 3).

UNSATURATION VS. PRESSURE AND OXYGEN CONCENTRATION

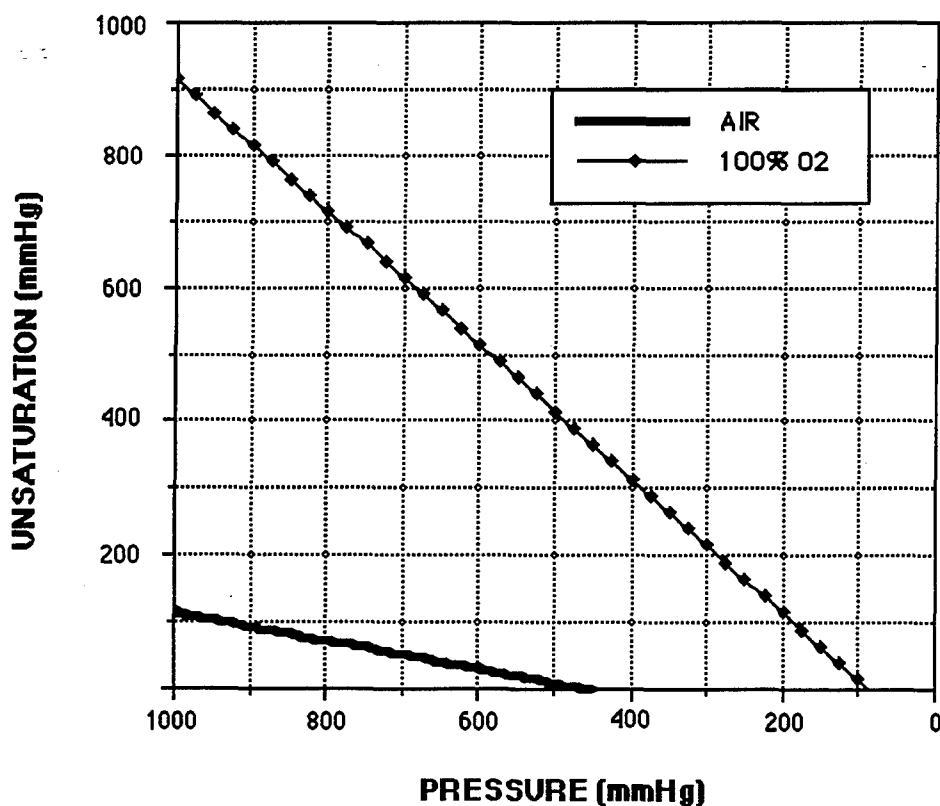


Figure 3. Unsaturation vs Pressure and Oxygen Concentration.

In contrast to diving, oxygen toxicity is not a threat at altitude. This allows breathing enriched air and 100% oxygen. Therefore, although the driving force favoring inherent unsaturation would be expected to decrease with increasing altitude, it could always be at its maximal level if 100% oxygen were used. In addition, on 100% oxygen, the risk of decompression sickness would be expected to decrease with time as nitrogen is eliminated from the body. With sufficient time, the oxygen window makes it possible for an aircrew to become completely denitrogenated, thereby eliminating the risk of DCS.

A final difference that significantly affects the calculation of decompression procedures for either diving or altitude concerns the time course of the inert gas loading and unloading. In diving, the individual starts with tissues saturated at ground level. During the dive the increased pressures cause more inert gas to be picked up by the tissue. In diving, therefore, the only tissues that need be considered in calculating safe decompression limits are those which could, in the length of time of the dive, attain a partial pressure of nitrogen sufficient to cause supersaturation upon ascent. In other words, tissues that take more time to saturate must be considered only in proportion to the length and depth of the dive. Based on this consideration, diving models for non-saturation diving have typically used inert gas exchange equations with tissue half-times of 5-180 minutes. The half-time represents the time required for the tissue partial pressure to reach half of the final equilibrium value for a given change in pressure.

For ascent to altitude, a person can be assumed to start with inert gas tissue pressures completely equilibrated with the atmosphere at ground level. While some tissues can be denitrogenated fairly quickly, those that respond most slowly to a change in the environment assume great importance at altitude. Previous altitude models have often set prebreathing requirements based on tissue half-times of 360 minutes or longer. Any model developed for use at altitude must take these factors into consideration.

5. REVIEW OF THE LITERATURE ON DCS MODELING

An extensive and impressive body of literature on DCS modeling is available. Driven primarily by the need for safe decompression procedures for underwater construction and escape from submarines, all of the early decompression models were developed for the hyperbaric field. Only in more recent times have serious attempts at mathematically modeling altitude decompression sickness been made (17,30,44,93,157,184).

Despite the considerations outlined above that limit the direct application of hyperbaric decompression sickness models to the hypobaric field, some of the concepts and algorithms implemented in these models may be useful. At any rate, they should serve as a starting point from which to develop or build up the additional factors necessary for an accurate altitude DCS model. Fortunately there are several good reviews of previous DCS modeling work. A good, concise summary of the significant advances in this area can be found in the Hamilton's paper in DCS Workshop Proceedings (121). Vann's chapter on the physiology of DCS in Diving Medicine (161) provides a comprehensive review of both the relevant physiology and modeling concepts. Hempleman (61) and Wienke (177) provide a more detailed review of the mathematical treatments.

The potential contributions from this wealth of literature were recognized at the very beginning of the altitude decompression computer research and development effort. Numerous existing diving models were reviewed. Although much fewer in number, previously proposed decompression models for altitude were also reviewed. This review included models of many types that focused on issues such as: diffusion and perfusion of inert gas, parallel and serial arrangement of multiple tissue compartments, bubble dynamics, and models for excursion from saturation diving. Also, an interesting model used to predict tissue gas concentrations for anesthesia administration during surgery was also reviewed for potential applicability. The significant models included in this review are listed in the following table.

Table 2. Models reviewed for applicability to development of an altitude decompression computer.

Diving models:	Haldane	US Navy
	Hills	US Navy E-L
	Huggins	DCIEM (Kidd-Stubbs)
	Hempleman	RNPL
	Wienke	Hamilton/Peterson
	Yount/Kunkle	Vann/Gernhardt
Altitude models:	NASA/JSC	Van Liew & Hlastala
	Gernhardt	Conkin
	Esa-Hennessy	Albanese et al.
	Fryer	
Other models:	Eger's anesthesia model	

Detailed discussion of all the models reviewed during this effort is not possible in this report. The following section provides a review of the significant material. This overview of previous work should provide the proper perspective for the subsequent sections describing the theoretical development of the algorithms that were implemented in the prototype altitude DCS computer. For a more detailed discussion of the literature, the reader should see the reviews mentioned above.

5.A. Hyperbaric Decompression Models

Perhaps the greatest impact in the field of decompression modeling was the early work of Boycott, Damant, and Haldane (19,60). In order to set down more stringent guidelines for the decompression of divers and caisson workers, Boycott et al devised what may be called the first tissue model. Their model focuses on inert gas exchange and uses the degree of supersaturation of the tissues as the predictor of DCS. In the interest of simplicity, they represented the body tissues as one lumped compartment, uniform both in composition and in blood supply. The inert gas exchange between tissue, blood and the environment was then described based primarily on the role of perfusion. The differences in nitrogen solubility of lean and fat tissue and blood were used to incorporate the known differences in rates of gas exchange. Many models were built from the foundation laid by Boycott, Damant, and Haldane, thus the theory merits some detail. The following material is paraphrased from "The Prevention of Compressed Air Illness" (19).

It had been observed that fatty tissue constitutes 15% of the mass of an average man and can dissolve approximately six times more nitrogen per unit volume than either blood or lean tissue. Given this, one may determine that there would be about 75% more nitrogen in a volume of saturated tissue than in the same volume of saturated blood { $[1(0.85) + 6(0.15)] / 1 = 1.75$ }. (Actually, Boycott, Damant and Haldane calculated a value of 1.7. The numbers used here are for explanation of the concept only; the end result is essentially the same). Taking into account the differences in solubility and the fact that the ratio of tissue to blood in the body is about 20:1 by volume, then at saturation there would be approximately $1.75 \times 20 = 35$ times more nitrogen dissolved in the body than in the blood.

If the partial pressure of nitrogen in the environment were to increase, there would be an initial deficit in the tissues with respect to the blood. This is because the blood is assumed to be instantly equilibrated with the environment due to both the mechanisms of gas transfer at the lung and the large surface area across which gas exchange occurs, while tissue gas concentrations may only be changed by the slower transfer of gases across the tissue and blood interface. This resulting concentration gradient

provides the driving mechanism for tissue uptake of inert gas. However, if nitrogen is considered to be the only inert gas, the relationships established earlier show that saturated blood could deliver only 1/35th of the total deficit with each pass through the tissues. For example, if one unit volume of nitrogen were needed to bring the tissues to saturation level, then with one round the blood would have added $(1/35) * 1 = 0.0286$ of a unit volume to the tissues. With the second pass, it would add $(1/35)*(1-0.0286) = 0.0278$. The effect continues such that on the third pass the amount of nitrogen delivered to the tissue is $(1/35)(1-(0.0286+0.0278)) = 0.0270$, and so on with each subsequent pass. The net effect is that a smaller amount of nitrogen is being added with each pass, with the actual amount transferred proportional to the ever-decreasing deficit. If the tissue had an initial volume of nitrogen, say V_o , then at the end of an interval of time, t_1 , it would have a new volume of nitrogen, $V_o * (1+0.0286)$ and at the end of the next time interval, it would have, $V_o * (1+0.0286+0.0278)$ and so on. This concept is often referred to as perfusion-limited inert gas exchange, since the time required for the blood to make each pass through the circulation is considered to be long compared to the time for gas to diffuse from the blood into the tissue.

This relationship is shown graphically in the following plot (Figure 4). Since the volume of dissolved gas per unit volume of solvent is a concentration, and since concentrations of gases are more familiarly described as partial pressures based on Henry's Law, the vertical axis of the chart is in partial pressure of nitrogen in the tissue.

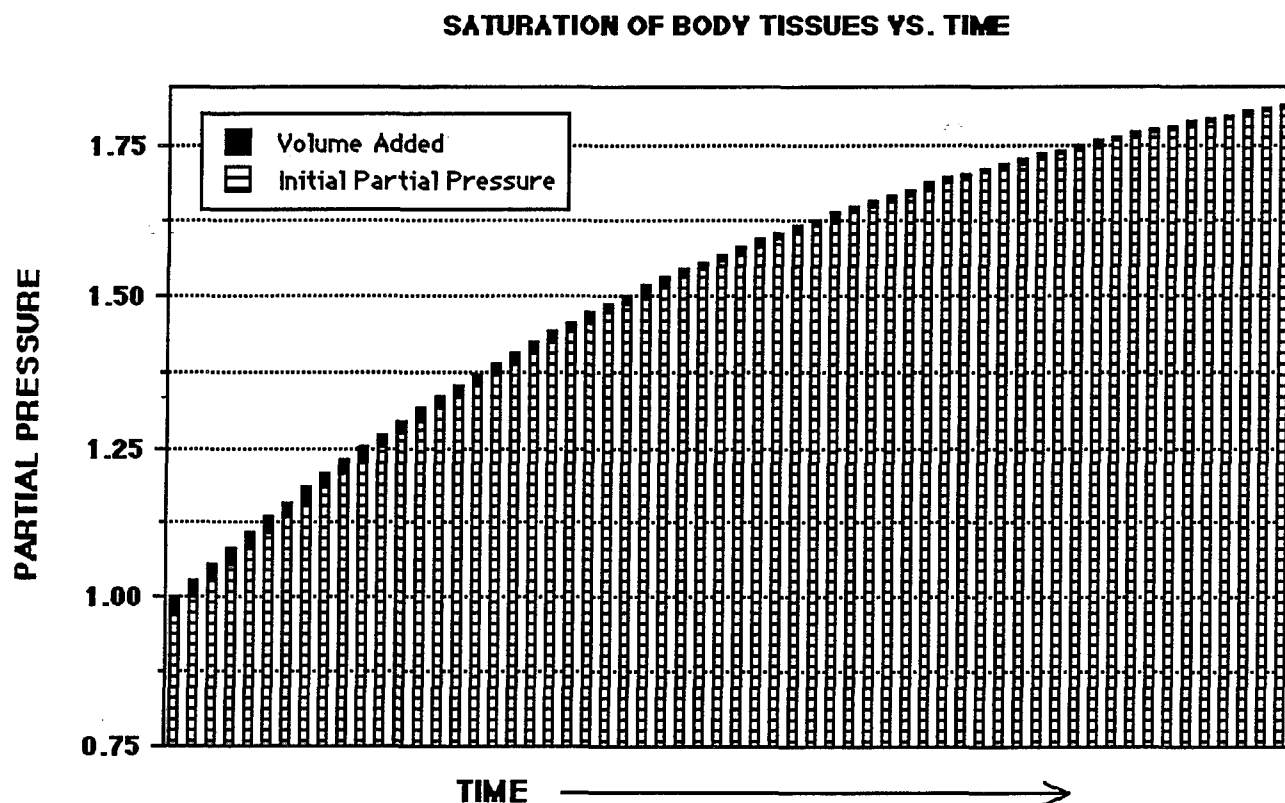


Figure 4. Uptake of nitrogen in tissues as predicted by the Haldane model.

Using this concept of perfusion-limited inert gas exchange, uptake of inert gas by the body can be mathematically described as an exponential, time-dependent process using the following equation:

$$P(t) = P_a + (P_o - P_a) * \exp(-kt). \quad \text{Eqn (1)}$$

where

$P(t)$ = partial pressure of nitrogen in the tissues
 P_o = initial nitrogen tissue pressure
 P_a = ambient nitrogen partial pressure
 k = time constant of gas uptake
 t = time tissue is exposed to P_a

Once the above equation is established, it may be recognized that the body is not uniform, and that the rate of inert gas uptake in a particular part of the body will vary widely with tissue fat content, effective blood perfusion, distance from the heart, etc. These differences may be accounted for by using different time constants in the above equation. Therefore, the partial pressure of nitrogen in a particular tissue of the body may be calculated using an exponential equation and its representative time constant. Because of the complexity involved in the real process of gas exchange between the tissue, blood and environment and individual variances in body composition, the time constants for these exponential equations cannot be directly related to actual physiological parameters. These values were simply chosen so that the spectrum of observed half saturation times was well represented.

The above model was derived for uptake of gas due to increases in ambient pressure. In the event of a rapid reduction in ambient pressure, the gradient is in the opposite direction and inert gas moves from the tissues to the blood to the environment. Provided no gas comes out of solution, desaturation of the tissues will be described by the same equation as tissue saturation.

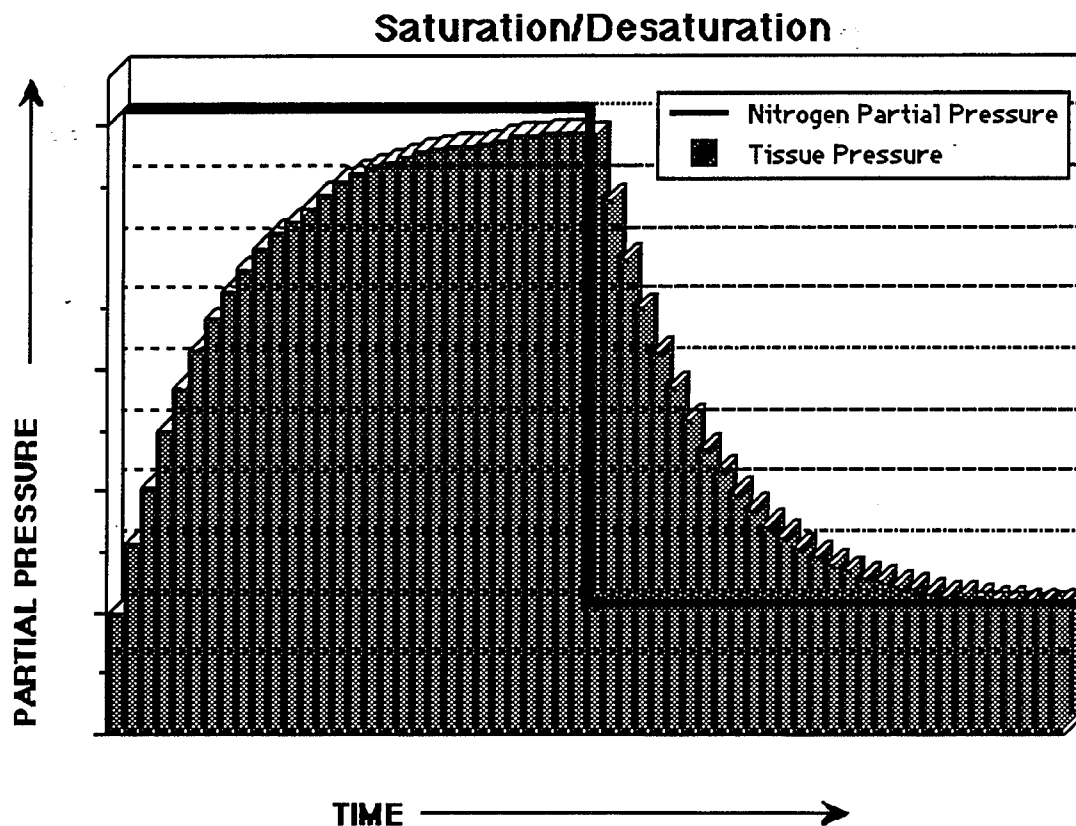


Figure 5. Nitrogen Uptake and Elimination in Tissue.

It is obvious, both from equation (1) and the above diagram (Figure 5), that, in the absence of a separated gas phase, the driving force for inert gas uptake or elimination is the difference between partial pressures of inert gas in the tissue and the ambient environment. It was experimentally determined that

the tissues could withstand a certain degree of supersaturation without gas phase separation. Haldane observed that tissues exposed to a given pressure for a "long" time could be exposed to a pressure reduction equal to half the previous level without posing significant risk of decompression sickness. This 2:1 ratio was based on total pressures. When only the inert gas is considered, the limiting ratio is actually 1.58:1.

The key to an efficient decompression then, would be to optimize the pressure difference so that gas is eliminated from the system as quickly as possible without causing bubble formation. Using multiple tissue compartments with various tissue half-time values, Haldane developed decompression limits for safe ascent from different depths such that, for each specified dive profile, the acceptable supersaturation ratio was never exceeded for any tissue compartment. Whenever a compartment exceeded the allowable limit, a decompression stop was required to allow the gas exchange processes time to catch up. The time required at each decompression stop was determined such that the controlling tissue could withstand a subsequent pressure drop equivalent to 10 fsw without again exceeding the acceptable supersaturation ratio.

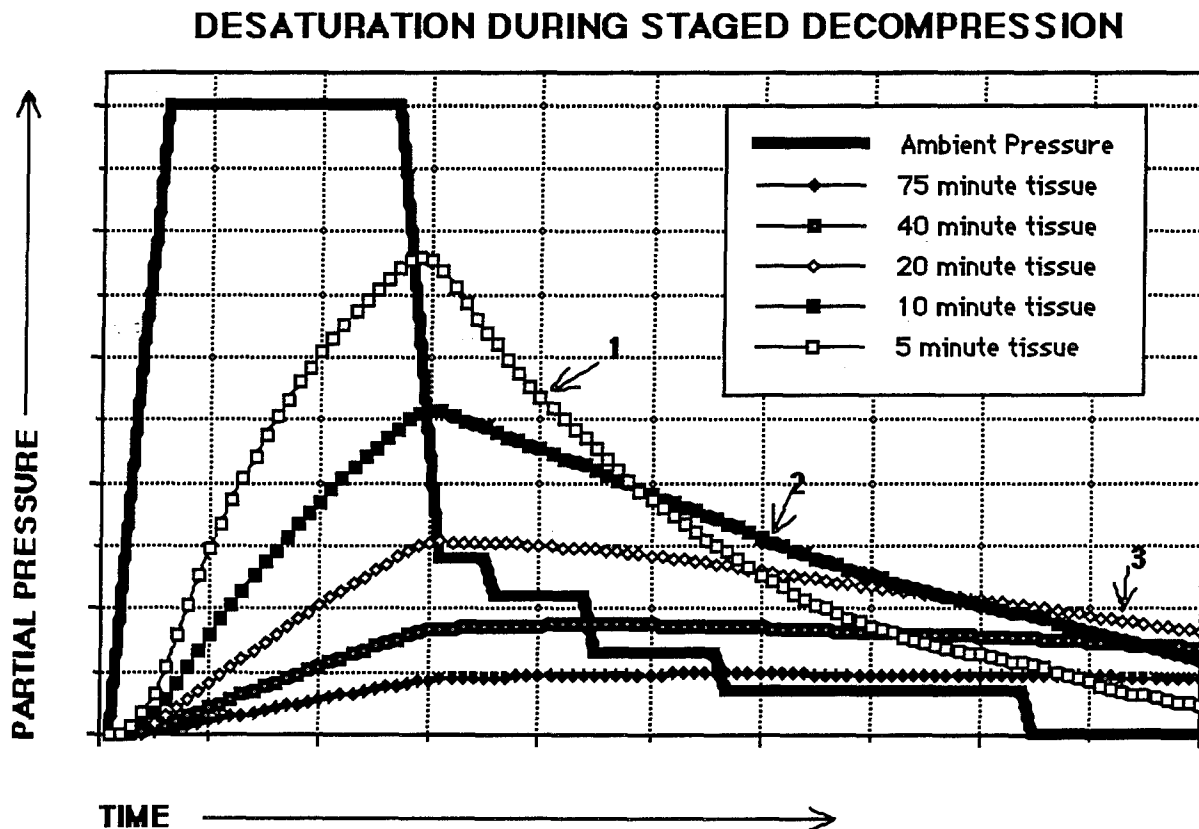


Figure 6. Illustration of Inert gas partial pressures in various tissue compartments as a function of time during a staged decompression. Arrows indicate which tissue is the rate-limiting factor for different phases of the decompression.

As can be seen from Figure 6 above, the ascent depth is not necessarily controlled by the same tissue throughout the dive. During the early stages, the fast tissues control the ascent rate limits. As time progresses the gas load in the fast tissues is removed and the slower tissues become the rate limiting factor.

Using this approach, Haldane developed a set of decompression tables for dives of various depths and bottom times. He used tissue half times of 5, 10, 20, 40 and 75 minutes, based on

physiological perfusion rates. These tables were conservative for short dives and inadequate for longer or deeper dives, indicating that larger tissue half times may be needed (62,83).

In response to this inaccuracy, the US Navy modified the Haldane model to produce a new set of dive tables in the 1950s (43). The main differences between the US Navy model and Haldane's model are: 1) six tissue compartments are used instead of five (the USN half-time constants were 5, 10, 20, 40, 80, 120 minutes), and 2) partial pressures of inert gas rather than total pressures were used in calculating the limits. This model produced the US Navy Standard Air Decompression Tables, which have been used as the basic standard for computing hyperbaric decompression procedures.

Although reliable for short dives, like Haldane's tables, the Navy tables were also inadequate for the deeper and longer dives, e.g., below 130 fsw for more than 30 minutes or for decompression times greater than 60 minutes (60). To compensate for these limitations, Workman (181) introduced the concept that the acceptable supersaturation ratio that can be tolerated without gas phase separation increases with both decreasing depth and decreasing tissue half time. Mathematically, this was accomplished by using a set of acceptable supersaturation ratios that varied with depth for each tissue. The ratios were referred to as M-values. The M-value is analogous to the maximum degree of supersaturation a tissue may possess at a specific depth to produce negligible risk of DCS. Using this approach, a set of curves were developed giving the M-value for each tissue compartment as a function of ascent pressure. The limiting tissue ratios defined by these curves were then used to develop decompression schedules for different dive profiles.

In order to more easily handle dives using multiple breathing gases, Schreiner used the sum of partial pressures due to each inert gas present to compute a total tissue pressure, which was then compared to the set of limiting tissue ratios. Variations in the rate of gas exchange for different gases was allowed through use of different half-times for each gas within the same tissue compartment. Like Haldane, Schreiner's original selection of halftimes were based on measured blood flows (130). However, these values have been modified to better match diving experience and can no longer be realistically linked to physiological blood flows (130).

Schreiner's model, commonly known as the "Tonawanda II" model or the Haldane-Workman-Schreiner method, also incorporated the partial pressures of carbon dioxide and water vapor when computing the inert gas partial pressure present at the alveoli (130). The resulting inert gas partial pressure was then used as the driving force for gas exchange with the tissues rather than the partial pressure of inert gas in the ambient environment. Although this difference is of little importance in diving since the alveolar CO_2 and water vapor partial pressures are small compared to the ambient pressure, it may be important for hypobaric exposures.

Another variation of the original Haldane model was developed by Thalman at the USN Experimental Diving Unit, (141,142,143) in an attempt to come up with a single model that would work equally well for both short dives and longer, deeper dives. Based on an extensive set of experimental data, he proposed that the exponential relationship governing uptake of inert gas on descent was not valid for ascent due to the formation of bubbles. Instead, an empirically determined linear relationship was used to calculate elimination of inert gas during decompression. This approach indirectly accounts for the slowed rate of denitrogenation due to gas phase separation during decompression without actually attempting to calculate the size of this gas phase. In addition, it predicts a higher residual level of nitrogen in the tissues than the exponential model. Though this would be expected to produce safer decompression schedules for repetitive dives, its profiles have been shown in many instances to be less conservative than the standard US Navy model (83).

At the Royal Navy Physiological Laboratory (RNPL) a diffusion model based on the concept of tissue slabs was used to calculate tissue inert gas concentrations. The RNPL model represents the body as a block of tissue with one face held at ambient pressure. The driving force for inert gas uptake or elimination is the slope of the concentration gradient (61,127). This is conceptually illustrated in Figures 7

and 8. The first curve shows the relative tissue nitrogen concentrations at some arbitrary time after an exposure to increased ambient pressure. The second figure shows the gas concentrations that would occur at some time during a subsequent decompression. The partial pressure of nitrogen in the tissues may therefore be calculated as a solution to the diffusion problem, and is a function of both distance and time. Like the other tissue models, a decompression is considered safe so long as the ratio of the greatest tissue gas tension to ambient pressure does not exceed the acceptable supersaturation level.

DIFFUSION OF INERT GAS INTO TISSUE SLAB

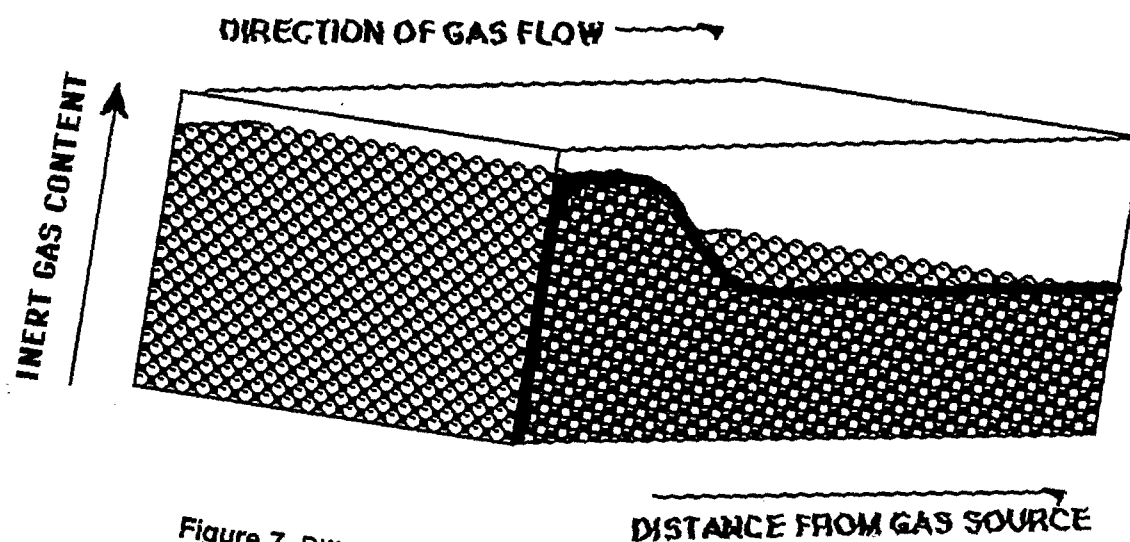


Figure 7. Diffusion of inert gas into tissue slab.

DIFFUSION OF INERT GAS FROM TISSUE SLAB

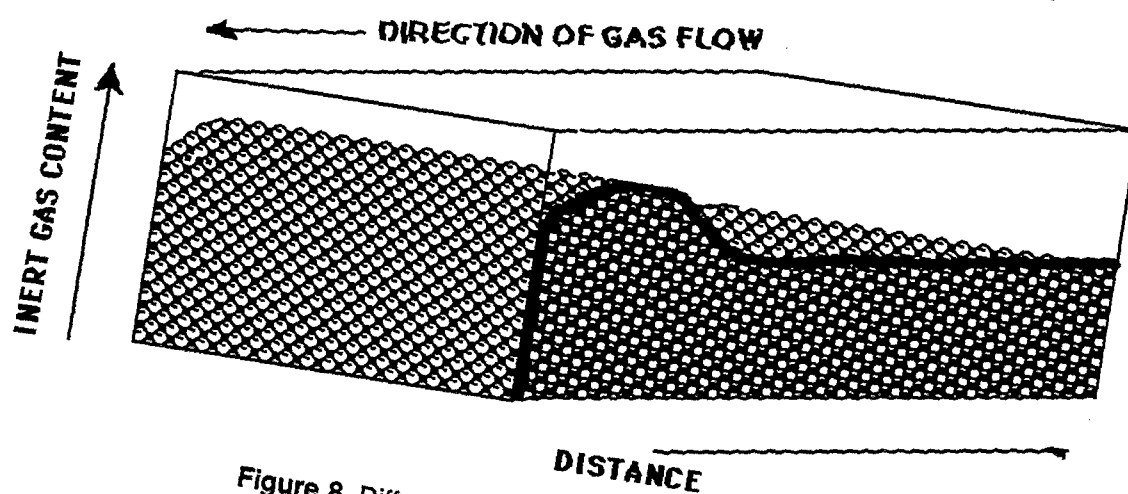


Figure 8. Diffusion of inert gas out of tissue slab.

An entirely different approach was employed in the development of the Kidd-Stubbs model used to develop the Canadian Defense and Civil Institute of Environmental Medicine (DCIEM) (in Toronto)

tables. This work is based on the gas exchange kinetics of a pneumatic analog consisting of 4 small chambers connected in series with only the first chamber exposed to ambient pressure. This device was used in real time to control the diver's exposure. The orifices connecting each chamber were sized to provide results roughly matching the USN tables. Unfortunately, manufacturing problems associated with drilling the small holes connecting the chambers limited the widespread use of this system. To overcome these problems, a computer model was developed at the DCIEM and refined by Nishi to mathematically solve the equations governing gas flow between the chambers of the pneumatic analog. The output of these equations provides the gas tensions for each compartment used to control the dive, based on the Haldanian concept of limiting supersaturation. Although the model has no basis in physiological mechanisms of gas exchange, the results provided reasonably successful air tables (113).

In the late 1960s, Hills developed his thermodynamic model (39,46). Inert gas exchange is assumed to be diffusion-limited and is described by the following equation:

$$(\Delta p)_r = x \Delta P \cdot \left(1 - \pi \sum_{n=1}^{\infty} \frac{\{J_0(r\alpha_n) \cdot Y_0(a\alpha_n) - Y_0(r\alpha_n) \cdot J_0(a\alpha_n)\} \cdot \exp(-\alpha_n^2 \cdot Dt)}{\left[\frac{J_0(a\alpha_n)}{J_1(b\alpha_n)} \right]^2 - 1} \right)$$

Eqn (2)

where α_n is the root to this equation:

$$J_0(a\alpha_n) Y_1(b\alpha_n) - Y_0(a\alpha_n) J_1(b\alpha_n) = 0$$

Eqn (3)

and

- $(\Delta p)_r$ is the change in the tissue pressure at any given location
- x is the fraction of inert gas in the capillary gas
- ΔP is the change in ambient pressure
- J_0, J_1 ordinary Bessel functions of the first kind, and of the zeroth and first order respectively
- Y_0, Y_1 ordinary Bessel functions of the second kind, and of the zeroth and first order respectively (68,72,78).

Although Hills claims that these equations are easily solved using Legendre quadrature, they become much more complex if one assumes the possibility of a separated gas phase. Furthermore, they are probably not necessary for the altitude situation, as will be explained later. Hills has shown evidence, however, that use of his radial bulk diffusion equation offers better prediction of several sets of data (68,75). Also, the complexities arising from the effect of a separated gas phase on the inert gas content of the tissues do not pose a problem in Hills' calculation of dive tables. In previous models, the difference between the ambient pressure and the tissue pressure was increased to just below bends provoking. Because a linear relationship had been established between inert gas elimination and this difference in pressure, maximizing this difference was believed to provide the greatest driving force for inert gas elimination. However, Hills assumes that the tissues are incapable of sustaining excess inert gas in solution. This zero-supersaturation criteria requires that all excess gas will either be eliminated via perfusion, or dumped into a separated gas phase (76). Because formation of gas bubbles decreases the rate of elimination of inert gas (11,71,78,161,188), Hills' thermodynamic model requires that the decompression be such that there is no possibility of bubble formation. According to the concept of inherent unsaturation, or the oxygen window (15,70,148,152,157), tissue in equilibrium with its environment will always have a total dissolved pressure of gases somewhat lower than the total ambient pressure. The ambient pressure may therefore be reduced to this lower tissue pressure without initiating the formation of a separated gas phase. Hills' decompression is therefore staged such that the "inherent unsaturation" is the driving force for inert gas elimination. While profiles matching those predicted by Hills' thermodynamic model have been used successfully for thousands of Okinawan pearl divers (103), this model, like the Haldanian tissue models, requires the individual to follow a rigid decompression format, and does not provide a risk assessment for the individual who may need to overstep the bounds of a "safe" decompression. The major deficiency of the thermodynamic model then, is in the estimation of the

size of the gas phase, or, in fact, the estimation of any sort of decompression strain whatsoever. If a risk analysis is to be provided in lieu of a strict yes/no assessment, this is a vital ingredient.

5.B. Hypobaric Decompression Model

While Hills took pains to avoid the separation of gas from solution in his calculation of the dive tables, his model seems to mark a transition from reliance upon traditional supersaturation models to increased interest in those that depended upon bubble size as the indicator of DCS.

Bubble models try to predict the size of the gas phase evolved from solution by equating the pressure inside the bubble with the pressure outside of the bubble (21). Inside pressure may be seen as those factors encouraging growth of the bubble. This is usually assumed to be equal to the partial pressure of inert gas in the tissues plus the pressure of CO₂, O₂, and water vapor. Conversely, the outside pressure would tend to shrink the bubble, and would be composed of the total ambient pressure, plus the pressure due to surface tension and from tissue elasticity. Most models ignore tissue effects, assuming that they are negligible (9,91,92,151,184).

The "critical released gas volume" hypothesis (64) led to the conclusion that decompression schedules could be developed by following the relation:

$$P_1 = a P_2 + b \quad \text{Eqn (4)}$$

where

P_1 the pressure to which the tissue has been equilibrated
 P_2 the pressure to which it is just safe to decompress
 a, b constants determined experimentally.

Starting with mass balance, rapid equilibration between dissolved and released gas is assumed. The total quantity of gas in the system may then be equated to the amount dissolved in the tissues plus the amount in the bubble:

$$S \cdot p_{1\alpha} = S \cdot p_{2\alpha} + V \cdot p_{2\alpha} \quad \text{Eqn (5)}$$

where

S solubility of the inert gas
 $p_{1\alpha}$ partial pressure of inert gas in the tissues before phase separation
 $p_{2\alpha}$ partial pressure of inert gas in the tissues after phase separation
 V volume of released gas per volume of tissue that is just below the bends-provoking limit.

The pressure of gases in the tissues is then equated to the pressure of gases in the bubble:

$$p_{2\alpha} + P(\text{O}_2, \text{CO}_2, \text{H}_2\text{O}) = P_2 + \frac{2\sigma}{r} + \delta \quad \text{Eqn (6)}$$

where

$P(\text{O}_2, \text{CO}_2, \text{H}_2\text{O})$ the sum of the partial pressures of oxygen, carbon dioxide, and water vapor in the tissues, 126 mmHg

- P_2 the pressure to which the subject is decompressed
 σ surface tension, 0.0179 N/m (39)
 r average bubble radius, 1.41 mm (67)
 δ the deformation pressure that will just induce pain at nerve endings, 10 mmHg (85)

Using these values and solving equations (5) & (6) simultaneously, the following relation was obtained

$$P_1 = A \cdot P_2 + B \quad \text{Eqn (7)}$$

where

$$A = 1 + \frac{V}{S} \quad \text{Eqn (8)}$$

$$B = A \cdot 74 + P_{O_2} \quad \text{Eqn (9)}$$

and

P_{O_2} is the partial pressure of oxygen in the breathing mix

Though it makes some dubious assumptions in its calculations of the size of the total evolved gas phase, experimental evidence suggests that this equation correctly defines the boundary between bubble formation and no bubbles (104). Therefore, this model could potentially be modified for use in aviation. Instead of determining an ascent pressure so that pain-inducing bubbles are only avoided, it could be used to predict the size of a bubble volume and the resulting decompression strain at a particular pressure. A model that does just this has been created by NASA (124). A review of the results of trials of this model does not seem to offer exceptional correlation between the predicted and actual strain.

An alternative use of bubble models is for the prediction of the time required for bubble dissolution (97). This assumes that DCS is unavoidable, and predicts the best method and required length of treatment. Supported by experiments of bubble growth in gelatin, the bubble lifetime was found to be:

$$L \approx \frac{r_0^2 \sqrt[3]{p_1 + \delta} + \sqrt[3]{(p_0 + \delta)^2}}{2 R T D S (p_1 + \delta - \tau)} \quad \text{Eqn (10)}$$

where

- p_1 treatment pressure (if subject is recompressed)
 p_0 initial ambient pressure
 r_0 initial radius of the bubble
 δ tissue deformation pressure
 R universal gas constant
 T temperature in degrees Kelvin
 D the diffusion constant $1.88 \times 10^{-5} \text{ cm}^2/\text{s}$ (165)
 S solubility $6.73 \times 10^{-13} \text{ mol}/(\text{dyn-cm})$ (105)
 τ gas tension in the tissue, assumed to be the sum of the inert gas tension, and the tension of oxygen in the tissue, found by the relation

$$\frac{d\xi}{dt} = 0, \quad \xi_b < \xi_c \quad \text{Eqn (11)}$$

$$\frac{d\xi}{dt} = k (\xi_b - \xi), \quad \xi_b > \xi_c \quad \text{Eqn (12)}$$

where

- ξ tissue tension of oxygen with and initial value of 46 mmHg
- ξ_b arterial tension of oxygen
- ξ_c maximum tension of oxygen that can be metabolized by the tissue.

This model ignores the effects of surface tension, since it was derived for use at depth, where surface tension would be assumed to be small compared to the hydrostatic pressure. Also, it does not provide for any sort of analysis during the decompression. However, it does acknowledge that decompression sickness may not always be avoidable, and provides a solution if DCS does develop.

One of the earliest bubble models was devised by Bateman and Lang (9). In their experiments, they found the rate of growth of bubbles in aqueous media to correspond reasonably well to their theoretically derived equation:

$$\frac{dV}{dt} = \frac{4\pi\alpha T\delta \cdot (p_1' - p_1) \cdot \sqrt[3]{\frac{3V}{4\pi N}}}{273p} \quad \text{Eqn (13)}$$

where

- α solubility of nitrogen in water at 37°C
- δ diffusivity of nitrogen in water
- p_1' partial pressure of dissolved gas in the tissues
- p_1 partial pressure of nitrogen in the bubble
- p total force acting on the bubble, assumed to be equal to the hydrostatic pressure plus pressure due to surface tension
- V total volume of evolved gas
- N total number of bubbles
- T temperature (K).

The desired result is the total volume of the gas out of solution. Bubble volume, however, does not have a one-to-one correspondence with bubble radius. As is illustrated by Figure 9, a relatively large change in volume may produce only a small change in radius, especially after the initial stages of growth.

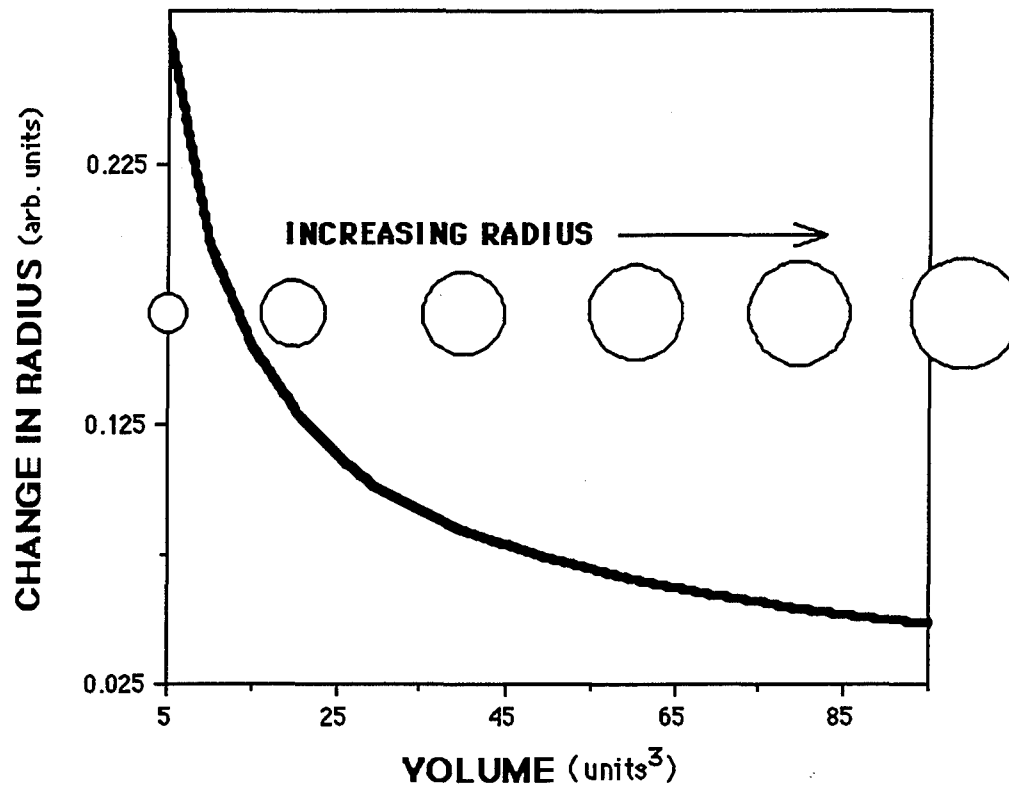


Figure 9. Change in Bubble Radius vs Volume.

Because decompression sickness is believed to be attributable to the mechanical effects of bubbles in the body (i.e., deformation of pain receptors or blockage of small blood vessels), many subsequent bubble models try to predict the bubble radius as opposed to the volume.

Van Liew's model (153) originally ignored surface tension as well as tissue effects. This was justified on the grounds that his calculations would err on the side of conservatism, but nevertheless was included in later calculations (150). He derived the following equation for the rate of change of the bubble radius with time:

$$\frac{dR}{dt} = (\alpha_t D K_1) \left(1 - \frac{P_{tis}}{P_{bub}}\right) \left(\lambda + \frac{1}{R}\right) \quad \text{Eqn (14)}$$

where

- R bubble radius
- α_t solubility of N_2 in the tissue, between 1 and 5 times the solubility in blood
- D diffusivity of N_2 in body fluids, $0.00132 \text{ cm}^2/\text{min}$
- K_1 factor to convert the pressure being used into bar
- P_{tis} the partial pressure of N_2 in the tissue
- P_{bub} the partial pressure of N_2 in the bubble
- λ the perfusion factor

$$\lambda = [(\alpha_b \cdot K_2 \cdot Q) / \alpha_t \cdot D]^{0.5} \quad \text{Eqn (15)}$$

where

- α_b solubility of N_2 in blood, 0.0144 (ml/gm)/bar
- K_2 constant for the effectiveness of blood flow, 1
- Q tissue perfusion rate (ml/ml)/min

As is the case with most bubble models, the calculations are highly circular. For example, P_{tis} is influenced not only by the washin or washout of inert gas from the tissues, but also by that gas that diffuses into or out of the bubble. P_{tis} is described by the following equations:

$$P_{tis} = \frac{V_t}{\alpha_t V} \quad \text{Eqn (16)}$$

where

- V_t volume of N_2 in the tissue volume, in ml
- v tissue volume, ml.

and V_t is dependent both on the washout of inert gas from the tissue and the amount that enters or leaves solution from the gas phase such that

$$\frac{dV_t}{dt} = \alpha_b Q (P_{tis} - P'_{tis}) + \frac{dV}{dt} \quad \text{Eqn (17)}$$

where

- P'_{tis} initial pressure of N_2 in the tissues for a time step
- P_{tis} final pressure of N_2 in the tissues for a time step
- V bubble volume, ml

If the barometric pressure is not constant with time (as during ascent), then

$$P_{tis} = P_B - F_{IO_2} P_B - P_{ACO_2} - P_{H_2O} \quad \text{Eqn (18)}$$

where

- P_B barometric pressure, bar
- F_{IO_2} fraction of oxygen in the inspired air
- P_{ACO_2} partial pressure of CO_2 in the alveolar gas, 0.053 bar
- P_{H_2O} partial pressure of water vapor in gas saturated at body temperature, 0.062 bar for the above equation. Also,

$$P_{bub} = P_B - (P_{tO_2} + P_{tCO_2} + P_{H_2O}) + \frac{2\gamma}{R K_3} \quad \text{Eqn (19)}$$

where

- P_{tO_2} the partial pressure of O_2 in the tissues, 0.053 bar
 P_{tCO_2} the partial pressure of CO_2 in the tissues, 0.059 bar
 γ the surface tension, 50 dynes/cm
 K_3 conversion factor, 106 (dynes/cm)/bar

This model offers a description of bubble growth that seems intuitively correct, but has not been tested for correlation to DCS. It has shown good correlation with experimental results for the absorption of inert gas pockets in the rat (148) but these may be a little different from the results that would be expected from smaller bubbles with greater volume-to-surface area ratios, and greater surface tension values. While these calculations may seem complicated and tedious, they enable predictions of gas bubble growth to be made for slow pressure changes and for profiles composed of more than one change in pressure or breathing mix. Once slow or multiple pressure changes are allowed, then tension gradients may develop in the tissue due to the effects of perfusion, as well as diffusion of gas into the bubble. Previous analyses of this type assumed only one instantaneous pressure drop (45,92,110) in order to avoid these complications.

Of course, a compromise could be made to make the gas bubble growth model more realistic for altitude decompression, but somewhat more manageable than the stringent mathematical interpretation of Van Liew. Instead of going through the rigors of calculating the tissue inert gas concentration gradient as affected by diffusion of gas into the bubble, and the washin or washout of gas from the tissue due to perfusion, a reasonable assumption would be that the tissue is well stirred except for a radial diffusion zone surrounding the bubble (3). The gradient in this zone could then be approximated by a linear function:

$$\frac{\partial C}{\partial r} = \frac{(C_i - C_s)}{d} \quad \text{Eqn (20)}$$

where

- C_i the concentration of inert gas in the tissue at the outer boundary of the diffusion zone
 C_s the concentration of inert gas in the tissue at the bubble boundary
 d the width of the diffusion zone.

The derivative of the radius with time can then be calculated as:

$$\frac{dR}{dt} = \left(\alpha \frac{k}{d} \right) (P_{gl} - P_l - \frac{2\sigma}{R}) - \frac{\left(\frac{RM}{3BT} \right) \left(\frac{dP_l}{dt} \right)}{\left(\frac{M}{BT} \right) \left(P_l + \frac{4\sigma}{3R} \right)} \quad \text{Eqn (21)}$$

where

- α solubility of inert gas in the tissues
 k diffusion coefficient of the inert gas in liquid
 d width of the radial diffusion zone
 P_{gl} tissue inert gas pressure outside of the diffusion zone given by

$$\frac{dP_{gl}}{dt} = -L_1 (P_{gl} - P_l), \text{ where } L_1 \text{ is determined experimentally}$$

P _i	pressure of inert gas in the breathing mix
M	molecular weight of the gas
B	universal gas constant
T	temperature in degrees Kelvin
σ	coefficient of surface tension
R	bubble radius

These models also assume pre-existing gas nuclei of such a size that surface tension does not cause them to be re-absorbed. Mathematical models have established that a gradient is formed during flow of gas out of a bubble, which may impede dissolution of that bubble (79). Because bubble growth from a nucleus is not considered, this may possibly affect the gradient of dissolved gas around the bubble, and thus the subsequent rate of growth or decay of the bubble.

Many models ignore the early growth process because it is not understood how a bubble can grow from nothing. Since the pressure due to surface tension is proportional to the reciprocal of the radius of the bubble, this pressure would effectively be infinite when the radius is close to zero. The pressure of gases inside the bubble would then have to be enormous in order to balance the pressure due to surface tension, resulting in an infinite gradient for diffusion of gases out of the bubble. Yount's model (182,186,190) does consider the events of initiation and early growth of a bubble. These events are not, however, assumed to have a substantial effect upon inert gas uptake or elimination, which is described by the common exponential equation. In order to describe bubble growth from pre-existing nuclei, the varying permeability model (VPM) (186,187) assumes that there is some sort of surface active agent that reduces surface tension in the bubble as bubble volume decreases. When the radius, and thus surface area, of the bubble decreases, the surfactant molecules clinging to liquid gas interface crowd closer together. During compression, the surfactant molecules may become so tightly packed that the bubble radius cannot decrease unless some of the surfactant molecules are expelled from the liquid-gas interface. This resistance to the effects of surface tension is called the skin compression. While in reality the skin compression will increase as the radius decreases, these effects are ignored in the VPM, and only changes caused by the addition or deletion of surfactant molecules are calculated. The liquid medium is considered to be a reservoir or sink for surfactant molecules, and changes in the skin compression are calculated as a function of the rate of accretion or deletion of surfactant molecules from the nuclear skin (186). It is assumed that bubbles of varying radii are interspersed within the liquid medium. Only those bubble nuclei with a sufficiently large radius will grow in response to a given differential between the ambient pressure and the inert gas tension in the tissue. As this differential increases, nuclei of smaller radius may be activated. Conversely, nuclear radius may be affected by changes in the skin compression, thereby increasing or reducing the number of nuclei that will grow in response to a given pressure differential. The decompression strain is calculated as the number of bubbles that have grown above a certain minimum radius. Safe decompression is predicted so that the calculated safe bubble number is not exceeded. While this model has been demonstrated to show good agreement with data on rats and humans (184,185), it is currently more concerned with strict prevention of DCS rather than prediction of risk.

Finally, one of the few models to incorporate the effects of tissue elasticity was also one of the few developed specifically for altitude. Like the others, Gernhardt (54) equates the pressure of the gases in the bubble to the sum of the forces acting on the bubble. However, in addition to the hydrostatic pressure and the pressure due to surface tension, he also incorporates the pressure due to the resistance of the tissue to deformation. The tissue deformation pressure is thus defined by:

$$T_D = 4\pi R^3 \cdot \frac{H}{3} \quad \text{Eqn (22)}$$

where

R radius of the bubble

H bulk modulus of the tissue expressed as the ratio of the change in pressure to the change in volume

Tissue inert gas content is assumed to be perfusion limited, while gas content of the bubble is diffusion limited. The change in the volume of the bubble is found by:

$$\frac{dV}{dt} = \frac{\alpha AD (P_T - P_B)}{h P_B} - \frac{V}{P_B} \frac{dP_B}{dt} \quad \text{Eqn (23)}$$

where

α solubility of gas in the tissues
A surface area of the bubble
D diffusivity
 P_B pressure in the bubble, defined as the sum of the hydrostatic pressure, pressure due to surface tension, and the tissue deformation pressure
V initial volume of the bubble
h effective thickness of the diffusion barrier between the bubble and the tissues
 P_T inert gas tension in the tissue, given by

$$P_T = P_0 + [x(P_0 - vt) - P_0][1 - \exp(-Qt \frac{\alpha_b}{\alpha_t})] \quad \text{Eqn (24)}$$

where

P_0 initial inert gas tension in the tissue
x fraction of inert gas in the breathing mix
v rate of ascent
t time
Q effective blood perfusion
 α_b solubility of the inert gas in the blood
 α_t solubility of the inert gas in the tissue

These equations, like Van Liew's, are highly interdependent.

Most of the models described up to this point have given an output of a particular decompression strain, whether this be tissue ratio, evolved gas volume, or bubble radius. In order to relate this strain to a probability of DCS, the methods of maximum likelihood have been developed (144,157,158,166). Using a maximum likelihood analysis, the parameters of any given model are adjusted such that the theoretical predictions are as close as possible to the actual outcome of a selected database (177).

As is evident, the algorithms used in the determination of the decompression strain, and in the assessments of the effects of this strain, can become quite complicated and tedious. One way to circumvent the need to perform all of these calculations is to develop an analog. These operate on the principle that many physical systems are governed by the same mathematical laws. Therefore, a system in which quantities are directly measurable (unlike the human body) can be used to represent the body.

Analogues for decompression were originally developed as a way to advise divers having no contact with the surface. Because it is inconvenient for a diver to carry a dive table, and it is rather difficult to put meters on the body to alert the individual to what is going on, the next best thing was to develop a system that would respond to the environment in a way similar to the human body and that would conveniently display its internal data. Since most of the models that had been used to develop the dive

tables relied upon the assumption that the uptake/elimination of gas from the body is a time-based function, it was reasonable to try to find a physical system in which the change of a particular parameter could be predicted by the same equations. Fortunately, there are many such systems from which to choose, the basic governing equations being modified only for constants and initial and boundary conditions.

Electrical systems have also been used as analog for the human body (106,107,139). In these systems voltage is related to gas pressure, current to gas flow (mass per unit time), resistance to gas diffusion resistance (pressure per unit gas flow), and capacitance to gas volume (gas mass per unit pressure). The great advantages of electric analog over other types of analog is that there are no moving parts, and they can be sufficiently time scaled to be used for predictive purposes as well as for real-time applications. One disadvantage is that they are quite sensitive to temperature. This would not normally be a problem, as most offices are temperature controlled. Unfortunately, most electric analogs will give the same predictions as the simple exponential used by most tissue models. There is no method to calculate the volume of gas that could come out of solution. A non-linear element would need to be introduced in order to mimic the effects of a separated gas phase on the elimination of inert gas from the system.

There are several disadvantages to analogs that would make them less desirable as a predictive tool for DCS:

- There is the possibility of mechanical failure, or the deterioration with time of moving parts.
- Most of them are designed for real-time applications, which would make using them for prediction of DCS rather difficult.
- Any decompression strain predicted by these analog would still need to be related to the severity or risk of DCS. A hybrid computer would then be required, with the analog part producing the decompression strain, and the digital part interpreting the risk of decompression sickness.
- There is currently no way to deal with the effect of phase separation on off-gassing.

6. ALTITUDE DECOMPRESSION COMPUTER CONCEPT DEFINITION

Development of the current altitude decompression computer concept has evolved during the course of this project. Analyses of operational requirements and various approaches to DCS risk assessment were used as a basis for defining the framework of the Armstrong Laboratory's altitude DCS model development efforts. This section reviews the results of the concept definition portion of the feasibility study. First the requirements and model development guidelines are reviewed. The remaining material in this section describes how these were translated into a conceptual altitude DCS model. The concluding sections address the implementation and evaluation of the preliminary model developed during this effort.

6.A. Requirements for an Operational Altitude Decompression Computer

The basic concept of the altitude decompression computer has already been presented. To reiterate, the altitude decompression computer will serve as a standardized tool for assessment and management of DCS risk in USAF flight operations. The same computer will also provide a standardized approach for risk management in altitude chamber training and research operations. A similar computer could also be used for managing DCS risk associated with extravehicular activity onboard the Shuttle and Space Station Freedom. The final implementation of these devices into operational systems may take several forms. For instance, mission planning and support may be accomplished on desktop computers or portable laptop systems on the ground before and during the flight while cockpit or pressure-suit-mounted devices could provide real-time input to the aircrew during flight.

An analysis of potential applications for the envisioned altitude decompression computer was used to identify the key requirements that must be addressed for successful development of the desired product. These requirements are discussed below.

Requirement #1:

The system must provide a relative assessment of the risk of altitude DCS rather than a simple yes/no prediction of impending DCS. One of the primary outputs should be the estimated probability of getting DCS for a given flight profile, expressed as a percent. This is necessary to allow evaluation of available options where, under certain circumstances, accepting a high risk of DCS may be the least costly alternative.

Requirement #2:

The system must also be capable of providing information about how to maintain the risk of DCS within user-defined acceptable limits. This may be in the form of answers to questions such as: How much prebreathe is required? What is the maximum safe altitude and/or duration at altitude? How does changing cabin and/or pressure suit differentials affect the risk of DCS?, etc.

Requirement #3:

The software in the final version must be compatible with implementation in multiple configurations. This may include different hardware platforms as well as different user interfaces, depending on the particular requirements for each application.

Requirement #4:

The operational systems must be structured in such a way that subsequent software updates can be readily incorporated. Improvements in both the spectrum of scenarios that can be evaluated by the model and the accuracy of these evaluations are expected based on operational experience and future research. This requirement will provide a means for easily transitioning these improvements to the field.

7. ALTITUDE DCS MODEL DEVELOPMENT GUIDELINES

Along with the above design requirements, a set of guidelines were developed for the altitude decompression computer development process. These guidelines were distilled from analyses of: 1) previous experience in decompression model development in both the hyper- and hypobaric fields; 2) the differences between these fields as mentioned earlier; and 3) DCS protection options for current and future operational missions. The guidelines are summarized below. Details on the rationale behind the guidelines are provided in the discussion that follows on the structure of the proposed model. Guidelines for altitude decompression computer development:

1. Modeling efforts should be based on physiological and physical mechanisms to the greatest extent possible, not just a curve fit of available data.
2. The software shall have a modular framework to facilitate evaluation and incorporation of multiple algorithms.
3. Development of the model/computer shall proceed in an evolutionary fashion with verification of each phase as it is developed.
4. The initial model development work should be based on existing databases and relevant *in vitro* data, with refinement based on additional research where necessary.
5. The final version of the model must be validated using a selective series of human altitude chamber trials that adequately covers the broad spectrum of exposures that the model will be used to evaluate.

8. STRUCTURE OF THE CONCEPTUAL ALTITUDE DCS MODEL

The development of the altitude decompression sickness risk assessment model has been influenced by the basic guidelines given above. Of primary importance is the goal to develop a model based on physiological and physical principles rather than relying on a purely empirical foundation. This theory-based approach should provide better reliability when extrapolating the model's predictions to new scenarios for which experimental data is not currently available.

However, since the precise mechanisms of decompression sickness have not yet been defined, we must compromise somewhat between the two approaches. To do this, we propose to implement mathematical representations of the relevant physical and physiological processes associated with altitude DCS. These mathematical expressions will yield numerical outputs that can then be combined to provide a composite estimate of the "DCS stress" imposed on a crew member by any given flight profile. Finally, the calculated DCS stress will be correlated with physiological outcomes, e.g., incidence, severity and latency of DCS and venous gas emboli, through the use of appropriate statistical techniques. These calculations may be modulated either directly or indirectly by additional calculations that provide a means of accounting for predisposing factors and individual variability. This conceptual structure is shown in Figure 10 below.

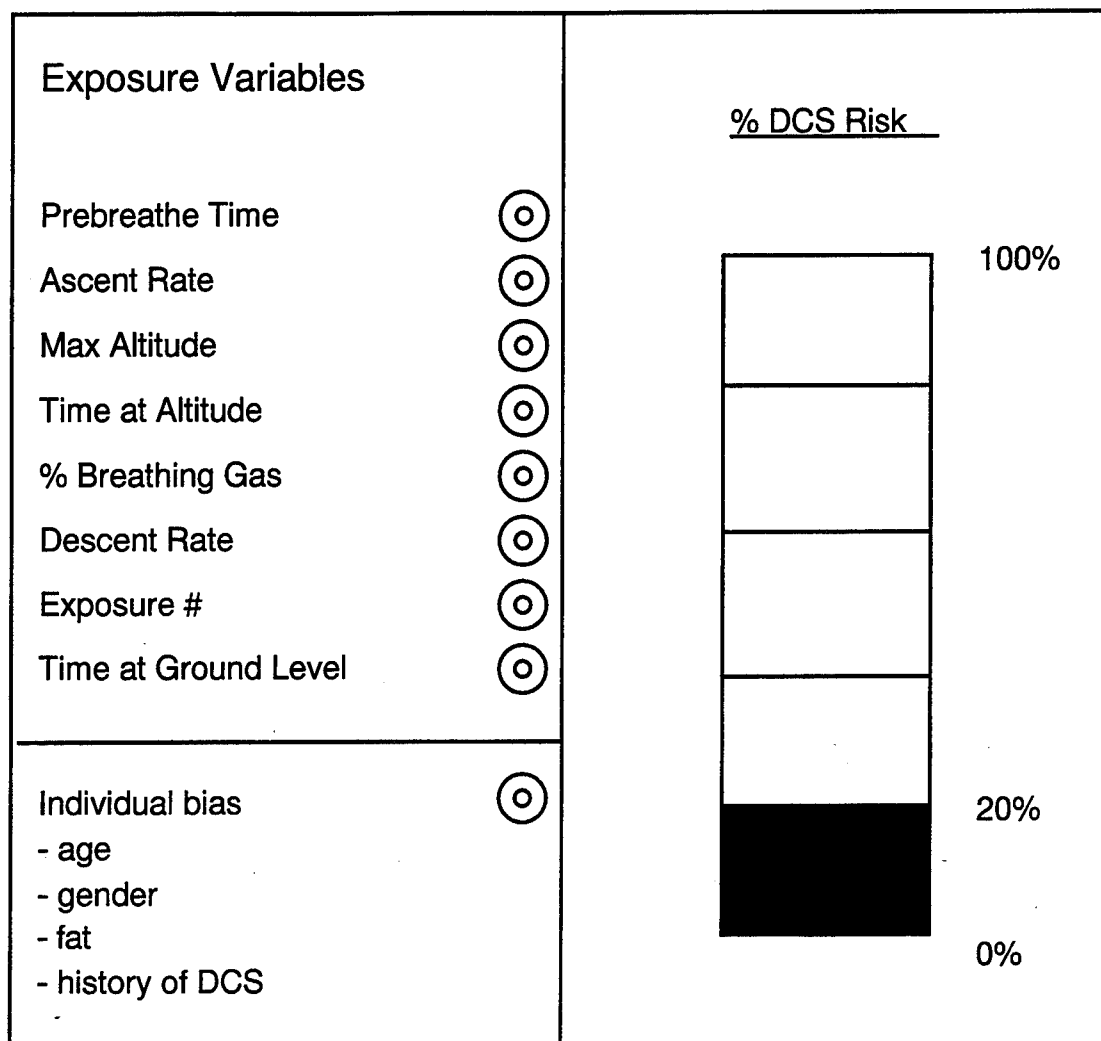


Figure 10. Conceptual Altitude DCS Risk Assessment Model.

This "quasi-physiological" model is being developed in an evolutionary process using a modular framework to allow incorporation and evaluation of multiple algorithms, testing various approaches from several existing models, and composed of the following gross components:

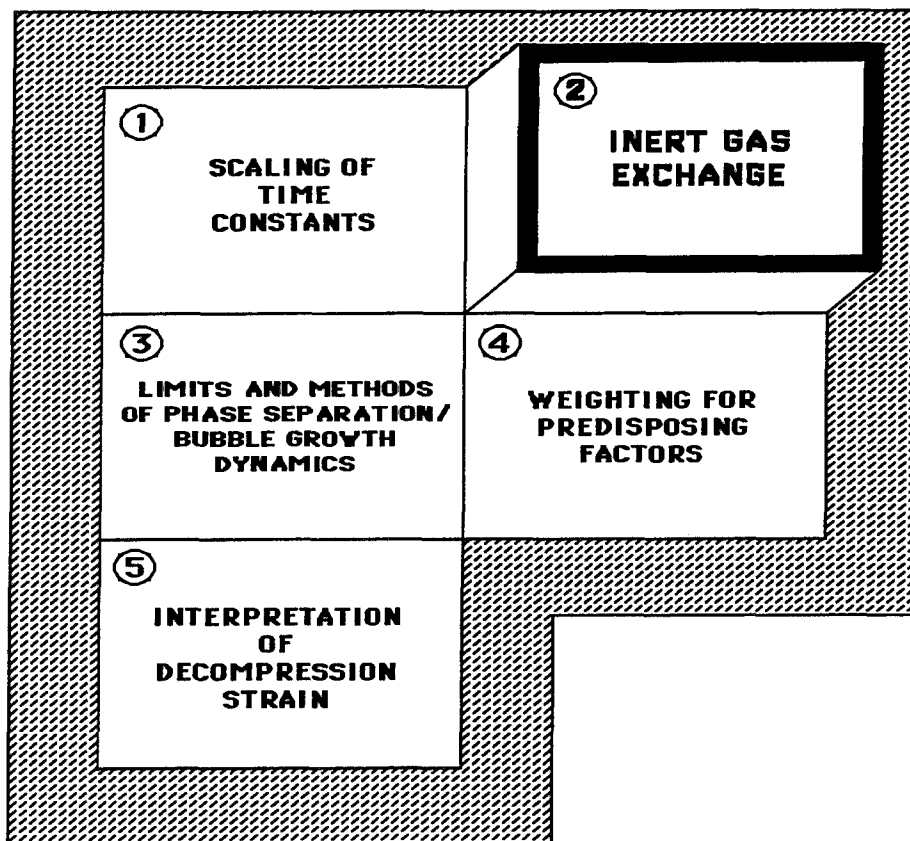


Figure 11. Gross component of working model.

The core of the model consists of inert gas exchange algorithms coupled with equations governing the dynamics of gas phase separation and bubble growth. Since different mechanisms may be dominant for different exposure conditions, the various predictive algorithms may be combined through an appropriate weighing scheme. The final output is in the form of an estimated probability of getting DCS expressed as a number between 0 and 100 percent. This represents the basic altitude DCS model. Further research and development could expand this concept to provide additional information on predicted severity and latency of symptoms and efficacy of available DCS risk reduction procedures.

Along with this modular framework, our approach emphasizes verification, validation and subsequent refinement of the various portions of the model in an iterative fashion throughout the development process. Initial validation will be accomplished by comparing model predictions with experimental DCS outcomes from available databases. Ultrasound imaging data, such as that reported by Olson, Webb and others (117,125,174) will be used to validate the bubble growth portion of the model. For final validation of the entire model, an appropriate number of manned altitude chamber tests will be required. Once the model has been proved in this manner, the prediction equations will be implemented in software on computer systems that can be used by operational personnel.

9. PRELIMINARY DCS MODEL DEVELOPMENT EFFORTS

The preliminary modeling efforts accomplished during the feasibility study were undertaken as an exercise to support the following objectives: 1) familiarization and evaluation of previous approaches to modeling DCS; 2) demonstration that development of an altitude DCS risk assessment model is technically feasible; and 3) identification of the critical areas where additional research is required. Thus

the development and implementation of these computer models provided the practical exercise necessary to tie all phases of this study together. With the conclusion of the feasibility study, this preliminary modeling work becomes even more important, since it provides the foundation from which will evolve the full-scale altitude DCS model and, in turn, the operational altitude decompression computer.

Detailed discussion of both the theoretical development and computer implementation aspects of the modeling effort are presented below. First, however, an overview of the entire model is presented. This overview should allow the non-technical readers to get the flavor of the process without getting bogged down in the technical details. The overview section should also better prepare those readers interested in the more technical aspects of the model for the subsequent discussion of the theory and implementation. This section of the report concludes with a discussion of some of the results obtained with the current model. It is emphasized that this preliminary model was developed for feasibility assessment purposes rather than for absolute accuracy. Verification and documentation of this software is still in progress. The results obtained from this modeling effort must therefore be evaluated accordingly.

9.A. Overview of DCS Model Development

Many decompression models have been created to delineate the boundaries of DCS. These models have been used to produce decompression procedures (decompression tables) for diving. While the diving models provide a basis for developing an altitude model, important issues not addressed in decompression procedures for diving must be taken into consideration for altitude.

One important difference between the requirements for decompression procedures at altitude versus diving is the nature of the mission. A diver usually begins a mission by descending to some water depth. During a diver's descent and bottom time there is no risk of DCS. The risk is during the return to sea level and after surfacing. At that time the mission is over and decompression time can be extended at will. Thus, most diving decompression procedures are based on a binary yes/no output. It is generally accepted that the form of DCS associated with altitude exposure is milder than that associated with diving. In many flight missions an aircrew must deal with other risks in addition to DCS. Because of these differences and depending on the nature of the other risks, an aircrew may accept relatively high levels of DCS risk. Thus, an altitude decompression model must output a 0% to 100% scale of risk rather than a binary response.

The overall objective of all decompression procedures is the prevention or reduction of DCS injury. In the diving field, since Haldane's classic work was published in Boycott et al (1908), there have been decompression guidelines (tables). For over 30 years, the Standard US Navy Air Decompression Tables have been the world standard for DCS prediction and prevention in the diving world. The diver can either look up in a table what needs to be done in decompression, or consult a dive decompression wrist computer that provides decompression information. It is estimated that over 50% of recreational divers now wear dive computers. Similarly, the USAF altitude decompression computer development is aimed at hardware and software to guide exposure to the low-pressure environment.

In contrast to the diving field, the aviation field has never had an organized, standard approach for predicting decompression sickness risk. Currently, in response to an inquiry concerning the DCS risk for a new or unusual altitude exposure, one of three approaches is used. A literature search can be initiated to find a matching study in a "scattergram" of over 50 year of DCS research. This is time-consuming and, often, unsuccessful. If the question is of high priority, a study specific to that issue can be initiated. This is also expensive and time consuming, but will most likely provide the answer. Most often, however, the "best guess" approach on an individual's memory and experience is used. A more rational approach would be to take this wealth from the last 50 years of DCS research and use it as the basis for the development of an altitude decompression model to serve as the operational "standard" for the altitude field.

The current development of such an altitude decompression computer has the following objectives provide:

1. "Cockpit or pressure suit" real-time readout of DCS risk under constantly changing conditions.
2. Capability for evaluating various options in high-altitude mission planning.
3. A tool for improved altitude chamber crew safety and manning control.
4. Desktop DCS risk analysis capability.

The immediate goal of this effort is to define the architecture (or framework) and the algorithms (or software) for the decompression model. The final product will be a software package that will serve as the altitude decompression "standard" and will lead to hardware development to provide the USAF with DCS risk assessment capability for a variety of operational settings.

The preliminary altitude DCS risk assessment model developed during this feasibility study (hereafter referred to as the Model) predicts the probability of getting DCS-based on principles of perfusion-limited inert gas exchange and diffusion-mediated growth of an evolved-gas phase. Actually, the current Model has three different models (or algorithms) that provide three different estimates of risk. These risk prediction algorithms were developed based on a sub-set of the previously recorded experimental DCS data stored in the Armstrong Laboratory's Hypobaric DCS Database (170). The data set used for the current model covers a total of 404 subject exposures on 13 different altitude chamber research protocols. All protocols employed male volunteers who performed minimal to moderate exercise during 6-8 hr exposures to simulated altitudes ranging from 9000 to 30,000 feet. The informed consent of each subject involved in these experiments was obtained in accordance with Air Force Regulation 169-3.

The general flow of the Model is shown in Figure 12. The process begins with the user entering the various mission parameters such as: duration of prebreathe, if any; ascent rate and exposure altitude; mission duration; and percentage of nitrogen in breathing gas. The software then computes two measures of DCS stress that are converted into three estimates of DCS risk or probability of getting DCS during the exposure, based on the three different dose-response equations. At this point we have not addressed issues such as severity and latency of DCS or factors such as exercise, age, and other parameters that may affect individual susceptibility.

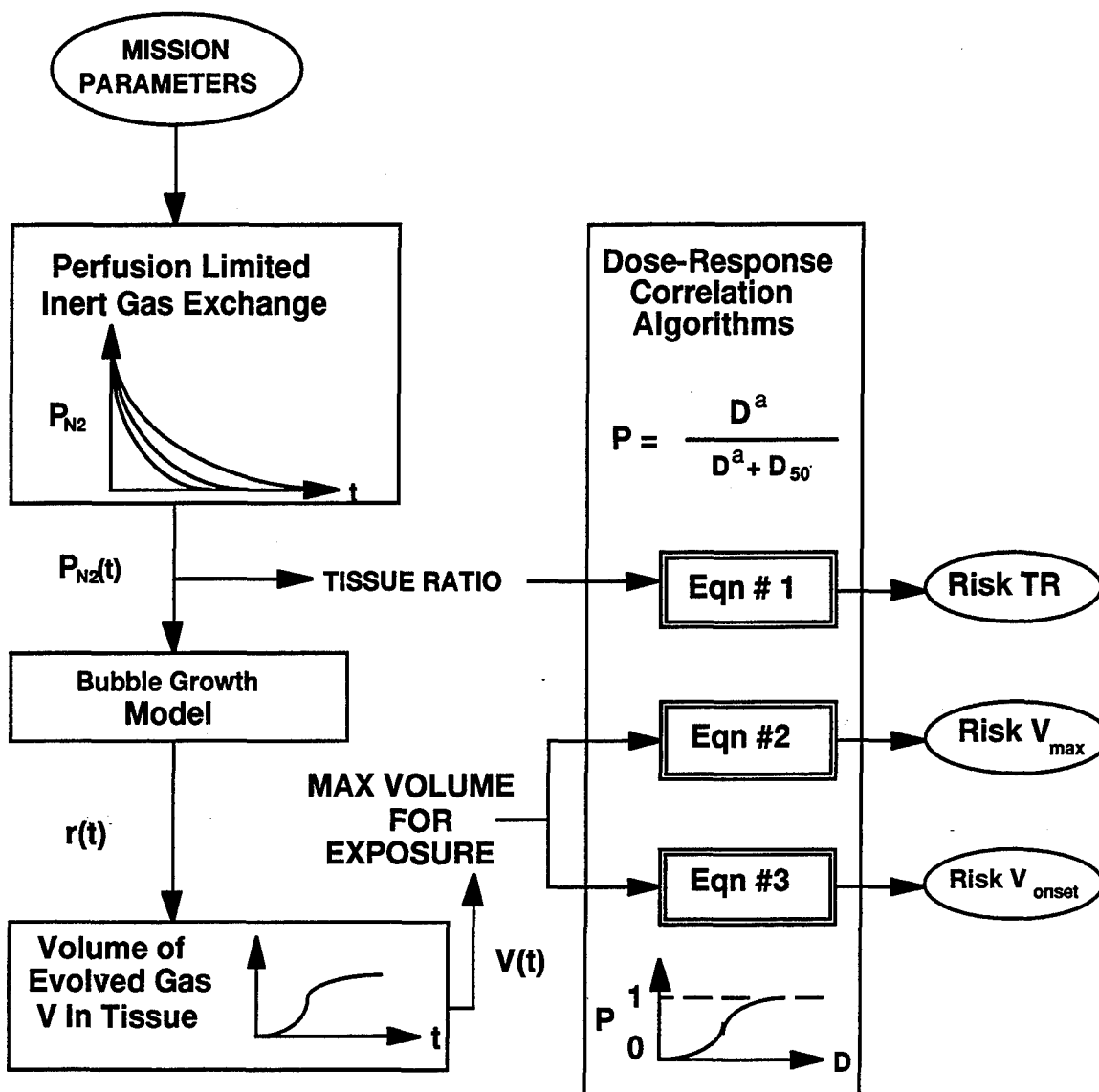


Figure 12. Armstrong Laboratory Altitude DCS Model.

The first measure of DCS stress calculated by the Model is the Haldanian tissue ratio (TR) that gives the ratio of the partial pressure of nitrogen in body tissues ($P_{N_2}t$) just prior to decompression to the ambient environmental pressure at the exposure altitude. This is computed by calculating the $P_{N_2}t$ for each time step based on the standard perfusion-limited exponential gas exchange algorithm. Following the traditional approach used in previous DCS models, we mathematically represent the body as multiple tissue compartments with different nitrogen washout halftimes. Although the model is set up to handle multiple-tissue half times, to date, all of our prediction equations have been based on a 360 minute half-time tissue.

The second measure of DCS stress is based on an estimate of the maximum volume of evolved gas per unit tissue developed during the decompression and is denoted as V_{max} . The use of this parameter, rather than just looking at the size of a single bubble, is based on the assumption that the total gas load imposed on the tissue should be a better indicator of impending DCS. Also, this parameter may be better suited for future comparison with experimental venous gas emboli grades recorded using ultrasound echoimaging and Doppler systems. The volume of evolved gas is computed by calculating the

radius of a hypothetical spherical bubble composed of nitrogen gas for each time step. The bubble growth equations in our model are based largely on the work of Gernhardt, Van Liew and Hastala. The bubble growth dynamics are governed by: 1) conservation of mass between dissolved and gaseous nitrogen; 2) force balances between the ambient pressure outside the bubble, the internal pressure of the gas in the bubble and the forces due to surface tension and tissue elasticity; and 3) expansion of the gas in the bubble due to Boyle's Law effects. The calculated bubble radius is then used to estimate the total volume of evolved gas per unit tissue for each time step based on an assumption of uniform bubble density throughout the tissue. The time-based volume data is then compared to select the maximum volume encountered during the altitude exposure.

The two measures of DCS stress, tissue ratio and maximum volume of evolved gas, serve as inputs to the three correlation equations used to independently predict the probability of getting DCS. These equations describe the well known, sigmoidally shaped dose-response curve given by the Hill equation (73). Each of the equations has a different set of coefficients that were determined by non-linear least squares regression techniques.

In an attempt to incorporate the concept of DCS latency and to partially account for the individual variability of DCS outcome across subjects for a given exposure, we also computed a third estimate of DCS stress. This third parameter may be defined as the volume of evolved gas/unit tissue at the time of DCS onset for each subject and is denoted V_{onset} . For those subjects who did not report any DCS symptoms during the entire exposure, the value of V_{onset} was set equal the maximum volume, V_{max} . The same non-linear least squares regression analysis was then used to determine a new set of correlation equation coefficients based on the V_{onset} data for each of the 404 subject exposures. This represents the third dose-response curve implemented into our model. Although the coefficients for this last equation were determined using the V_{onset} data, it is impossible to know beforehand if or when a given individual will get DCS symptoms. Therefore, when analyzing new exposure profiles with the Model we use the maximum volume of evolved gas, V_{max} , as input to the V_{onset} risk prediction equation.

9.B. Theoretical Development of the Underlying Mathematical Models

This model makes the assumption that stable bubble nuclei exist in tissue. The model then describes the growth of bubble nuclei in a thoroughly perfused tissue. The theory used in the model is described in detail below starting with the definition of perfusion and what perfusion describes mathematically. The theory then derives the equations used to describe the diffusion of gas into a bubble. A relationship is then found for the growth of a bubble as gas diffuses into the bubble. Since gas bubbles can grow not only as a result of diffusion but also as a result of changes in ambient pressure as described by Boyles law, a relationship is found between the growth of a bubble and the change in ambient pressure. Finally, as nitrogen diffuses into a bubble, tissues are depleted of nitrogen. Therefore, an equation is found that accounts for the nitrogen lost from the tissue due to diffusion into gas bubbles.

All equations implemented in the program are marked with an asterisk. The implementation section of this paper discusses how the equations are implemented in the program to predict DCS.

B.1. Perfusion

A mole balance can be done on a tissue to determine the rate at which the gases are entering and leaving a tissue. In this case it is assumed that tissues are perfusion limited in the exchange of gases. The following equation expresses the rate of gas exchange in the case of perfusion.

$$P = P_a + (P_o - P_a) \exp(-kt) \quad \text{Eqn (25)}$$

where

- P = the partial pressure of the gas at time t
 P_a = the partial pressure of the gas entering the tissue
 P_0 = the partial pressure of the gas in the tissue at time $t=0$
 k = the time constant which is related to tissue half time

The perfusion equation can be thought of in terms of a perfectly mixed tank as shown in Figure 13.

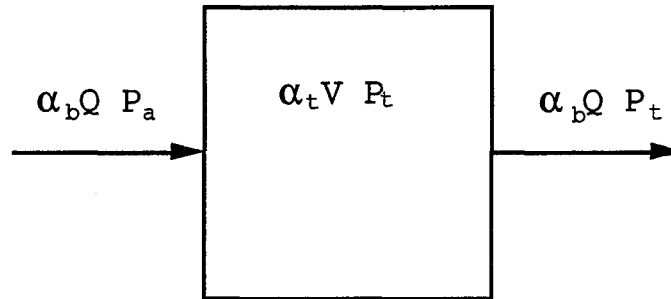


Figure 13. Perfusion

Blood with a certain concentration of nitrogen flows into the tissue, which mixes the blood such that every point in the tissue has the same concentration of nitrogen. Since the volume remains approximately constant the same amount of blood must leave the tissue as enters the tissue. Doing a mass balance on the tissue the following expression is obtained:

$$\frac{\text{Change in volume of } N_2}{\text{time}} = \frac{\text{Volume } N_2 \text{ in}}{\text{time}} - \frac{\text{Volume } N_2 \text{ out}}{\text{time}}$$

or

$$\alpha_t V \frac{dP_t}{dt} = \alpha_b Q (P_a - P_t)$$

Eqn (26)

where

- α_t = solubility of nitrogen in tissue
 α_b = solubility of nitrogen in blood
 Q = flow rate of blood into the tissue
 P_a = partial pressure of nitrogen in the blood
 P_t = partial pressure of nitrogen in the tissue
 t = time
 V = volume of tissue

Let $k = \alpha_b Q / (\alpha_t V)$, then the following first order differential equation is obtained:

$$\frac{dP_t}{dt} = k (P_a - P_t)$$

Eqn (27)

with the initial condition:

$$P_t(0) = P_{t0} \quad \text{Eqn (28)}$$

This can be solved by separating the variables time and tissue pressure P_t and integrating the time and tissue pressure.

$$\int \frac{dP_t}{(P_a - P_t)} = \int k \, dt \quad \text{Eqn (29)}$$

After integrating both sides of the expression above the following expression is obtained:

$$\ln(P_a - P_t) = -k t + C_1 \quad \text{Eqn (30)}$$

where C_1 is an integration constant. The expression is then solved in terms of tissue pressure as:

$$P_t(t) = P_a - C \exp(-kt) \quad \text{Eqn (31)}$$

Using the initial condition the constant C can be determined.

$$P_t(0) = P_a - C \quad \text{Eqn (32)}$$

Substituting in the expressions for k and C the following expression is obtained.

$$P_t(t) = P_a + (P_{t0} - P_a) \exp\left(-\frac{\alpha_b Q t}{\alpha_t V}\right) \quad \text{Eqn (33)}$$

The constant k is usually reported in terms of a tissue half time where the tissue half time is the amount of time required to reach half the final change. This occurs at the time $t=ht$ when the $\exp(k \, ht)$ equals one half as shown below.

$$\exp(-k \, ht) = \frac{1}{2} \quad \text{Eqn (34)}$$

$$k \, ht = \ln(2) \quad \text{Eqn (35)}$$

$$k = \frac{\alpha_b Q}{\alpha_t V} = \frac{0.693}{ht} \quad \text{Eqn (36)}$$

B.2. Bubble Diffusion

It is thought that gas diffuses into and out of a bubble down a diffusion gradient. The flux of gas exchange between a bubble and the tissue is described by a form of Fick's law.

$$J = D \frac{\Delta C}{\Delta X} \quad \text{Eqn (37)}$$

$$J = \frac{D (C_t - C_b)}{h} \quad \text{Eqn (38)}$$

J = Molar flux of gas

D = Diffusivity
 C_t = Concentration of gas in the tissue
 C_b = Concentration of gas in the bubble
 h = Effective thickness of diffusion barrier

Fick's law can be manipulated into a more convenient form using Henry's law. Henry's law states that the concentration of a component in liquid phase is equal to some constant times the partial pressure of that component in the gas phase.

$$k_i P_i = C_i \quad \text{Eqn (39)}$$

The Henry's constant k_i can be replaced by the solubility coefficient α_i . Henry's constant k_i has units of moles per volume liquid per unit pressure whereas the solubility coefficient has units of volume of gas per volume liquid per unit pressure. The ideal gas law can be used to relate the two at the standard conditions of the solubility coefficient as shown below.

$$K_i = \alpha_i (P_s / RT)_{\text{stand}} \quad \text{Eqn (40)}$$

$$C_i = \alpha_i P_i (P_s / RT)_{\text{stand}} \quad \text{Eqn (41)}$$

Since standard conditions are usually taken at one atmosphere the equation becomes:

$$C_i = \alpha_i P_i \left(\frac{1}{RT} \right)_{\text{stand}} \quad \text{Eqn (42)}$$

Care must be taken not to confuse units since the value of the solubility coefficient must be expressed in terms of atmospheres, otherwise a conversion factor is needed.

This derivation is mostly concerned with nitrogen, although the same equations apply to other gases. Figure 14 illustrates the flux of gas into the bubble under perfusion gas transport. By substituting the expression for concentration (42) into equation (38), Fick's law becomes:

$$J = \alpha D (P_t - P_b) P_s / RTh \quad \text{Eqn (43)}$$

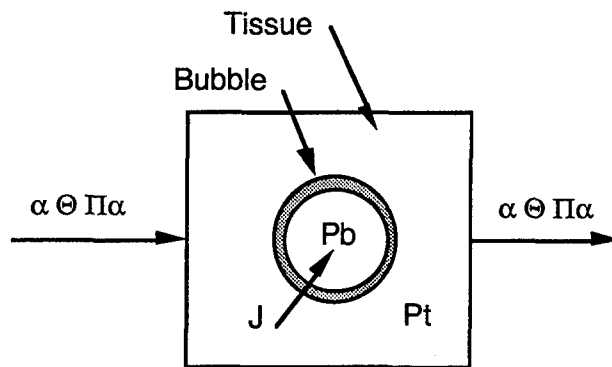


Figure 14. Bubble Diffusion

Where

J = Molar flux of gas
 D = Diffusivity

- h = Effective thickness of diffusion barrier between the bubble and the tissue
 P_b = Partial pressure of gas in the bubble
 P_t = Partial pressure of gas in the tissue
 R = Ideal gas constant
 T = Temperature
 α = Solubility of gas in the tissue

Multiplying the equation for Fick's law in terms of partial pressure by the area of the bubble interface gives the number of moles of gas n per unit time diffusing into the bubble.

$$J A = \frac{\alpha A D (P_t - P_b)}{R T h} = \frac{dn}{dt} \quad \text{Eqn (44)}$$

Assuming nitrogen obeys the ideal gas equation (45) and taking the derivative of the number of moles with respect to time at constant temperature (49), the following expression for the change in number of moles with respect to time is obtained:

$$n_i = \frac{P_i V}{R T} \quad \text{Eqn (45)}$$

$$\frac{dn}{dt} = \frac{P_b}{R T} \frac{dV}{dt} + \frac{V}{R T} \frac{dP_b}{dt} \quad \text{Eqn (46)}$$

Expression (23) can be equated to the flux equation (43). The gas constant and temperature cancel and the flux equation becomes:

$$\frac{\alpha A D (P_t - P_b)}{h} = P_b \frac{dV}{dt} + V \frac{dP_b}{dt} \quad \text{Eqn (47)}$$

In this derivation it is assumed that bubbles are spherical. The surface area and volume of a spherical bubble are:

$$A = 4 \pi r^2 \quad \text{Eqn (48)}$$

$$V = \frac{4 \pi r^3}{3} \quad \text{Eqn (49)}$$

The derivative of the volume of a bubble with respect to time gives the following expression.

$$\frac{dV}{dt} = 4 \pi r^2 \frac{dr}{dt} \quad \text{Eqn (50)}$$

The equations for the volume, area, and rate of change of volume for a spherical bubble were substituted into the flux equation to give the expression below.

$$\frac{\alpha D (P_t - P_b)}{h} = P_b \frac{dr}{dt} + \frac{r}{3} \frac{dP_b}{dt} \quad \text{Eqn (51)}$$

Next, a force balance is done on a bubble. There are four forces that must be balanced. The hydrostatic pressure from the environment acting on the bubble acts as an inward force on the bubble.

The surface tension of the bubble also generates an inward force that tends to shrink the bubble. Also, the tissue elasticity resists bubble growth.

Hydrostatic pressure is the pressure of the environment or the barometric pressure. The pressure due to surface tension is defined as $2\delta/r$, where δ is the surface tension and r is the radius of the bubble. The pressure as a result of tissue elasticity is defined as $4\pi r^3 H/3$, where H is the bulk modulus for the tissue. The pressure of the gas inside the bubble can be divided into two parts, the partial pressure due to nitrogen and the partial pressure due to other tissue gases (oxygen, carbon dioxide, and water). The bubble pressure can be equated to the three opposing pressures due to hydrostatic pressure, surface tension, and tissue elasticity.

$$P_b + P_{tg} = P_h + \frac{2\delta}{r} + \frac{4\pi r^3 H}{3} \quad \text{Eqn (52)}$$

$$4\pi r^3 NH/3 = (N_{(bub/Vtiss)} \cdot \Delta V_{bub} \cdot \Delta P) / (V_{tiss} \cdot \text{tissue})$$

where

- N = # of bubbles/ml in tissue
- P_b = partial pressure of nitrogen in the bubble
- P_{tg} = partial pressure of other gasses (O_2 , H_2O , CO_2) in the bubble
- P_h = hydrostatic pressure of the surrounding environment
- δ = surface tension of the bubble interface
- r = radius of the bubble
- H = bulk modulus of the tissue

The bubble equation (52) is solved for P_b and the derivative taken with respect to time holding P_{tg} and P_h constant to give the following expression.

$$\frac{dP_b}{dt} = \left(-\frac{2\delta}{r^2} + 4\pi r^2 H \right) \frac{dr}{dt} \quad \text{Eqn (53)}$$

This expression can then be substituted into the expression for gas diffusion (51) into the bubble to arrive at the expression below.

$$\frac{\alpha D (P_t - P_b)}{h} = \left(P_b - \frac{2\delta}{3r} + \frac{4\pi r^3 H}{3} \right) \frac{dr}{dt} \quad \text{Eqn (54)}$$

This equation can be solved in terms of the derivative of the radius, or the rate of change in the radius.

$$\frac{dr}{dt} = \frac{\alpha D (P_t - P_b)}{h \left(P_b - \frac{2\delta}{3r} + \frac{4\pi r^3 H}{3} \right)} \quad \text{Eqn (55)*}$$

The above expression expresses the rate of bubble growth as gas diffuses into a bubble, but it does not account for free expansion of a gas as a result of a change in pressure. Boyle's law describes the free expansion of an ideal gas at constant temperature moving from state one to state two.

$$P_1 V_1 = P_2 V_2 \quad \text{Eqn (56)}$$

Boyle's law can be applied to a spherical bubble by substituting equation (26) for the volume of a sphere into equation (56).

$$(P_b + P_{tg})_1 (r^3)_1 = (P_b + P_{tg})_2 (r^3)_2 \quad \text{Eqn (57)}$$

Using equation (34) and equation (29) for the force balance on the bubble, an expression is obtained that can be used to predict the final radius r_2 of a bubble for a change in ambient pressure. Equation (35) requires iterative numerical methods to solve for the value r_2 which satisfies the expression below.

$$f(r_2) = P_{h2} + \frac{2\delta}{r_2} + \frac{4\pi H r_2^3}{3} - (P_b + P_{tg})_1 \left(\frac{r_1}{r_2}\right)^3 = 0 \quad \text{Eqn (58)*}$$

B.3. Gas Exchange between Tissue and Bubbles

The perfusion equation describes the exchange of nitrogen with the environment; however, nitrogen may also leave the tissue phase and move inside the bubble. The nitrogen balance becomes:

$$(\text{moles } N_2 \text{ in tissue})_{t1} = (\text{moles } N_2 \text{ in tissue})_{t2} + (\text{moles } N_2 \text{ diffused into bubbles}) \quad \text{Eqn (59)}$$

$$n_{t1} = n_{t2} + n_{b2} \quad \text{Eqn (60)}$$

The number of moles of nitrogen in the tissue is described by a form of Henry's law similar to equation (42) except concentration is expressed as $C_t = n_t/V_t$.

$$n_t = \left(\frac{1 \text{ atm}}{RT}\right)_{\text{stan}} \alpha_t P_t V_t \quad \text{Eqn (61)}$$

The number of moles of nitrogen that move into the bubbles is described in terms of the ideal gas law by equation (62).

$$n_{b2} = P_b \left(\frac{\Delta V N}{R T}\right) \quad \text{Eqn (62)}$$

$$\Delta V = \frac{4\pi(r_2^3 - r_1^3)}{3} \quad \text{Eqn (63)}$$

where

- P_b = pressure in the bubble
- P_t = pressure in the tissue
- ΔV = change in volume of a single bubble
- N = number of bubbles per volume of tissue
- n_{b2} = change in number of moles of nitrogen in the bubble
- n_t = number of moles of nitrogen in the tissue

Substituting the relationships for n_t and n_b , equations (61) and (62) respectively, into the nitrogen balance, the following expression is obtained for the partial pressure of nitrogen in tissues as a result of gas diffusion into bubbles.

$$(P_{tN_2})_2 = (P_{tN_2})_1 - \frac{N P_b 4 \pi (r_2^3 - r_1^3)}{\alpha_t 3} \quad \text{Eqn(64)*}$$

The value for N, the number of bubbles per ml of tissue, is not known, so a value of 1000 bubbles/ml of tissue was assumed. It is not clear if this is a reasonable guess or not.

B.4. Correlation with database

Once a model for predicting the growth of bubbles in tissue was developed, the incidence of DCS was correlated with a DCS Database. The exact mechanism of DCS is not clearly understood. It is thought that DCS is related to inert gas bubbles developing in tissue. However, different individuals will not all bend under the same circumstances. Furthermore, the same individual may bend one day and may not bend another day under the same exposure. In order to quantify this irregularity, it is necessary to take a statistical approach and report the incidence of DCS for some exposure.

The Hill equation (42) is one method that has been used for relating incidence of DCS to exposure dosage D. The exposure dosage can be any parameter related to decompression sickness, such as tissue ratio or bubble volume.

$$P = \frac{D^n}{D^n + D_{50}^n} \quad \text{Eqn (65)*}$$

When dosage D in equation (65) is equal to zero, the expression returns a probability of zero. When the dosage is infinite the probability is one. Thus, this expression bounds the probability between zero and one. The value D_{50} is the value at which there is a 50 % probability of DCS. The value of D_{50} determines the inflection point of the sigmoidal curve and also determines the steepness of the curve.

This equation can be linearized by inverting the expression and taking the logarithm of both sides of the expression.

$$\frac{1}{P} = 1 + \frac{D_{50}^a}{D^a} \quad \text{Eqn (66)}$$

$$\log\left(\frac{1}{P} - 1\right) = \log(D_{50}^a) - a \log(D) \quad \text{Eqn (67)}$$

Equation (67) is in the linear form $y = mx + b$, where $m = a$, $b = \log(D_{50}^a)$, and $y = \log(1/P - 1)$. Linear least squares of this expression can be used to fit DCS dosage data with incidence of DCS.

Another approach taken was the use of SAS non-linear regression on the VAX computer system. Non-linear regression will find a better correlation of probability, since it minimizes the sum of the errors in probability. The linear regression used in equation (44) minimizes the sum of the error of the $\log(1/P-1)$, which is not exactly what needs to be minimized. Furthermore, it cannot be used for cases in which $P=0$ or $P=1$.

9.C. Development, Evaluation and Documentation of the Preliminary Mathematical Altitude DCS Model and Its Corresponding Computer Implementation

The primary objective of the first year of effort is the development of the first generation Model through continued refinement and expansion of the preliminary model. During the first year,

development, implementation and evaluation of several candidate models in agreement with our "modular and evolutionary" development strategy will be finalized. Also during this year, it is expected that parameter identification will be completed and a detailed analysis/evaluation of the first generation Model using available *in vitro* and *in vivo* data will be initiated. The specific objectives for the first year require some additional background and are detailed below.

C.1. Mathematical Model Structure

Notations:

t_{hn}	: half time for nth tissue compartment (min)
r	: radius of the bubble (cm)
N_b	: number of bubbles/ml tissue
P_{N2t}	: partial pressure of N_2 in the tissue (mm Hg)
P_{N2b}	: partial pressure of N_2 in the bubble (mm Hg)
P_h	: hydrostatic pressure (mm Hg)
P_{mgb}	: partial pressure of $O_2+H_2O+CO_2$ in the bubble (mm Hg)
P_{amb}	: ambient pressure of N_2 (mm Hg)
a	: solubility
D	: diffusivity (cm^2/min)
h	: diffusion barrier thickness (cm)
d	: surface tension (dyne/cm)
F_{N2IN}	: inspired fraction of N_2
H	: bulk modulus for the tissue ((dyne/cm ²) (ml tissue/ml gas))
P_s	: standard pressure (mm Hg)
k	: time constant related to tissue half time
TR	: tissue ratio
V_b	: volume of the bubble (cm ³)
t	: time (min)
c_f	: conversion factor = 7.51×10^{-4} (mm Hg)/(dyne/cm ²)

Any relatively complete mathematical DCS model should account for at least the following phenomena: a) perfusion-limited inert gas exchange between blood and tissues (Haldanian model), b) the diffusion of inert gas across the tissue/bubble interface (Ficks' law), c) gas solubility, d) diffusivity, e) surface tension, f) tissue elasticity effects, and g) free expansion of a bubble due to decompression in accordance with Boyle's law. The preliminary model described in the feasibility study attempted to incorporate all of these factors. Previous investigators derived bubble growth equations (a collection of equations that describe the phenomena) using different assumptions, and hence obtained different models. Most papers have agreed on the perfusion equation:

$$P_{N_2t}(t) = P_{amb}(t) + (P_{N_2t}(0) - P_{amb}(t)) e^{-0.693t / t_{hn}} \quad \text{Eqn (68)}$$

and pressure force balance equation on a bubble.

$$P_{N_2b} + P_{mgb} = P_h + \frac{2d}{r} + \frac{4\pi}{3} r^3 H \quad \text{Eqn (69)}$$

However, opinions vary on deriving bubble radius equations. The three models used in the feasibility study include Van Liew's (153):

$$\frac{dr}{dt} = a D \left(1 - \frac{P_{N_{2t}}}{P_{N_{2b}}} \right) \left(\sqrt{\frac{k}{D}} + \frac{1}{r} \right) \quad \text{Eqn (70)}$$

and Gernhardt's (54).

$$\frac{dr}{dt} = \frac{a D (P_{N_{2t}} - P_{N_{2b}})}{h \left(P_{N_{2b}} - \frac{2d}{r} + \frac{4\pi}{3} r^3 H \right)} \quad \text{Eqn (71)}$$

In the third model (131,132), instead of assuming the diffusion from a planar surface as in Gernhardt's model, the equation was derived by using spherical coordinates.

$$\frac{dr}{dt} = \frac{a D (P_{N_{2t}} - P_{N_{2b}})}{h \left(P_{N_{2b}} - \frac{2d}{3(r+h)} + \frac{4\pi}{3} r^3 \frac{r}{r+h} H \right)} \quad \text{Eqn (72)}$$

This last approach is the one currently implemented in the preliminary model developed during the feasibility study. The values used for the parameters D , h , a , H , N_b and d in these equations need to be reviewed. Some of the parameters are not well defined in the literature and the values used in the preliminary modeling work are questionable. For example, the number of bubbles per milliliter tissue, N_b , is an unknown value, and a variable diffusion barrier, h , should be considered, instead of a constant as in Gernhardt's equation, to account for observed differences in bubble growth rates. In addition to the parameter identification, a more feasible bubble radius equation needs to be selected.

C.2. Parameter Identification Techniques

Parameter identification problems such as these are optimization problems, i.e., problems of minimizing an error criterion $J(s,z;q)$ over parameters q in Q , subject to s satisfying the DCS model as compared to experimental data z (from database). Here Q denotes the admissible parameter set, i.e., the collection of parameters that satisfy all (physiology) constraints, and q is the vector of parameters that need to be identified, $q=(D, h, a, H, N_b, d)$.

There are two techniques that will be used in parameter identification. The first approach is the one most commonly used in minimization: least square analysis. This method seeks to find the optimal parameter vector q that minimizes

$$J(s,z;q) = \sum_i |s_i - z_i|^2 \quad \text{Eqn (73)}$$

where $\{s_i\}$ can be the probability of DCS which is a function of parameter vector q , $f(D_i;q)$, for a given physical stress or dose D_i , e.g. tissue ratio or bubble volume, and $\{z_i\}$ is the probability of DCS determined from experimental outcomes in the database. Alternatively, the identification problem can be stated as seeking the optimal parameter vector q which maximizes the likelihood function (55)

$$J(\hat{P};q) = \text{Ln} \left(\prod_i \hat{P}_i^{x_i} (1 - \hat{P}_i)^{(1-x_i)} \right) \quad \text{Eqn (74)}$$

occurs), \hat{P}_i is the probability of DCS given by DCS mathematical model for a given dose D_i . The probability \hat{P}_i is a function of parameter q . The existence and uniqueness of the solution to the optimization problems will be studied.

The reasons for using the above two techniques are as follows. The least squares approach has been used successfully in many applications. The maximum likelihood approach has also been used previously and is especially well suited for optimization problems involving probabilistic outcomes. When certain conditions are satisfied, the two methods give essentially identical results. Since these conditions, for example, the probability distribution of the variable, are not easy to check, both methods will be applied in the model development work. Comparison of the results is expected to determine the more favorable method. In addition, during the out-years of this program, alternative techniques such as logistic regression and discriminant analysis will also be explored.

The mathematical model will be implemented on computers in FORTRAN. Calculations for solving gas exchange and bubble-growth equations are relatively simple. The size of the time step used in solving these equations will be studied to achieve minimum computing time and satisfactory accuracy. In solving optimization (minimization or maximization) problems, one of the computational methods (Gauss-Newton method, Marquardt method, steepest-descent method, etc.) will be used depending on the efficiency and accuracy of the method.

9.D. Computer Implementation of the Model

This investigation approached modeling DCS by first developing a computer model to predict physical parameters related to DCS such as tissue ratio, bubble radius and bubble volume. These physical parameters thought to be related to DCS were then correlated with a database of experimental data on decompression sickness. Once a link between the decompression sickness and the model-predicted physical parameters was established, the model could predict a likelihood of DCS for a variety of flight profiles. Figure 15 is a flow diagram of the approach taken in modeling DCS.

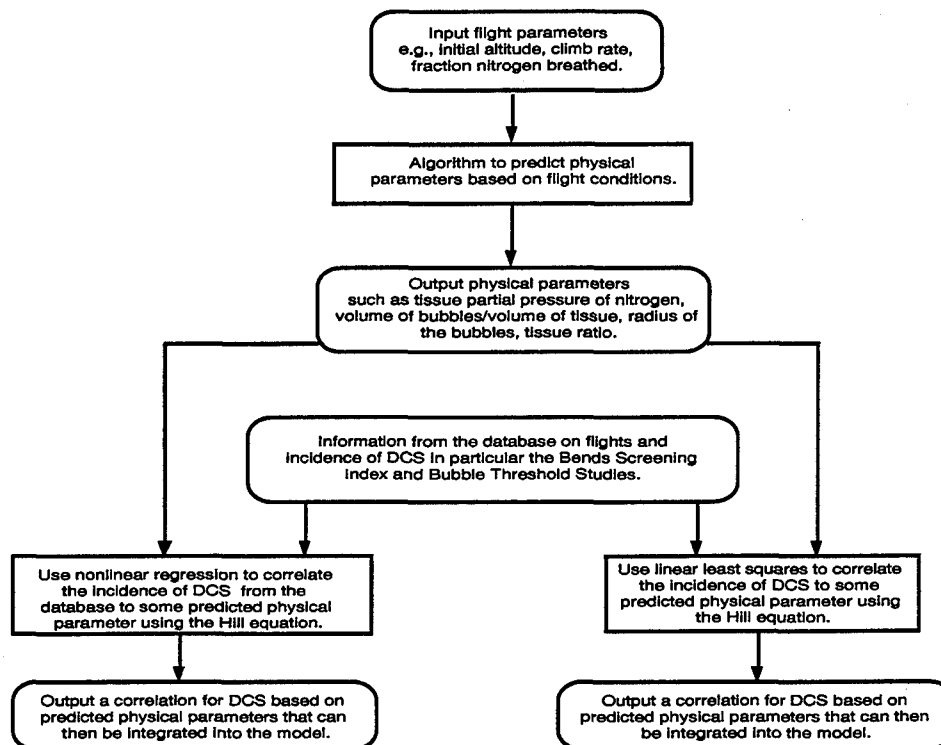


Figure 15. Implementation.

D.1. Program

The program begins by entering the data for a flight profile into the program. The program calculates and outputs a value for physical parameters such as bubble volume, bubble radius, tissue ratio, and partial pressure of nitrogen in tissue over time. The values of these physical parameters are used in a correlation based on the data base to predict the likelihood of DCS.

Lab View version 2.0.6 for the Macintosh, was used in solving the system of equations discussed in the theory. Lab View is a graphical-based programming system designed by National Instruments. Though Lab View is easy to use, more powerful numerical methods are available on the networks, such as VAX network, which could be implemented in the program. This would decrease the amount of programming necessary. Furthermore, the decompression sickness database and SAS (Statistical Analysis System) is on the VAX network. Thus, the entire DCS problem could be worked without having to import files between different systems such as Macintosh and the VAX.

The program begins by calculating an array of time points based on the duration of the stage and the time increment desired. The program calculates the ambient pressure at each point based on interpolation of an Air Force Altitude Pressure Table. Also, the partial pressure of nitrogen fed by the Air Force regulator is calculated. These variables are then fed to a subroutine called "PMb," which then calculates the partial pressure of nitrogen in the tissue, bubble radius, and bubble volume.

The subroutine "PMb" first calculates a new tissue partial pressure at the next time step using the perfusion model. The model then calculates a new bubble radius in subroutine "Rad" based on a Boyle's law expansion $P_1V_1 = P_2V_2$. The value obtained for the radius is passed to subroutine "Dr," which calculates the change in radius of the bubble due to gas diffusion into a bubble, as described by equation

(55) in the theory section. Subroutine "Dr" uses an Euler's method integration of equation (55) defining the change in radius with diffusion. The effect of diffusion on tissue partial pressure is calculated in subroutine "Pt" based on equation (64). These steps are then repeated for each time step. Shown below in Figure 16 is a block diagram of the program with the equations solved at each subsequent step.

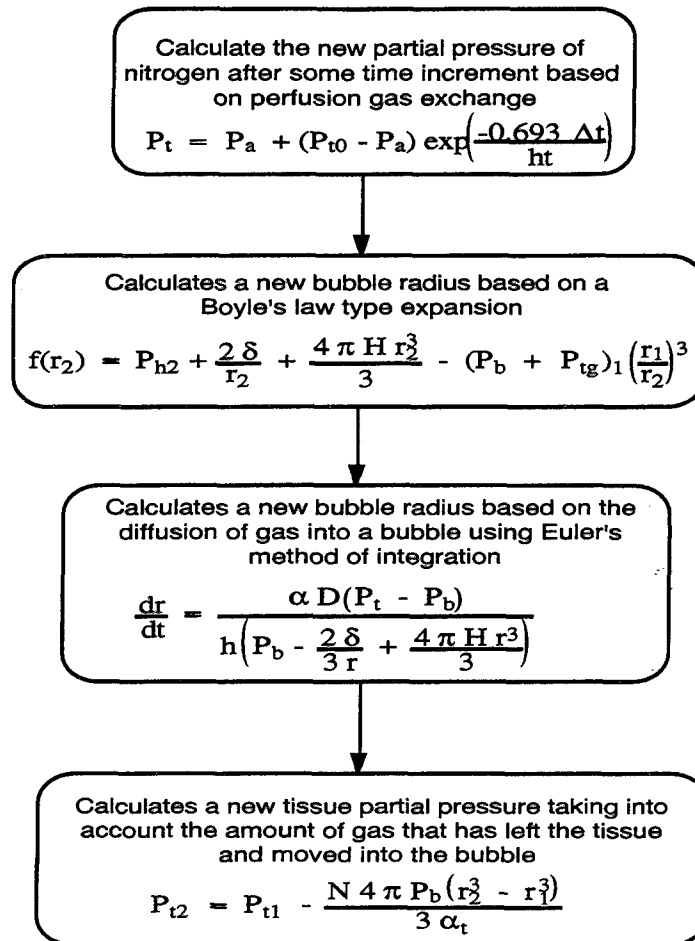


Figure 16. Program Flow Diagram.

The Program, in addition to the main algorithms shown in Figure 15, has subroutines that support the program. An algorithm passes data on altitude and barometric pressure called "Press vs. Alt array," which is interpolated by subroutine "P vs. A". Another subroutine "Reg" simulates an Air Force regulator by passing data on the fraction of nitrogen versus altitude-based curve fit of the data obtained from Aviation Medicine. The regulator can be turned off and the fraction of nitrogen can be entered at the control panel.

The values used for the constants in the model are, initial radius $R_0 = 3.0E-04$ cm, surface tension, $\delta = 30$ dyne/cm, diffusivity, $D = 2.0E-08$ cm²/s, diffusion barrier thickness, $h = 3.0E-04$ cm, and nitrogen solubility in tissue, $\alpha_t = 0.0125$.

D.2. Integration with Database

Once the program for predicting the physical parameters such as tissue partial pressure, tissue ratio, bubble radius, and bubble volume had been developed, various exposures from the database were run. The physical parameters of the output were then correlated with the incidence of DCS reported in the database for corresponding exposure.

Several methods were investigated for correlating the physical parameters from the model with incidence of DCS. The first method used was a linear least squares correlation between incidence of DCS indicated in the database and the maximum bubble volume developed for a given exposure.

Another approach investigated was use of SAS nonlinear regression of each individual's decompression data. This approach looked at correlating each individual's DCS with the bubble volume. This approach was statistically better, since exposures with no incidence could be used in correlating DCS. The linearized form of the Hill equation cannot be used for exposures with no incidence of DCS.

Twelve exposure studies with decompression ranging from 9,000 to 30,000 feet with various gas mixtures were used to correlate the model with DCS incidence data. The model output the tissue ratio, bubble volume and partial pressure of nitrogen over the time for each exposure.

Once a correlation for the incidence of DCS was found, a subroutine was created which predicted the probability of DCS for some exposure. After all the physical parameters are calculated for a flight profile, subroutine "P_{tr}" and "P_v" calculate the probability of DCS from physical parameters calculated in the model.

10. RESEARCH NEEDS

The preliminary mathematical model was based on several assumptions: a) the existence of stationary gas bubbles in tissue, b) that the body is one uniform tissue, i.e., that all tissues have the same concentration of nitrogen, and c) constant temperature. In addition to those assumptions, the model does not account for factors such as gas expansion driven by water vapor pressure at low absolute pressures, variations in physiological parameters, and individual differences in the ability to withstand tissue supersaturation and gas emboli. Integration of these factors into the mathematical model will be attempted using the data generated by the proposed parallel *in vitro* and *in vivo* research. Once the mathematical model is modified, parameter identification will be repeated to optimize the enhanced model.

Finally, the 360 min. tissue half-time is most commonly used in altitude decompression modeling. This is based on empirically derived results for a few specific types of exposures. Since the Model will serve many flight scenarios, it may be necessary to incorporate a number of tissue half-times to cover a large spectrum of exposures. In addition, we will attempt to relate bubble growth equations to the tissue ratio (TR) using available VGE data recorded in the AL DCS Research Database.

10.A. Verification of the Basic Physical and Physiological Concepts upon which this Preliminary Model Is Built through *in Vitro* Studies

The purpose of the proposed *in vitro* experiments is: 1) to relate bubble dynamics to DCS symptomatology, 2) to help develop the concepts used in constructing the Model, 3) to verify these concepts in the laboratory, and 4) to "troubleshoot" the Model during development. It is not possible to verify all basic principles in decompression modeling. The approach, therefore, is to identify those that have the greatest impact on the Model and also lend themselves to investigation using *in vitro* experimentation. The following first year research effort dealing with such basic concepts will be investigated.

A.1. Bubble Growth

The DCS models described in the literature includes equations describing bubble growth. The detailed derivation of the bubble growth equations is shown in Appendix A. However, in order to use these equations, it is necessary to know the appropriate size range. To determine this range, this laboratory has developed *in vivo* bubble-sizing techniques using echo imaging systems. One of these techniques uses buoyancy or flotation rates to determine size (117, 118). *In vitro* sizing techniques have also been used and include microscopic range, small gauge wires, and microspheres. Although preliminary research suggests that the bubbles involved in DCS are, at least during the early stages, in the microscopic range, further confirmation of these findings is required.

With bubble size in the microscopic range, optical magnification recording systems are required to follow bubble formation and growth. In particular, equipment needed includes fiber optic light sources, microscopes with adjustable magnification and focal length, as well as equipment to record the images (camcorder) and process them (computer-based image analysis software).

The process of generating bubbles of known size is difficult in itself. A small altitude chamber is necessary to simulate the exposures. However, altitude alone is not enough to produce bubbles, even though bubble nuclei may be present. High-frequency sonic or ultrasonic shock waves can produce bubbles in the appropriate size range. Development of the bubble generating device that mimics *in vivo* bubble formation mechanisms is more desirable. In addition, work is also in progress on developing other bubble-generating methods, including the use of surface active materials and fat-water interfaces.

It is well known that both diffusion and perfusion play vital roles in any DCS model because these processes bring nitrogen in the vicinity of a bubble. But preliminary work shows that convection currents are also important. Quiescent fluid can have large concentration gradients that will change very slowly as long as the fluid is undisturbed. Therefore, a method that can simulate such motion processes in the laboratory will be developed. The ability to circulate nitrogen-laden or depleted fluid in the region of growing bubbles may also be required. Furthermore, the relationship between bubble growth and degree of tissue supersaturation or N_2 tissue ratio (TR) will be studied. Although it is generally believed that the initial bubble growth phase is a rapid event (on the order of a few seconds), preliminary experiments have shown that as the TR is lowered, bubble growth slows dramatically. Since prebreathing lowers the TR, an aviator who has prebreathed and is on 100% O_2 can be at a relatively high altitude, yet may have a low TR, resulting in bubble growth much slower than expected. In addition, the current model assumes that the only gas participating in the diffusion process into or out of the bubble is N_2 . However, the effect of the other gases, e.g., O_2 , CO_2 , water vapor, is not well understood, especially at higher altitudes. This effort will employ techniques similar to those described above. Preliminary work has indicated that such *in vitro* experiments are possible.

During the first year, the bubble growth equations described earlier were experimentally validated using the above techniques and equipment. In addition, in combination with the ongoing *in vivo* investigation, the relationships between bubble formation, bubble growth and DCS symptomatology will be explored in an attempt to mathematically described the dynamics of the relationships.

A.2. Factors Affecting Bubble Formation

The risk of developing altitude DCS is directly related to the risk of developing bubbles in the body. The exact mechanisms involved in bubble formation in the body have been elusive. Bubble formation is an obvious, yet very difficult factor to include in the Model development.

It has been postulated for a long time that some kind of bubble nuclei always exists in the body, even at ground level (65,84,85). It is not clear exactly what these nuclei are. Some think of them as extremely small stable microbubbles, while other believe they are concentration of inert gas that form a

"potential" for bubble formation. For several years, this laboratory has attempted to clarify the relationship between altitude exposure and bubble formation. It is clear from this work that the transformation is not a simple Boyle's Law phenomenon. Nucleation sites and conditions supporting this transformation are poorly understood. There are several discrete stages in this process. Tribonucleation, cavitation, and many other phenomena modulated by factors such as altitude and surface tension are involved in the bubble production. Nevertheless, the potential for these nuclei to grow into symptomatic bubbles with exposures to altitude is of prime importance to the Model development. This research will not attempt to define bubble nuclei *per se*. Instead, it will focus on three factors thought to influence bubble formation: altitude, stable microbubbles, and surface tension.

Preliminary experiments in this laboratory have shown that some microbubbles (not what most investigators would refer to as bubble nuclei) less than 10 microns in diameter are stable and difficult to grow with altitude exposure. Other bubbles grow spontaneously to over 100 microns when exposed to altitude. The number and size of stable microbubbles generated by low-energy sonic shock waves at various altitudes in fluid in which the surface tension is adjusted to that of plasma will be defined. The number and size of these stable microbubbles in the formation and growth of symptomatic bubbles will be examined.

Surface tension is believed to be of major importance to *in vivo* bubble dynamics. Walder (162) found that subjects who were more prone to develop DCS were the ones with lower plasma surface tension. La Place's Law dictates that the force on a bubble is directly proportional to the surface tension, and inversely proportional to the diameter. If this were true, microbubbles could not exist. Apparently, surface tension is only one of the factors involved. In general, high surface tension will hinder bubble formation and low surface tension will allow bubbles to form. The surface tension can be reduced by a number of surfactants in the body. The most obvious location is the lungs, which have high concentrations of surfactant. In the joints, lubrication fluid can act as a surfactant. The effect of surface tension on bubble formation and growth will be studied *in vitro*, exposing the fluid to altitude after surface tension has been set to desired levels by the addition of surface-active ingredients. We propose to mathematically describe the effects of altitude and surface tension on bubble formation.

A.3. DCS Latency Period

It is well known that there is a latency period associated with DCS symptoms after arrival at altitude (124). This latency period, which may be as long as several hours, may make short missions or altitude chambers run relatively safe. One of the required outputs of the Model is the latency period for a given altitude exposure. Thus, a theoretical basis for the latency period calculation is needed. The causes of this latency period are not well understood. Latency is thought to be related to both bubble dynamics and physiological mechanisms. Van Liew (147) has suggested that latency is due to five mechanisms:

1. The time it takes bubbles to grow to a symptomatic size.
2. A continuous process of bubble formation under conditions that permit further growth.
3. The time it takes for dissolved N_2 to reach the site where it can be used by a growing bubble.
4. The time it takes bubbles to migrate from a site where they are silent to a site where they produce symptoms.
5. The time it takes DCS bubble precursors to migrate into a nitrogen-rich area where they can develop.

In vitro studies have shown that the size of microbubbles in water depends upon both the altitude at which they form and the time given to form (116). It has been suggested that latency is the result of the

time required for evolved gas volume (number and size of bubbles) to become sufficiently large enough to engender symptoms. Bubbles of the size found circulating in subjects with DCS will be observed microscopically and the growth times compared with the known latency periods.

Secondly, the proposed mechanism in which the shell of tissue surrounding a bubble into which nitrogen is being carried by perfusion, and out of which nitrogen is leaving by diffusion into the bubble, will be investigated and related to the latency. Van Liew (147) has derived a bubble-growth equation using this shell concept. An estimate of the thickness of this shell may be possible by noting how close two bubbles must be before they interfere with each other's growth rate. This shell thickness, in turn, may be related to the latency.

10.B. Elucidation and Quantification through in Vivo Human Studies of Specific Physiological Concepts Currently Ill-defined but Necessary for this Model Development

B.1. Exercise at Altitude

The effect of varying levels and types of exercise at altitude on incidence and latency of DCS and intravascular gas emboli will be quantified. Exercise will be studied in terms of energy expenditure and mechanical effects. A current AL protocol titled "Effect of Exercise on Altitude Decompression Sickness," will be modified to reflect the need to integrate exercise as a predisposing factor into the Model. This ongoing study has the current objective to quantify the effects of isometric and isotonic exercise both using arms and legs on the development of altitude decompression sickness. The data from this study will be the basis for the mathematical bias imposed on the Model. Much of the preliminary work of the protocol has been completed (47,176). A stack-weight machine was designed and instrumented to allow measurement of isometric or isotonic exercise performed with the arms or legs. An advanced metabolic measurement system capable of breath-by-breath analysis of low-level oxygen consumption data was used during subject training. Criterion tests were administered for maximal oxygen consumption (VO_2 max) and maximal voluntary contraction. Procedures were developed for equating and individualizing the isometric and isotonic work by means of oxygen consumption (% of VO_2 max). The altitude chamber and facilities used for this study are the same ones that have been used for human decompression sickness studies over the past 3 decades at AL. They have all physiologic and safety monitoring equipment already installed, including Doppler, 2D echocardiography, ECG, and communications pass through, as well as video recording capability. A hyperbaric treatment is immediately adjacent to the chamber and a treatment team is on hand during each exposure.

Both military and/or civilian subjects participate in this study. Subjects are tested and trained at ground level to perform a specific amount of isometric and isotonic exercise using the arms or legs. They then undergo up to three resting exposures to identify the altitude to be used for the remaining exposures, starting with 29,000 feet. Four exposures at this selected altitude follow. The effects of the two types of exercise, isometric and isotonic, and the effects of upper body and lower body exercise are measured in terms of incidence and time to onset of intravascular bubbles and DCS. The endpoint of DCS is considered as met with Grade 2 (mild-to-moderate constant pain) or any neurologic or other serious manifestation of DCS. Subjects who do not develop DCS at altitude will remain in the chamber for four hours. The independent variables in this investigation are the type of exercise and body region. The dependent variables are the incidence and time of onset of intravascular gas emboli and limb pain. The sample size of 24 was chosen based on the estimation of DCS incidence and onset times from previous work. Using calculations for a binomial distribution, and a one-tailed test of significance, 24 subjects give a power of .95 at the .05 level. With a continuous distribution, the sample size gives a good chance of identifying a small difference between rest and exercise, and a fairly large difference between exercise types. It is the purpose of this study to continue ongoing research of a controlled series of altitude exposures in which the degree of exercise, as well as the type of exercise, is well defined. The method described earlier for documenting DCS incidence and latency and quantifying *in vivo* intravascular gas

emboli will be used. The results are stored in the AL DCS Database and the data will be used to develop a method for biasing the Model for exercise.

B.2. DCS and intravascular gas emboli above 30,000 ft and the impact of PPB on N₂ elimination at these high altitudes

In the event of a sudden loss of aircraft cabin pressure at high altitudes, hypoxia (decreased O₂ in the inspired air) is the primary acute threat. The use of positive pressure breathing (PPB) for protection against hypoxia at high altitudes is well established. During 100% O₂ breathing at altitudes above 34,000 ft, the partial pressure of alveolar O₂ (PO₂) in the lungs starts to fall below normal sea-level pressure. At altitude greater than 40,000 ft, the PO₂ becomes inadequate to maintain homeostasis unless O₂ is delivered under positive pressure. PPB requirements have been established for altitudes above 34,000 ft and consist of a range of acceptable airway pressure at any given altitude (2). These requirements have been designed to maintain PO₂ levels of at least 60 mmHg for routine flight, and not less than 30 mmHg following emergency rapid decompression.

Excess nitrogen is removed from the tissue in two ways. Bubbles grow by inward diffusion of N₂ from tissues. With increasing altitude, O₂, CO₂, and vapor pressure remain constant whereas N₂ partial pressure is reduced. This enhances the tissue supersaturation and can lead to accelerated bubble growth (beyond the Boyle's Law effect) as the N₂ gradient between tissue and bubble is increased (155). The other path of process of N₂ from the tissue is by diffusion into the blood and transport by the circulatory system to the lungs for elimination. This process is facilitated by breathing 100% O₂ prior to ascent to altitude and during the exposure. Interventions that increase the rate of N₂ elimination from the body may decrease DCS risk. These interventions include exercise, head-out immersion, supine body position, raised ambient temperature, negative pressure breathing and vasodilator drugs (7). The physiological mechanisms by which these interventions accelerate N₂ elimination are increases in cardiac output and tissue perfusion.

Positive pressure breathing has been shown to decrease Xenon 133 (Xe₁₃₃) elimination from adipose tissue (7) and, thus, may impair elimination of other inert gases as well. Its effect on N₂ elimination has never been investigated. However, PPB is known to increase peripheral pooling in the circulation and reduce cardiac output, thus, potentially reducing N₂ elimination and increasing DCS risk.

At altitude, the total (cumulative) N₂ elimination is rapid during the first 10 min of 100% O₂ breathing then continues at a slower rate (107). That is, the slope defining the relationship between time at altitude and N₂ elimination will change at altitude requiring PPB, and N₂ elimination will be at a slower rate with PPB above 30,000 ft than without PPB below 30,000 ft. Thus, at the higher altitudes, the risk of DCS may be higher and the PPB effect may need to be incorporated into the Model.

In addition, in order to remove hypoxia as a variable, we will determine whether O₂ delivery to the brain is sufficient by continuously monitoring transcranial arterial oxygen saturation (SaO₂). Little physiological data on O₂ levels exist for human exposures to these high altitudes involving PPB.

The independent variables in this investigation are exposure altitude, exposure duration, and use of positive pressure breathing for altitude. The dependent variables are the incidence and time of onset of DCS and intravascular gas emboli as detected by precordial echo imaging/Doppler.

Whole body nitrogen elimination measurements have limited value in DCS research because they are a blend of off-gassing nitrogen from all anatomical areas and, therefore, cannot be correlated with specific symptomatology. For example, during exercise, N₂ elimination from the vast muscle tissues is several orders of magnitude greater than other tissues and can overwhelm the measurements. Such readings will tell us little about joint tissues, neurological tissues, etc., that are of great importance to the clinical condition. On the other hand, in order to compare N₂ elimination with and without PPB, a system

for quantifying N_2 elimination from the body is useful and will be developed in this program. This will include techniques for sampling and analyzing N_2 in the inspired and exhaled gas throughout the experiment.

11. AREAS REQUIRING FURTHER RESEARCH

The following areas require further research:

- A. Gas exchange issues
- B. Evolved Gas Dynamics and Phase Separation Issues
- C. Methods of estimating DCS stress or "dose"
- D. Methods of calculating physiological response to DCS stress
- E. Methods for incorporation of pre-disposing factors
- F. Consolidation of existing experimental data

11.A. Research Requirements in Support of the Model Development

The feasibility study pointed out several major deficits in our knowledge base of information required for successful development of the Model. This lack of information exists both in basic knowledge and in the AL DCS Database. Although other important deficits exist, four areas are especially important to the Model development and are, therefore, included in this proposed research program. These areas include: a) processes governing bubble formation and growth, b) DCS above 30,000 ft and the effect of positive pressure breathing on denitrogenation, c) exercise at altitude as a predisposing factor, and d) the effects of repetitive altitude exposures on DCS risk.

A.1. Process governing bubble formation and growth

The vast majority of basic information on bubble dynamics is derived from the hyperbaric field. The formation and behavior of gas bubbles in the low pressure environment is different than in the high pressure environment and is not as well documented. Although many diving decompression models rely solely on Haldanian theory, it is clear from the feasibility study that bubble dynamics must be incorporated into the altitude Model. Therefore, the basic assumptions on bubble formation and growth will be evaluated with *in vitro* experimentation. The size DCS bubbles grow to, bubble rates altitude, bubble formation requirements, the effect of surface active substances, and other questions are pertinent to the Model development.

A.2. DCS above 30,000 feet and the effect of PPB on denitrogenation

Essentially no reliable DCS database exists today for DCS and bubble formation above 30,000 ft. Such empirical data are crucial to the development of the model. Without it, the applicability of the model would be limited to below 30,000 ft. Thus, one of the major first-year goals is to expand the DCS Database to the higher altitudes.

In addition to the lack of databases for the higher altitudes, basic denitrogenation information is not available. For the lower altitudes, the relationship between altitude and whole body N_2 elimination has been documented and appears to be linear after the first 10 minutes (108). At higher altitudes, and especially at the altitudes requiring PPB, this relationship is undefined. The slope defining the relationship between altitude and N_2 elimination may change and N_2 elimination may be lower with PPB above 30,000 ft than without PPB below 30,000 ft. Thus, at the higher altitudes, the risk of DCS may be higher. The basic algorithms of the Model may require modifications with increasing altitudes.

A.3. Exercise at altitude as a predisposing factor

It is well established that exercise affects a person's altitude DCS tolerance (51). Gray (58), for example, showed in 1943 that a person's DCS threshold can be lowered by as much as 5000 ft by exercising at altitude, and that the relative importance of DCS as the cause of forced descent from altitude increases with exercise (57,58). Unfortunately, very little quantitative data are available in the literature (33,94,96,156). Therefore, the degree of threshold change cannot be correlated with the degree of exercise. Also lacking is any attempt to correlate the type of exercise with DCS outcomes. This is complicated by the considerable controversy regarding the comparison of isometric and kinetic (dynamic) exercise in terms of energy usage and muscle mechanics (37,109,133,179). Consequently, one can only speculate on the relative role of tribonucleation and metabolite accumulation in the etiology of limb bends. Does the shearing action of overlapping muscle sheaths during active exercise produce *de novo* bubble nuclei in the tissue and thereby predispose one to bends? It is becoming more important from an operational viewpoint to define and to quantify the relative contributions of various types of exercise to DCS parameters. Likewise, it is necessary to determine the effects of various degrees and types of exercise on VGE and DCS in order to integrate an exercise bias into the Model.

A.4. The effects of repetitive altitude exposures on DCS risk

Multiple altitude exposures with short ground level intervals are common in some operational settings. It is generally thought that such repetitive exposures will result in higher incidence of DCS than single exposures. The repetitive aspect of DCS was reviewed recently by Furr and Sears (53). This paper found that the literature was confounding; studies supported an increase, decrease, and no change in susceptibility to DCS associated with repetitive exposures. Furthermore, no usable database for repetitive altitude exposures exists. Yet the Model must be capable of predicting DCS risk for multiple flights.

The nitrogen in all tissues at ground level is at an equilibrium (saturated). If ambient pressure is reduced, the tissues are said to be supersaturated, i.e., the PN_2 in the tissues is higher than ambient. However, during the altitude exposure, the tissue denitrogenate at an exponential rate. Upon returning to ground level, the tissues renitrogenate at a similar rate. Since it may take as long as 24 hours for the tissues to return to the ground level equilibrium after a flight, if a second flight is initiated within that time, denitrogenation will start at a lower level, and supersaturation will be less (assuming similar altitude exposures). From a strictly gas diffusion/perfusion standpoint, repetitive flights should result in a reduced DCS risk. However, supersaturation can result in bubble formation and growth in parallel with the denitrogenation. Since bubbles are thought to have a longevity in certain tissues lasting hours to days, each repetitive exposure would lead to bubble growth and, thus to increased DCS risk. This picture is complicated further by the fact that rarely are a series of repetitive flights exactly the same. Variables such as altitude, prebreathing time, rates of ascent and descent, time at altitude, ground level intervals and number of flights must all be taken into consideration by the Model for accurate risk assessment.

An investigation is proposed for the out-years of the project that will provide the Model with both the theoretical basis and the empirical database necessary for its use in repetitive flight situations. *In vitro* studies will attempt to define the bubble formation and growth algorithms. Human research using echo imaging and DCS symptoms as end points during representative repetitive series of flights will provide the database for the Model development.

12. ROAD MAP FOR ALTITUDE DECOMPRESSION COMPUTER DEVELOPMENT

Our approaches emphasizes verification, validation and subsequent refinement of the various portions of the Model in an iterative fashion throughout the development process. Without an integrated validation process, the development cannot proceed because there is no way of knowing the accuracy and limitations of the evolving models. Results from validation of each phase provide the data necessary to direct the continuing development.

Procedures for validating decompression procedures were outlined at a 1989 workshop. This information has been published in a document titled "Validation of Decompression Tables" (130). Although aimed at the diving field, many of the guidelines can be applied to the development of this altitude Model. The validation procedures outlined below were derived from that document. In short, it is a two-step procedure: 1) test the model against available DCS databases, 2) test the model experimentally on human subjects at simulated altitude in a chamber.

12.A. Verification with DCS Databases

Initial validation will be accomplished by comparing model predictions with experimental DCS outcomes from available databases. There are two modern research altitude DCS databases available: 1) NASA JSC, and 2) USAF AL. Both the USAF and NASA have extensive computerized records of DCS and venous gas emboli data obtained from many years of research. The AL Hypobaric DCS Research Database (172) is the largest and most extensive since it is the only one that contains intravascular bubble data obtained with echo imaging techniques. Thus, this is the primary database that will be used in the model development.

The AL DCS Database is a VAX-based relational database system with 211 data fields per subject exposure. Complete records of venous gas emboli observed following movement of each limb are available for each 15 min segment of every exposure. The time course of all reported DCS symptoms is also recorded. Detailed coded information on the type and the severity of each symptom is recorded. The complete pressure profile, breathing mixtures for each exposure, selected personal anthropometric data and medical history of each subject are also recorded. As of 22 September 1992, 1076 exposures were recorded in the database. Efficient sorting and extracting procedures have been developed to produce computer-generated tables and other documents. This resource has been used extensively in support of many publications.

In addition to the AL and NASA Database, an additional source of useful data is the World War II research on DCS. The numerous studies conducted during and following WWII, as well as some of the newer studies, were recently compiled into a single computerized database by Conkin (28). Although these data have some limitations, Conkin's databank will be useful in modeling the severe end of the spectrum of clinical DCS manifestations. Most of these early studies were part of various aircrew screening programs. As a result, they contain large number of individuals. Unfortunately, much of the detailed data from the individual flight records have been lost. Another major problem with this old data is that both the endpoints for terminating the exposure and the symptom classification system used in these early studies varied significantly and are not consistent with the endpoints currently used. Despite these shortcomings, it should be possible to correlate some of these variables by carefully reviewing and comparing the detailed records based on symptomatology rather than classification of DCS. This would provide a critical volume of data that, due to stricter limitations on human experimentation, could never be repeated today.

A significant problem that must be dealt with in developing models of decompression sickness is the typically low incidence rates that occur on the milder exposures. To obtain sufficient statistical power in the data analyses, a large number of subjects is required for each study. The cost of doing such a large study is high. Therefore, it is imperative that all available data is consolidated into a common framework that

will give more statistical power than relying only on data obtained at any one research center. Using this approach will minimize the need for new experimental work.

12.B. Experimental Trials

Final validation of the model will, however, require experimental trials exposing human volunteers to selected altitude profiles in hypobaric chambers. The subjects will be monitored for DCS symptoms and intravascular gas emboli with echo imaging systems. The data on the DCS and VGE incidence and latency will be used to determine the validity of the model and to guide ongoing modifications to the model.

The method developed by the AL for human DCS research has been described in several papers (6,42,114,115,117,118,123,173). It is currently in use on four experimental protocols. In addition, a quantitative measure of decompression stress, intravascular gas emboli, is achieved with a non-invasive ultrasonic echo imaging/Doppler system (Hewlett Packard SONOS 1000) that permits precordial monitoring, by both visual and audio means. Gas emboli can be clearly seen and heard in all chambers of the heart, the pulmonary artery, the inferior vena cava, and other peripheral vessels. All data from these studies are coded and transferred into and stored in the AL DCS Database described above.

12.C. Goals and Approach

The feasibility study has shown that development of a working model is possible. We propose to initiate a full scale model development program that will produce the mathematical DCS Model that could ultimately be incorporated into an operational altitude decompression computer. Based on the preliminary work accomplished during the feasibility study, development and validation of the altitude decompression Model for the USAF is expected to take five years.

The multidisciplinary nature of this project requires a team of investigators and technicians with a wide spectrum of training and experience. In addition, altitude chamber crews and human subjects will be extensively utilized. Development and evaluation of candidate algorithms for DCS risk assessment require a flexible computing environment. The preliminary model was implemented using the LabView software package by National Instruments. This software has good user interfaces for inputting data and displaying results. However, due to the graphical nature of the software, direct control over the lower-level computational processing is limited. For this reason, future model development will be accomplished using FORTRAN. FORTRAN provides a common language that can be supported on a wide variety of computers. As the model software development progresses, the FORTRAN code can be linked to other packages such as MATLAB or LabView for easier display and analysis of results.

The mathematical model will be implemented on an 80486 microprocessor-based personal computer using FORTRAN. The flight profile and personal information can be input either from terminal (screen) or from a file. The output will be either in data or in graphs. The software MATLAB will be used to demonstrate the graphs and to do data comparisons. The FORTRAN code can be incorporated into MATLAB for more efficient operation. The model will calculate the physical stress related to DCS such as tissue ratio, bubble size, and bubble volume. The physical stress will then be correlated with experimental data on DCS. Once the link between DCS and the model-calculated physical stresses is established, the validity of the model will be evaluated. When the model has been refined to an acceptable degree of accuracy, it will be used to assess the risk of DCS associated with a variety of flight profiles.

Software development will be accomplished using a modular approach. Candidate algorithms will be implemented and tested against the available data from both *in vitro* and *in vivo* experiments. It is anticipated that no single algorithm will adequately model the entire range of potential altitude exposures. This will be addressed by combination of multiple algorithms. The proposed software development will be accomplished in an evolutionary fashion starting with simpler models and adding complexity where required to adequately match the experimental data.

C.1. First-year goals

Building on the preliminary model developed during the feasibility study, three parallel efforts will be initiated during the first year of the program:

1. Development, evaluation and documentation of the preliminary mathematical altitude DCS model and its corresponding computer implementation.
2. Verification of the basic physical and physiological concepts upon which this preliminary model is built through *in vitro* studies.
3. Elucidation and quantification through *in vivo* human studies of physiological concepts currently ill-defined but necessary for this model development.

Altitude D.C.S. Model Development Milestones

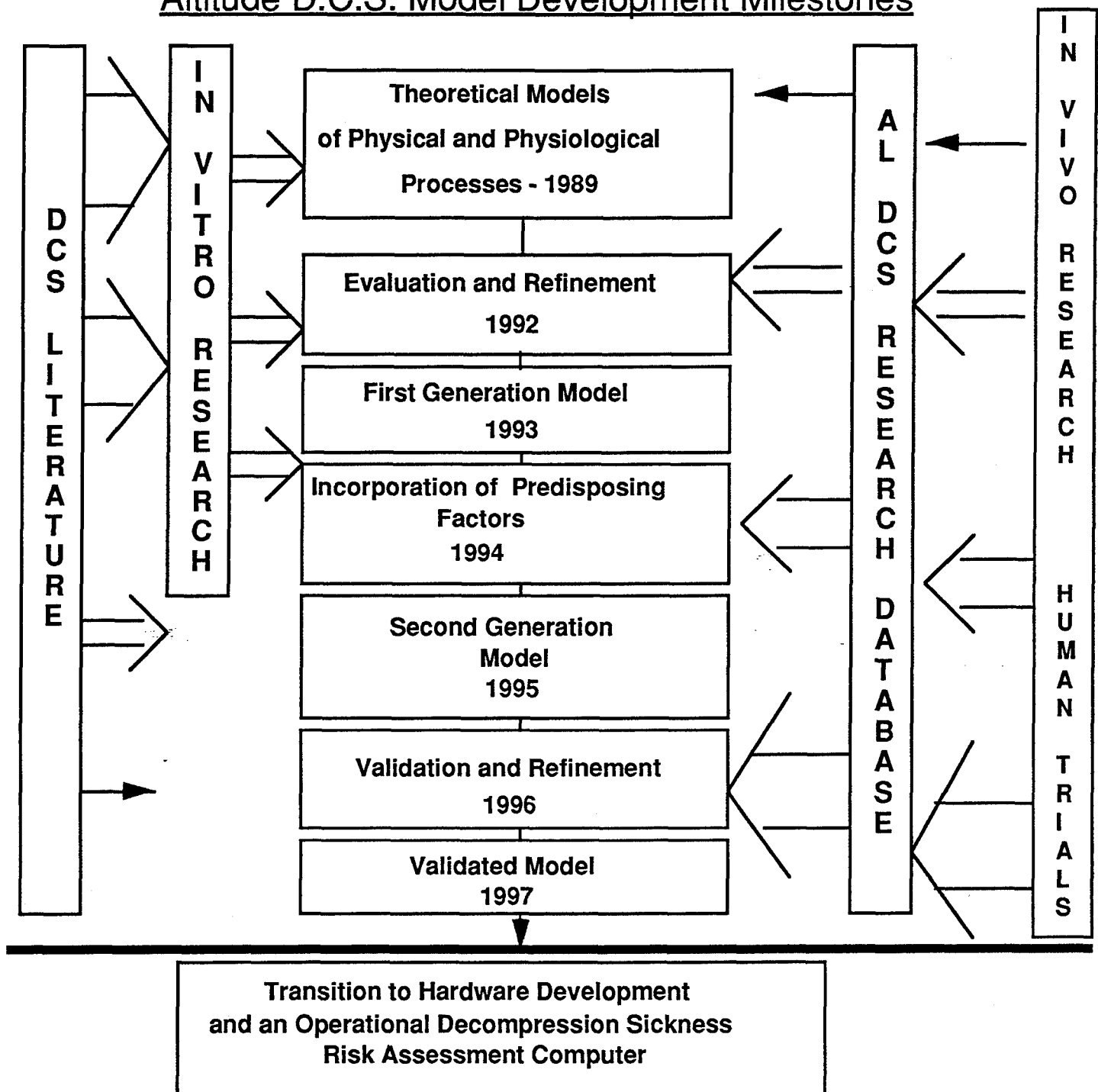


Figure 17. Altitude DCS Model Development Milestones

12.D. Outyear goals

Ongoing efforts should improve the validity of the model based on the incorporation of additional experimental data. Future efforts will also focus on expanding the scope of the model to include other factors known to affect DCS risk, i.e., level of exercise, repetitive exposures. Specific plans for future research include parametric studies to determine effects of variations in selected model parameters on the accuracy of the DCS risk predictions as well as refinement in selected model parameters and expansion of the model based on:

1. Additional data on the incidence and latency of DCS symptoms.
2. Correlations with experimental data on incidence and time course of venous gas emboli.
3. Verification of the bubble growth portion of the model against data from both *in vivo* and *in vitro* ultrasound echo imaging studies.

D.1. Continuation of year 1 objectives

It is expected that all of the studies listed above will continue into at least the second year. They will be initiated first because they represent the basic building blocks of the model or address the major gaps in the database and require an early start.

D.2. Incorporate predisposing factors and individual variability (biases)

DCS from all types of environments has a high level of individual variability. However, altitude DCS appears to have the highest. Therefore, in contrast to diving models, this model will contain methods for biasing the answer in order to reduce the variability. Ideally, correction factors have been implicated over the years. Some have a scientific basis, others are part of the "folklore" of DCS. In addition, some of these factors that have generated considerable scientific interest may not be of high importance. The magnitude of their impact on DCS may be disproportionately small and therefore, they will not be considered for the model. A variety of predisposing factors that are considered important in the etiology of DCS will be evaluated for consideration for the model and will be dealt with in two ways. If the factor has been dealt with sufficiently in the past, and its effect is well documented, and the decision is made that it has a major influence on DCS, data from the literature will be used to integrate a bias into the model. This category includes such factors as age, body fat, hydration, and gender. If a factor is considered to be important and sufficient data are in the literature, research will be initiated to determine its effects on DCS and the data entered into the database. The influences listed below are currently in the latter category:

1. PPB
2. Exercise
3. Repetitive exposures

D.3. Develop "read-out" configuration

Because altitude DCS occurs during the mission, not only should the Model output display percent risk, it should also provide information on how severe the symptomatology will be, and the time progression of that risk while at altitude. This information will provide as much capability as possible in order to maximize mission effectiveness.

D.3a. Severity scale

A variety of DCS end-points have been used over the years (175). Most frequently the Golding (56) Type I/Type II classification has been used. Recently, this classification has been dropped by many because it is inadequate and counterproductive (48, 90). The NASA model (29) used a three-level scale to describe DCS risk: VGE, pain, and serious symptoms. A four-level scale risk assessment approach is proposed for this Model readout. This will enable selection of not only percent risk but also the type and severity of risk. The four scales are, in general, in increasing order of severity:

1. venous gas emboli and arterial gas emboli
2. pain
3. neurological symptoms
4. chokes (respiratory distress)

The empirical data for the first two scales, as discussed above, will be obtained from the AL DCS Research Database. However, because of the conservative nature of the studies that contribute to that database, studies dating back several decades will be used to verify the more severe scales. These old databases may require organization and computerization to make them useful to the modeling effort. Some of this work is ongoing at other research centers and subcontracting for such required databases may be needed.

D.3b. Latency and resolution

The onset time to DCS has been used effectively for many years in the USAF to enable certain operational altitude exposures to be accomplished with minimal risk of DCS. The latency period has been discussed and will be an output of the Model. Another portion of a flight profile that can be useful will be referred to as the resolution period (174). If an individual goes to altitude breathing 100% O₂ and stays there a long enough time, the bubbles and DCS tend to resolve. This is because the continuing denitrogenation process at some point reduces the N₂ levels so low that bubbles can't be maintained. As can be seen in Figure 18, the time frame between these two relatively safe regions is the area of concern.

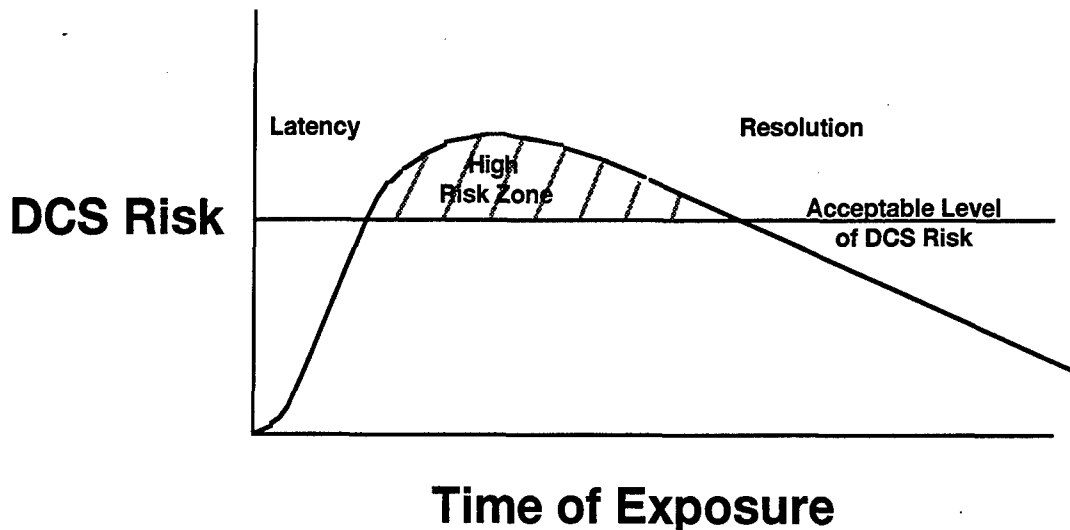


Figure 18. Flight profile of DCS risk

It is the region in which one will want to ask the Model to change variables in such a way as to bring down the risk level, i.e., increase prebreathing, change breathing gas, change altitude, etc. The model must be capable of incorporating these effects in order to provide accurate risk assessments in all three of these regions.

D.4. Human subject validation trials

Testing of a decompression model with human subject trials is one of the basic requirements for the acceptance of any model. Unless this is done, a model remains a purely theoretical computer exercise with no validity. This is clearly defined in the validation workshop previously discussed (56). One of the basic design concepts of our Model is that any part of it can be modified at any time. Its development will incorporate this capability. During the human trials phase, the Model will be continuously refined as data becomes available.

It is expected that the human trials phase will last approximately two years. The experimental protocol for the human trial will be written and processed through the AL human use committee and the Surgeon General's Office during the third year of the project. Since not all situations can be validated, obviously the testing protocol will require great care in the selection of which representative flight profiles will be used to validate the model. That selection will take into account the profiles already used from the databases, and the portion of the model with the lowest confidence.

D.5. Final software package for transition development of operational device

Upon completion of the verification process, the model will be finalized in the software formats and languages determined to be most desirable for transition to software and hardware development.

13. CONCLUSIONS

Work to date on development of an altitude DCS risk assessment model shows great promise. Ongoing efforts should improve the validity of the model based on inclusion of additional experimental data. Future efforts will also focus on expanding the scope of the model to include other factors known to affect DCS risk, i.e., level of exercise, age, repetitive exposures, flying after diving, etc. Specific plans for future research include parametric studies to determine effects of variations in selected parameters on accuracy of DCS risk predictions. Also, we plan to refine and expand the model based on:

1. Additional data on the incidence and latency of DCS symptoms.
2. Correlations with experimental data on incidence and time course of venous gas emboli.
3. Verification of bubble growth model against data from echo imaging studies.

In closing, we believe the final product of this research will provide a tool that will be of direct use to field personnel in both planning and executing operational missions impact, i.e., results in better assessment of DCS risk. The same product will also provide a standardized approach for risk management in altitude chamber training and research operations.

14. REFERENCES

1. Adler HF. Dysbarism. USAFSAM Aeromedical Review #1-64. 1964;166pp.
2. Air Standardization Coordinating Committee. Minimum Physiological Requirements for Aircrew Demand Breathing Systems. ASCC Air Standard 61/22A, 12 Feb 1988.
3. Albanese RA., et al. Bubble dynamics and delayed decompression sickness. Tab E, 22 pp. In: Special study group report. Altitude decompression sickness among U.S. Air Force Academy Cadets. USAF School of Aerospace Medicine. Jun 1978.
4. Ashman MN., et al. A nonlinear model for the uptake and distribution of halothane in man. *Anes* 33(4):419-429 (1970).
5. Aukland K., et al. Measurement of local blood flow with hydrogen gas. *Circ Res* 14:164-187 (1964).
6. Baas CL, Olson RM, Dixon GA. Audio and visual ultrasonic monitoring of altitude decompression. 26th Annual SAFE Symposium Proceedings. 1989;22-6.
7. Balldin UI. Denitrogenation. p.235. In: Proceedings of the 1990 Hypobaric Decompression Sickness Workshop. Pilmanis A.A. (Ed.) USAF Armstrong Laboratory Special Report # USAFAL-SR-1992005. 1992. Brooks AFB, TX.
8. Bateman JB. Susceptibility to decompression sickness: The effects of prolonged inhalation of certain nitrogen-oxygen mixtures compared with those of exposure to pure oxygen. *Comm. Aviat. Med. Report #364*. 1944;23pp.
9. Bateman JB and Lang J. Formation and growth of bubbles in aqueous solutions. *Canad J Res* E23:22-31 (1945).
10. Battino R and Clever HL. The solubility of gases in liquids. *Chem Rev* 66: 395-463.
11. Baz A. and Abdel-Khalek. Effect of intravascular bubble on perfusate flow and gas elimination rates following a simulated decompression of a model tissue. *Undersea Biomed Res* 13(1):27-43 (1986).
12. Behnke AR, Thompson RM, Shaw LA. The rate of elimination of dissolved nitrogen in man in relation to the fat and water content of the body. *Am J. Physiol.* 1935;114:137-46.
13. Behnke AR. The application of measurements of nitrogen elimination to the problem of decompressing divers. *U.S. Naval Medical Bulletin*. 1937;35:219-40.
14. Behnke AR. Physiologic studies pertaining to deep sea diving and aviation, especially in relation to the fat content and composition of the body. *The Harvey Lectures* 1942:198-226 (1942).
15. Behnke AR. The isobaric (oxygen window) principle of decompression. *Transactions of the 3rd Annual Conference of the Marine Technology Society, San Diego, California*, 1967.
16. Behnke AR., et al. The rate of elimination of dissolved nitrogen in man in relation to the fat and water content of the body. *Am J Physiol* 114:137-146 (1935).
17. Bigelow JH., et al. Altitude bends in humans: an investigation using mathematical models and a computer. R-1002-PR, Aug 1972.

18. Bove AA and Davis JC. Diving Medicine, 2nd ed. WB Saunders Company. p29-49 (1990).
19. Boycott AE, Damant GCC, Haldane JS. The prevention of compressed-air illness. J. Hyg. London. 1908;8:342-456.
20. Boyle R. New pneumatical experiments about respiration. Philosophical Transcripts, 5, 1670;2011-2058.
21. Buckles RC. The physics of bubble formation and growth. Aerospace Med:1062-1069 (1968).
22. Buhlmann AA. Gas uptake, gas elimination. Decompression theory: Swiss practice, pp. 105-112 In: T. E. Berghage (chairman). The Seventeenth Undersea Medical Society Workshop, Bethesda, Maryland. UMS Publication Number 29WS(DT), Sept 1978.
23. Butler BD. Cardiopulmonary effects of decompression bubbles. p53 In: Proceedings of the 1990 Hypobaric Decompression Sickness Workshop. Pilmanis A.A. (Ed.) USAF Armstrong Laboratory Special Report # USAFAL-SR-1992-005. 1992. Brooks AFB, TX.
24. Campbell JA. Changes in the tensions of O₂ and CO₂ injected under the skin and into the abdominal cavity. J Physiol 59:1-6 (1924).
25. Chadov VI and Iseyev LR. Variation on the maximum acceptable coefficient of supersaturation during altitude decompression. Kosmicheskaya Biologiya i Aviakosmicheskaya Meditsina 23(3):58-62 (1989).
26. Chapra SC and Canale RP. Numerical methods for engineers: with personal computer applications. New York: McGraw-Hill, 1985.
27. Chilcoat RT., et al. Computer assistance in the control of depth of anaesthesia. Br J Anaesth 56:1417-1432 (1984).
28. Conkin J, Bedahl SR, Van Liew HD. A computerized databank of decompression sickness incidence in altitude chambers. Aviat. Space Environ. Med. Vol 63, No. 9, p.819-824, 1992.
29. Conkin J, Dierlam JJ, Stanford J Jr, Riddle JR, Waligora JM, Horrigan DJ. Increase in whole-body peripheral vascular resistance during three hours of air or oxygen prebreathing. NASA Technical Memorandum 58261. 1984;14pp.
30. Conkin J, Edwards BF, Waligora JM, Horrigan DJ Jr. Empirical models for use in designing decompression procedures for space operations. NASA Technical Memorandum 100456. 1987;45pp.
31. Conkin J, Edwards BF, Waligora JM, Stanford J Jr, Gilbert JH III, Horrigan DJ Jr. Updating empirical models that predict the incidence of aviator decompression sickness and venous gas emboli for shuttle and space station extravehicular operations. Update of NASA Tech. Memorandum No. TM100456. August, 1990.
32. Conkin J, Van Liew, HD. Failure of the straight-line DCS boundary when extrapolated to the hypobaric realm. Aviat. Space Environ. Med. IN PRESS.
33. Conkin J, Waligora JM, Horrigan DJ Jr, Hadley AT III. The effect of exercise on venous gas emboli and decompression sickness in human subjects at 4.3 psia. NASA Technical Memorandum 58278. 1987;21pp.

34. Cowles AL., et al. Tissue weights and rates of blood flow in man for the prediction of anesthetic uptake and distribution. *Anesthesiology* 35(5):523-526 (1971).
35. Crank J. The mathematics of diffusion. London: Oxford University Press, 2nd ed., 1975.
36. Daniels S., et al. Micronuclei and bubble formation: a quantitative study using the common shrimp, *Crangon crangon*, pp. 146-157, In: A. J. Bachrach and M. M. Matzen. *Underwater Physiology VIII*. Bethesda: Undersea Medical Society, 1984.
37. Danoff PL, Danoff JV. Energy cost and heart rate response to static and dynamic exercise. *Arch. Phys. Med. Rehab.* 1982;63:130134.
38. Davis NR and Mapleson WW. Structure and quantification of a physiological model of the uptake and distribution of injected agents and inhaled anaesthetics. *Br J Anaesth* 53:399-405 (1981).
39. Davson H. A textbook of general physiology, 3rd ed. London: Churchill, 1964.
40. Decompression procedures for the safe ascent of aerospace personnel from ground level to altitude. Contract NAS 9-6978 to NASA, Union Carbide Corporation, 1968.
41. Dedrick RL. Animal scale-up. *J Pharmacokinetics* 1(5):435 (1973).
42. Dixon GA, Adams JD, Harvey WT. Decompression sickness and intravenous bubble formation using a 7.8 PSIA simulated pressuresuit environment. *Aviat. Space Environ. Med.* 1986;57:223-8.
43. Dwyer JV. Calculation of air decompression tables. Research Report 4-56. USN Experimental Diving Unit, Wash.DC. 1955;36pp.
44. Eger EI. II. A mathematical model of uptake and distribution, ch. 7, pp.72-87 In E. M. Papper and R. J. Kitz (eds.). *Uptake and distribution of anesthetic agents*. New York: McGraw-Hill, 1963.
45. Epstein PS and Plesset MS. On the stability of gas bubbles in liquid-gas solutions. *J Chem Phys* 18(11):1505-1509 (1950).
46. Ferris EB, Webb JP, Ryder HW, Engel GL, Romano J, Blankenhorn MA. The protective value of preflight oxygen inhalation at rest against decompression sickness. *Comm. Aviat. Med. Report* #132. 1943;8pp.
47. Fischer MD, Wiegman JF, McLean SA, Olson RM. Evaluation of four different exercise types for use in altitude decompression sickness studies (Abstract). *SAFE 92, Las Vegas*, 1992.
48. Francis TJR. Describing decompression illness. Royal Navy Institute of Naval Medicine Report #INM R91012, 1991.
49. Francis TJR. Neurological complications of decompression illness - mechanisms and pathology. p167. In: *Proceedings of the 1990 Hypobaric Decompression Sickness Workshop*. Pilmanis A.A. (ed.) USAF Armstrong Laboratory Special Report # USAFAL-SR-1992005. 1992. Brooks AFB, TX.
50. Fraser AM, Stewart CB, Manning GW. Review of Canadian investigations on decompression sickness. *Assoc. Comm. Aviat. Med. Rpt.* C-2503. 1943;49pp.
51. Fryer D.I. Subatmospheric decompression sickness in man. AGARDograph No. 125, Circa Publications, Pelham NY., 1969.

52. Fulton, JF. Decompression sickness: caisson sickness, diver's and flier's bends and related syndromes. Philadelphia, PA: W.B. Saunders Co., 1951.
53. Furr PA and Sears WJ. Physiological effects of repeated decompression and recent advances in decompression sickness research: A review. SAE Technical Paper #881072, 18th Intersociety Conference on Environmental Systems, 1988.
54. Gernhardt M. Tissue gas bubble dynamics during hypobaric exposures. SAE Technical Paper Series 851337. Fifteenth Intersociety Conference on Environmental Systems, San Francisco, California, July 1985.
55. Gerth WA, Vann RD, Southerland DG. Quasi-physiological decompression sickness incidence modeling. p253. In: Repetitive Diving Workshop. Lang MA and Vann RD (Eds), American Academy of Underwater Sciences Publication #AAUSDSP-RDW-02-92, 1992.
56. Golding, F.C.; P. Griffiths; H.V. Hempleman; W.D. Paton and D.N. Walder. Decompression sickness during construction of the Dartford tunnel. Br. J. Ind. Med.17, 167-180, 1960.
57. Gray JS. Aeroembolism induced by exercise in cadets at 23,000 feet. SAM Report, Project #227. 1944;3pp.
58. Gray JS. The effect of exercise at altitude on aeroembolism in cadets. SAM Report, Project #156. 1943;9pp.
59. Hamilton RW and Schreiner HR. Editorial summary: validation of decompression tables. In 37th UHMS Workshop, Validation of decompression tables, pp 163-167. UHMS Pub. 74(VAL) 1-1-88. Bethesda
60. Haldane JS and Priestley JG. Respiration. New Haven: Yale University Press, 1935.
61. Hempleman HV. Investigation into the decompression tables, report III, part A. A new theoretical basis for the calculation of decompression tables. RNPRC Report, UPS 131, MRC, London, 1952.
62. Hempleman HV. Tissue inert gas exchange and decompression sickness. Proceedings of 2nd Symposium on Underwater Physiology, Washington, D. C., 1963.
63. Hennessy TR. The equivalent bulk-diffusion model of the pneumatic decompression computer. Med Biol Engng 11:135-137 (1973).
64. Hennessy TR and Hempleman HV. An examination of the critical released gas concept in decompression sickness. Proc R Soc Lond B197:299-313 (1977).
65. Hills BA. Decompression sickness, Volume 1: The biophysical of prevention and treatment. Chichester: John Wiley & Sons, 1977.
66. Hills BA. A thermal analogue for the optimal decompression of divers: construction and use. Phys Med Biol 12(4):445-454 (1967).
67. Hills BA. A thermal analogue for the optimal decompression of divers: theory. Phys Med Biol 12(4): 437-444 (1967).

68. Hills BA. A thermodynamic and kinetic approach to decompression sickness. Ph.D. dissertation, University of Adelaide, Adelaide, Australia, 1966.
69. Hills BA. Decompression sickness. Volume 1: the biophysical basis of prevention and treatment. Chichester: John Wiley & Sons, 1977.
70. Hills BA. Effect of decompression per se on nitrogen elimination. *J Appl Physiol: Respir Environ Exercise Physiol* 45:916-921 (1978).
71. Hills BA. Limited supersaturation versus phase equilibration in predicting the occurrence of decompression sickness. *Clin Sci* 38:251-267 (1970).
72. Hills BA. Linear bulk diffusion into heterogeneous tissue. *Bull Math Biophys* 30:47-59 (1968).
73. Hills BA. Relevant phase conditions for predicting occurrence of decompression sickness. *J Appl Phys* 25(3):310-315 (1968).
74. Hills BA. The time course for the uptake of inert gases by the tissue responsible for marginal symptoms of decompression sickness. *Rev Subaqua Physiol* 1:255-261 (1969).
75. Hills BA. Thermodynamic decompression: an approach based upon the concept of phase equilibration in tissues. ch. 9, pp. 317-356 In: P. B. Bennett and D. H. Elliot (eds.). *The physiology and medicine of diving and compressed-air work*. London: Balliere, Tindall and Cassell, 1969.
76. Hills BA. Vital issues in computing decompression schedules from fundamentals. II. critical supersaturation versus phase equilibration. *Int J Biometeor* 14(2):111-131 (1970).
77. Hills BA., and D. H. LeMessurier. Unsaturation in living tissue relative to the pressure and composition of inhaled gas and its significance in decompression theory. *Clin Sci* 36:185-195 (1969).
78. Hills BA., et al. The zero-supersaturation approach to decompression: its fundamental basis and computerization with simultaneous oxygen optimization. pp. 100-118 In: R. W. Hamilton (ed.). *Development of decompression procedures for depths in excess of 400ft*. Washington: Undersea Medical Society, 1976.
79. Hlastala MP, Van Liew HD. Absorption of in vivo inert gas bubbles. *Respirat. Physiol.* 1975;24:147-158.
80. Hlastala MP. Transient-state diffusion in rat subcutaneous tissue. *Aerospace Med* 45(3):269-273 (1974).
81. Hlastala MP and Van Liew HD. Absorption of in vivo inert gas bubbles. *Resp Phys* 24:147-158 (1975).
82. Huggins KE. Computer/calculator solutions to decompression problems. (1984).
83. Huggins KE. Microprocessor applications to multi-level air decompression problems. Michigan Sea Grant College Program. MICHU56-87-201 (1987).
84. Ikels KG. Physical-chemical aspects of bubble formation. SAM Technical Report #69-60. 1969;7pp.
85. Ikels KG. Production of gas bubbles in fluids by tribonucleation. *J. Appl. Physiol.* 1970;28:524-7.

86. Inman VT and Saunders JB. Referred pain from skeletal structures. *J Nerv Ment Dis* 99:660-667 (1944).
87. International Commission on Radiological Protection. Report of the task group on reference man, p. 280-285. Oxford Pergamon, 1975.
88. Jauchem JR. Effects of exercise on the incidence of decompression sickness: a review of pertinent literature and current concepts. *Int Arch Occup Environ Health* 60:313-319 (1988).
89. Jones HB. Respiratory system: nitrogen elimination. pp. 855-871 In: O. Glasser (ed.). *Medical Physics*. Vol 2. Chicago: Year Book Publishers, 1950.
90. Kemper GB, Stegmann BJ, Pilmanis AA. Inconsistent classification and treatment of Type I/Type II decompression sickness. (Abstract) *Aviat. Space Environ. Med.* 1992;63:410.
91. Kety SS. The theory and application of the exchange of inert gas at the lungs and tissues. *Pharmacol Rev* 3:1-41 (1951).
92. Kislyakov YY. Dynamics of gas bubble growth in biologic tissues under decompression (mathematical model). *Rep Acad Sci USSR* 253:1012-1015 (1980).
93. Kislyakov YY and Kopyltsov AV. The rate of gas-bubble growth in tissue under decompression. mathematical modelling. *Resp Phys* 71:299-306 (1988).
94. Krutz RW Jr, Dixon GA. The effects of exercise on bubble formation and bends susceptibility at 9,100 m (30,000 ft; 4.3 psia). *Aviat. Space Environ. Med.* 1987;58:A97-A99.
95. Kumar KV, Powell MR, Gilbert JH, Waligora JM. Survival analysis of the association between symptoms and Maximum grade of circulating microbubbles during hypobaric decompression (Abstract). *Undersea Biomed. Research Suppl.* Vol 19; A110, p 71, 1992.
96. Kumar KV. Decompression sickness and the role of exercise during decompression. *Aviat. Space Environ. Med.* 1988;59:1080-2.
97. Kunkle TD and Beckman EL. Bubble dissolution physics and the treatment of decompression sickness. *Med Phys* 10(2):184-190 (1983).
98. Lam TH and Yau KP. Analysis of some individual risk factors for decompression sickness in Hong Kong. *Undersea Biomed Res* 16(4): 283-292 (1989).
99. Lambertsen CJ. Origins and evolution of pathophysiological concept, p3. In: *Proceedings of the 1990 Hypobaric Decompression Sickness Workshop*. Pilmanis A.A. (ed.) USAF Armstrong Laboratory Special Report # USAFAL-SR-1992-005. 1992. Brooks AFB, TX.
100. Lang MA, Hamilton RW (eds). *Proceedings of the American Academy of Underwater Sciences Dive Computer Workshop*. University of Southern California Sea Grant Publication USCSG-TR-01-89. 1988.
101. Lategola, M. T. Measurement of total pressure of dissolved gas in mammalian tissue in vivo. *J Appl Physiol* 19(2):322-324 (1964).
102. Lawrence JH, Jones HB, Berg WE, Henry FM, Ivy RC. Studies on gas exchange. Memorandum Report MCREXD-696-114. 1948;224pp.

103. LeMessurier DH and Hills BA. Decompression sickness: a thermodynamic approach arising from a study of Torres Strait diving techniques. *Hvalradets Skr* (48):54-84 (1965).
104. Lin YC. Species independent maximum no-bubble pressure reduction from saturation dive. pp. 699-706 In: A. J. Bachrach and M. M. Matzen (eds.). *Underwater Physiology VII*. Bethesda: Undersea Medical Society, 1981.
105. MacIntosh R., et al. *Physics for the anaesthetist*. Oxford: Blackwell Scientific, 1963.
106. Mapleson WW. An electric analogue for uptake and exchange of inert gases and other agents **:197-204 (1961?).
107. Mapleson WW. Circulation-time models of the uptake of inhaled anaesthetics and data for quantifying them. *Br J Anaesth* 45:319-334 (1973).
108. Marbarger JP, Kadetz W, Paltarokas J, Variakojis D, Hansen J, Dickinson J. Gaseous nitrogen elimination at ground level and simulated altitude and the occurrence of decompression sickness. SAM Report #55-73. 1956;20pp.
109. McArdle WD, Foglia GF. Energy cost and cardiorespiratory stress of isometric and weight training exercises. *J. Sports Med. Phys. Fitness*. 1969;9:22-30.
110. Meisel S., et al. Bubble dynamics in perfused tissue undergoing decompression. *Resp Phys* 43:89-98 (1981).
111. Morales MF and Smith RE. A note on the physiologic arrangement of tissues. *Bull Math Biophys* 7:47-51 (1945).
112. Neubauer JC, Dixon JP and Herndon CH. Fatal pulmonary decompression sickness: A case report. *Aviat. Space and Environ. Med.* 59, 1181-4 (1988).
113. Nishi RY and Lauckner GR. Development of the DCIEM 1982 decompression model for compressed air diving. DCIEM Report No.84R-44, 1984.
114. Olson RM, Dixon GA, Adams JD, Fitzpatrick EL, Koegel E. An evaluation of the ultrasonic precordial bubble detector. *AsMA Ann. Sci. Mtg. Preprints*. Anaheim, CA. 1980;10-11.
115. Olson RM, Krutz RW Jr, Dixon GA, Smead KW. An evaluation of precordial ultrasonic monitoring to avoid bends at altitude. *Aviat. Space Environ. Med.* 1988;59:635-9.
116. Olson RM, Krutz RW Jr. Significance of delayed symptom onset and bubble growth in altitude decompression sickness. *Aviat. Space Environ. Med.* 1991;62:296-9.
117. Olson RM, Pilmanis AA, Scoggins TE. Echo imaging in decompression sickness research. 29th Annual SAFE Symposium Proceedings. 1991;278-82.
118. Olson RM, Pilmanis AA, Scoggins TE. Use of echo imaging in decompression model development. (Abstract) *Aviat. Space Environ. Med.* 1992;63:386.
119. Papper EM and Kitz RJ. *Uptake and distribution of anesthetic agents*. New York: McGraw Hill, 1963.

120. Perl W and Chinard FP. A convection-diffusion model of indicator transport through an organ. *Circ Res* 22:273-298 (1968).
121. Pilmanis A.A. (ed.) Proceedings of the 1990 Hypobaric Decompression Sickness Workshop. USAF Armstrong Laboratory Special Report # USAFAL-SR-1992-005. 1992. Brooks AFB, TX
122. Pilmanis AA, Bisson RU. Incidence of decompression sickness (DCS) in high altitude reconnaissance pilots. (Abstract) *Aviat. Space Environ. Med.* 1992;63:410.
123. Pilmanis AA, Olson RM. Arterial gas emboli in altitude-induced decompression sickness (Abstract). 6th Annual Space Operations, Applications, and Research Symposium, Houston, 1992.
124. Pilmanis AA, Stegmann BJ. Decompression sickness and ebullism at high altitudes. In: "High Altitude and High Acceleration Protection for Military Aircrew." Proceedings of the NATO AGARD Symposium 71st Aerospace Medical Panel. Pensacola, FL. AGARD-CP516. 1991;11pp.
125. Powell MR. Doppler indices of gas phase formation in hypobaric environments: time/intensity analysis. NASA Technical Memorandum, Mar 1990.
126. Price HL., et al. The uptake of thiopental by body tissues and its relation to the duration of narcosis. *Clin Pharm Therap* 1:16-22 (1960).
127. Rashbass C. Investigation into the decompression tables. Report VI, New Tables, UPS Report 151, RNPRC, MRC, London, 1955.
128. Ross RS., et al. Measurement of myocardial blood flow in animals and man by selective injection of radioactive inert gas into the coronary arteries. *Circ Res* 15:28 (1964).
129. Roughton FJW. Diffusion and chemical reaction velocity in cylindrical and spherical systems of physiological interest. *Proc Roy Soc London SB*, 140:203-229 (1952).
130. Schreiner HR and Hamilton RW (Eds). Validation of decompression tables. 37th Undersea and Hyperbaric Medical Society Workshop. UHMS Publication 74(VAL) 1-1-88, 1989.
131. Scoggins TE, Ripley EP, Bauer DH, Pilmanis AA. Development of an altitude decompression sickness model. (Abstract) *Aviat. Space Environ. Med.* 1992;63:386.
132. Scoggins TE, Ripley EP, Melkonian AD, Pilmanis AA. Development of an operational altitude decompression computer: Feasibility study results. USAF AL Technical Report (In Preparation), 1992.
133. Sharkey BJ. A physiological comparison of static and phasic exercise. *Res. Quart.* 1;37:520-531.
134. Smith RE and Morales MF. On the theory of blood-tissue exchanges: I. fundamental equations. *Bull Math Biophys* 6:125-131 (1944).
135. Smith RE and Morales MF. On the theory of blood-tissue exchanges: II. applications. *Bull Math Biophys* 6:133-139 (1944).
136. Stegmann BJ, Pilmanis AA. Prebreathing as a means to decrease the incidence of decompression sickness at altitude. In: "High Altitude and High Acceleration Protection for Military Aircrew." Proceedings of the NATO AGARD Symposium 71st Aerospace Medical Panel. Pensacola, FL. AGARD-CP-516. 1991;8pp.

137. Stevens CD., et al. The rate of nitrogen elimination from the body through the lungs. *J viat Med* 18:111-168 (1947).
138. Stubbs RA and Kidd DJ. Control of decompression by analogue computer. Canadian Forces Medical Service. Institute of Aviation Medicine. Report #65-RD-8, Dec 1965.
139. Stubbs RA and Weaver RS. The transient response of an m-loop series filter with special application to the decompression problem in man. Linear model. DRET Report No.620. Defence Research Establishment Toronto, Sept 1968.
140. Tatnall ML., et al. Controlled anaesthesia: an approach using patient characteristics identified during uptake. *Br J Anaesth* 53:1019-1026 (1981).
141. Thalmann ED. A procedure for doing multiple level dives on air using repetitive groups. Navy Experimental Diving Unit Report Number 13-83 (1983).
142. Thalmann ED. Air N2O2 decompression computer algorithm development. Navy Experimental Diving Unit Report Number 8-85 (1985).
143. Thalmann ED. Computer algorithms used in computing the MK 15/16 constant 0.7 ATA oxygen partial pressure decompression tables. Navy Experimental Diving Unit Report Number 1-84 (1984).
144. Tikuisis P., et al. Use of the maximum likelihood method in the analysis of chamber air dives. *Undersea Biomed Res* 15(4):301313 (1988).
145. Van Liew HD. Bubble dynamics. p 17. In: Proceedings of the 1990 Hypobaric Decompression Sickness Workshop. Pilmanis A.A. (ed.) USAF Armstrong Laboratory Special Report # USAFAL-SR-1992005. 1992. Brooks AFB, TX.
146. Van Liew HD. Gas exchanges of bubbles in tissues and blood. In: *The Physiological Basis of Decompression*. (RD Vann, Ed.). 38th Undersea and Hyperbaric Medical Society Workshop, UHMS Publication # 75(Phys)6/1/89,1989;73-85.
147. Van Liew HD. Simulations of the dynamics of decompression sickness bubbles and the generation of new bubbles. *Undersea Biomedical Research*, Vol.18, No.4, p.333, 1991.
148. Van Liew HD. Coupling of diffusion and perfusion in gas exit from subcutaneous pockets in rats. *Am J Phys* 214:1176-1185 (1968).
149. Van Liew HD. Gas exchanges of bubbles in tissue and blood. *Proceedings of the Thirty-Eighth Undersea and Hyperbaric Medical Society Workshop*, Durham, North Carolina, 1989.
150. Van Liew HD. Simulations of the growth of decompression sickness and transformation of gas nuclei to bubbles. (in press)
151. Van Liew HD. Tissue pO2 and pCO2 estimation with rat subcutaneous gas pockets. *J Appl Physiol* 17:851-855 (1962).
152. Van Liew HD., et al. Effects of compression on composition and absorption of tissue gas pockets. *J Appl Physiol* 20:927-933 (1965).
153. Van Liew HD, Hlastala MP. Influence of bubble size and blood perfusion on absorption of gas bubbles in tissues. *Respir. Physiol.* 1969;7:111-21.

154. Vann RD (Ed.). The physiological basis of decompression . 38th Undersea and Hyperbaric Medical Society Workshop, UHMS Publication # 75(Phys)6/1/89, 1989.
155. Vann RD, Gerth WA. Physiology of decompression sickness p. 35. In: Proceedings of the 1990 Hypobaric Decompression Sickness Workshop. Pilmanis A.A. (ed.) USAF Armstrong Laboratory Special Report # USAFAL-SR-1992-005. 1992. Brooks AFB, TX.
156. Vann RD. Exercise and circulation in the formation and growth of bubbles. In: Supersaturation and Bubble Formation in Fluids and Organisms, an International Symposium Kongsvoll. Brubakk AL, Hemmingsen BB, Sundnes G (eds.) 1989;235-63.
157. Vann RD. Likelihood analysis of decompression data using Haldane and bubble growth models. 9th Int'l Symposium on Undersea and Hyperbaric Physiol. 1987;165-81.
158. Vann RD. A likelihood analysis of experiments to test altitude decompression protocols for shuttle operations. (1986).
159. Vann RD. Exercise and circulation in the formation and growth of bubbles. pp.235-263 In: A. O. Brubakk, B. B. Hemmingsen, and G. Sundnes (eds.). Supersaturation and bubble formation in fluids and organisms, Kongsvoll, Norway, 1988.
160. Vann RD. Likelihood analysis of decompression data using Haldane and bubble growth models. pp 165-181. 9th International Symposium on Underwater and Hyperbaric Physiology. Bethesda, Maryland, 1987.
161. Vann RD. Mechanisms and risks of decompression. ch. 4, pp. 29-49 In: A. A. Bove and J. C. Davis (eds.). Diving medicine: physiological principles and clinical applications, 2nd ed. Philadelphia: W. B. Saunders Company, 1990.
162. Walder DN. Serum surface tension and its relation to the decompression sickness of aviators. J. Appl. Physiol. 1948;107:4344P.
163. Waligora JM, Horrigan DJ, Conkin J. The effect of extended oxygen prebreathing on altitude decompression sickness and venous gas bubbles. Aviat. Space Environ. Med. 1987;58:A110-A112.
164. Ward CA., et al. Relation between complement activation and susceptibility to decompression sickness. J Appl Physiol 62(3): 1160-1166 (1987).
165. Weast. Handbook of chemistry and physics. 70th ed. CRC Press, 1989.
166. Weathersby PK, Homer LD, Flynn ET. On the likelihood of decompression sickness. J. Appl. Physiol. 1984;57:815-25.
167. Weathersby PK, Survanshi SS, Homer LD, Parker E, Thalmann ED. Predicting the time of Occurrence of Decompression Sickness. J Appl Physiol 72:1541-1548, 1992.
168. Weathersby PK and Homer LD. Solubility of inert gases in biological fluids and tissues: a review. Undersea Biomed Res 7(4): 277-296 (1980).
169. Weathersby PK., et al. Stochastic description of inert gas exchange. J Appl Physiol: Respirat Environ Exercise Physiol (47): 1263-1269 (1979).

170. Weaver RS and Stubbs RA. The transient response of an m-loop series filter system with special application to the decompression problem in man. Non-linear model. DRET Report No. 674. Defense Research Establishment Toronto, Sept 1968.
171. Weaver RS., et al. Decompression calculations: analogue and digital methods. DRET Report No.703 Defense Research Establishment Toronto, Sept 1968.
172. Webb JT, Krutz RW Jr, Dixon GA. An annotated bibliography of hypobaric decompression research conducted at the Crew Technology Division, USAF School of Aerospace Medicine, Brooks AFB, Texas from 1983 to 1988. USAFSAM Technical Paper 88-10R. 1990;22pp.
173. Webb JT, Olson RM, Baas CL, Hill RC. Bubble detection with an echo-image/Doppler combined probe versus separate probes: A comparison of results. (Abstract) Undersea Biomed. Res. 1989; 16(Suppl):89-90.
174. Webb JT, Pilmanis AA. Resolution of high bubble grades at altitude. (Abstract) Aviat. Space Environ. Med. 1991;62:481.
175. Webb JT, Pilmanis AA. Venous gas emboli detection and endpoints for decompression sickness research. 29th Annual SAFE Symposium Proceedings. 1991;20-3.
176. Wiegman JF, McLean SA, Olson RW, Pilmanis AA. Metabolic monitoring of hypobaric subjects. Armstrong Laboratory Technical Report # AL-TR-1991-0057, 1991.
177. Wienke BR. Tissue gas exchange models and decompression computations: a review. Undersea Biomed Res, 16(1):53-89 (1989).
178. Wilhelm E., et al. Low pressure solubility of gases in liquid water. Chem Rev 77:219-262 (1977).
179. Wilmore JH, Parr RB, Ward P, Vodak PA, Barstow TJ, Pipes TV, Grimditch G, Leslie P. Energy cost of circuit training. Med. Sci. Sports. 1978;10:75-78.
180. Workman RD and Bornmann RC. Decompression theory: American practice. ch. 17, pp. 325-330 In: P. B. Bennett and D. H. Elliot (eds.). The Physiology and Medicine of Diving. Baltimore: Williams & Wilkins, 1975.
181. Workman RD and Reynolds JL. Adaptation of helium-oxygen to mixed gas scuba. NEDU Report 1-65, 1965
182. Yount DE, Hoffman DC. On the use of a bubble formation model to calculate diving tables. Aviat. Space Environ. Med. 1986;57:149-56.
183. Yount DE. Application of bubble formation model to decompression sickness in rats and humans. Aviat. Space Environ. Med. 1979;50:44-50.
184. Yount DE. Application of a bubble formation model to decompression sickness in fingerling salmon. Undersea Biomed Res 8(4):199-208 (1981).
185. Yount DE. Application of a bubble formation model to decompression sickness in rats and humans. Aviat Space Environ Med 50(1):44-50 (1979).
186. Yount DE. On the evolution, generation, and regeneration of gas cavitation nuclei. J Acoust Soc Am 71(6):1473-1481 (1982).

187. Yount DE. Skins of varying permeability: a stabilization mechanism for gas cavitation nuclei. *J Acoust Soc Am* 65(6):1429-1450 (1979).
188. Yount DE and Hoffman DC. Decompression theory: a dynamic critical volume hypothesis. pp. 131-146 In: A. J. Bachrach and M. M. Matzen. *Underwater Physiology VIII*. Bethesda: Undersea Medical Society, 1984.
189. Yount DE and Hoffman DC. On the use of a bubble formation model to calculate diving tables. *Aviation Space and Environmental Medicine* 57:149-156 (1986).
190. Yount DE and Strauss RH. Bubble formation in gelatin: a model for decompression sickness. *J Appl Phys* 47:5081-5089 (1976).
191. Yount DE., et al. Microscopic study of bubble formation nuclei. pp. 119-130 In: A. J. Bachrach and M. M. Matzen. *Underwater Physiology VIII*. Bethesda: Undersea Medical Society, 1984.
192. Yount DE., et al. Stabilization of gas cavitation nuclei by surface active compounds. *Aviat Space Environ Med* 48(3): 185-191 (1977).
193. Zwart A., et al. Multiple model approach to uptake and distribution of halothane: the use of an analog computer. *Comp Biomed Res* 5:228-238 (1972).

APPENDIX A

Derivation of Bubble Growth Equation

1. Introduction

In deriving the bubble growth equation, defined as change rate of bubble radius dr/dt , three basic laws are employed: Fick's law, Henry's law and ideal-gas (Boyle's) law. Several different bubble growth equations in the literature are all based on those three laws with different assumptions. The focus here is to derive those equations by Van Liew (1967), Van Liew and Hlastala (1969), Hlastala & Van Liew (1975) and Gernhardt (1985) from the same principles but different assumptions so that one bubble growth equation with acceptable assumptions could be chosen for the altitude DCS prediction model.

2. Three basic laws

Fick's Law

Fick's law has two forms, one is a gradient equation and the other is a differential equation. Each equation has different expressions according to the coordinate system chosen. In all following discussions, the substances considered are assumed to be isotropic and a generic letter e is assigned to represent the substance of interest.

Under the assumption, Fick's law in one dimension is (Crank 1975)

$$(1) \quad J_e = -D \frac{\partial C_e}{\partial x}$$

where

- J_e : rate of transfer of diffusing substance e per unit area of section
- C_e : concentration of diffusing substance e
- x : the space coordinate measured normal to the section
- D : diffusion coefficient.

If we restrict ourselves to cases in which the diffusion is radial, Eqn (1) can be expressed as

$$(2) \quad J_e = -D \frac{\partial C_e}{\partial r}$$

where r is radius.

The differential equation of diffusion in general is

$$(3) \quad \frac{\partial C_e}{\partial t} = \text{div} (D \text{ grad } C_e)$$

where

$$\text{div } C = \nabla \cdot C = \frac{\partial C_x}{\partial x} + \frac{\partial C_y}{\partial y} + \frac{\partial C_z}{\partial z},$$

$$\text{grad } C = \nabla C = \frac{\partial C}{\partial x} \mathbf{i} + \frac{\partial C}{\partial y} \mathbf{j} + \frac{\partial C}{\partial z} \mathbf{k},$$

and the subscripts x,y,z are the Cartesian coordinates. Assuming a constant diffusion coefficient, Eqn (3) in one dimension, the three dimension and radial diffusion become:

$$(4) \quad \frac{\partial C}{\partial t} = D \frac{\partial^2 C}{\partial x^2},$$

$$(5) \quad \frac{\partial C}{\partial t} = D \nabla^2 C = D \left(\frac{\partial^2 C}{\partial x^2} + \frac{\partial^2 C}{\partial y^2} + \frac{\partial^2 C}{\partial z^2} \right),$$

and

$$(6) \quad \frac{\partial C}{\partial t} = D \nabla^2 C = D \left(\frac{\partial^2 C}{\partial r^2} + \frac{2}{r} \frac{\partial C}{\partial r} \right) \quad \text{or} \quad \frac{\partial C}{\partial t} = D \nabla^2 C = D \frac{1}{r^2} \frac{\partial}{\partial r} \left(r^2 \frac{\partial C}{\partial r} \right)$$

respectively.

Ideal Gas Law

The ideal-gas law says that pressure times volume of the substance is constant, i.e.,

$$(7) \quad n_e R T = P_e V_e$$

where

- n_e = number of moles of the substance e
- R = ideal gas constant
- T = temperature
- P_e = pressure of the substance e
- V_e = volume of the substance e

or alternatively

$$(8) \quad n_e = \frac{P_e V_e}{R T}.$$

Henry's Law

Henry's law states that the concentration C_e of a substance in liquid phase is equal to some constant k_e times the partial pressure P_e of the substance in the gas phase,

$$(9) \quad C_e = k_e P_e.$$

By changing units and applying the ideal-gas law (7), Eqn (9) can be written as

$$(10) \quad C_e = \alpha P_e \left(\frac{P_s}{RT} \right)$$

where

- α = solubility of substance e
- P_s = standard pressure.

There is a connection between Eqn (8) and Fick's law Eqn (2), such that the rate of total substance transferred cross an area A is equal to the number of moles of the substance n per unit time, i.e.,

$$(11) \quad \frac{dn}{dt} = JA = -D \frac{\partial C}{\partial r} A.$$

Notice that Fick's law expression (2) is used since it is of our interest. Taking the derivative of Eqn (8), one obtains

$$(12) \quad \frac{dn_e}{dt} = \frac{d}{dt} \left(\frac{P_e V_e}{RT} \right) = \frac{1}{RT} \left(P_e \frac{dV_e}{dt} + V_e \frac{dP_e}{dt} \right).$$

3. Derivation of Equation

To be more specific, the problem of interest is the saturated (with Nitrogen N_2) tissue serving as a source of gas causing the gas concentration to decreases as it gets closer to the gas-tissue interface. Eqn (12) gives the rate of the number of moles of N_2 crossed gas-tissue interface

$$(13) \quad \frac{dn}{dt} = \frac{1}{RT} \left(P_b \frac{dV_b}{dt} + V_b \frac{dP_b}{dt} \right)$$

where

P_b = partial pressure of N_2 in the bubble
 V_b = volume of the bubble.

In a steady state in which partial pressure in the bubble does not change, (13) becomes

$$(14) \quad \frac{dn}{dt} = \frac{1}{RT} P_b \frac{dV_b}{dt}.$$

The partial pressure of N_2 in the bubble P_b can also be expressed through the pressure balance on the bubble:

$$(15) \quad P_b + P_{mg} = P_h + \frac{2\delta}{r} + \frac{4}{3}\pi r^3 H$$

where

P_{mg} = partial pressure of $O_2 + H_2O + CO_2$ in the bubble
 P_h = hydrostatic pressure
 δ = surface tension
 H = bulk modulus for the tissue.

Eqn (15) says that the total pressure $P_b + P_{mg}$ inside a bubble is balanced by the sum of hydrostatic pressure P_h , pressure due to surface tension $2\delta/r$ and pressure as a result of tissue elasticity $(4/3)\pi r^3 H$. Assuming that the interface of a bubble and the tissue has the shape of sphere, volume and area of the bubble are $V_b = (4/3)\pi r^3$ and $4\pi r^2$. Replacing dP_b/dt , dV_b/dt and V_b in Eqn (13) by:

$$\begin{aligned}\frac{dP_b}{dt} &= \left(-\frac{2\delta}{r^2} + 4\pi r^2 H \right) \frac{dr}{dt}, \\ \frac{dV_b}{dt} &= \frac{d}{dt} \left(\frac{4}{3}\pi r^3 \right) = 4\pi r^2 \frac{dr}{dt} = A \frac{dr}{dt}, \\ V_b &= \frac{4}{3}\pi r^3 = \frac{r}{3} A,\end{aligned}$$

Eqn (13) and (14) can be rewritten respectively as

$$(16) \quad \frac{dn}{dt} = \frac{1}{RT} A \left(P_b - \frac{2\delta}{3r} + \frac{4}{3}\pi r^3 H \right) \frac{dr}{dt},$$

and

$$(17) \quad \frac{dn}{dt} = \frac{1}{RT} A P_b \frac{dr}{dt}.$$

Combining Eqn (11) and Eqn (16), one gets the relationship between the gradient of concentration and the bubble growth rate dr/dt :

$$(18) \quad \frac{1}{RT} \left(P_b - \frac{2\delta}{3r} + \frac{4}{3}\pi r^3 H \right) \frac{dr}{dt} = -D \frac{\partial C}{\partial r}.$$

The above expression is the basic equation which will be used over and over again in developing bubble growth equations.

To develop the bubble growth equation, steady-state, i.e., $\partial C/\partial t = 0$ will be studied at first. A general solution to Fick's law expression (6) is (Crank, 1975)

$$\begin{aligned}\frac{\partial C}{\partial t} &= \frac{\partial}{\partial r} \left(r^2 \frac{\partial C}{\partial r} \right) = 0 \\ (19) \quad C &= G_2 + \frac{G_1}{r}\end{aligned}$$

where G_1 and G_2 are constants to be determined from a set of boundary conditions.

Case I

Assume that a bubble is spherical and surrounded by a shell with the thickness h , i.e. a bubble with the shell is like a hollow sphere shown in Fig 1.

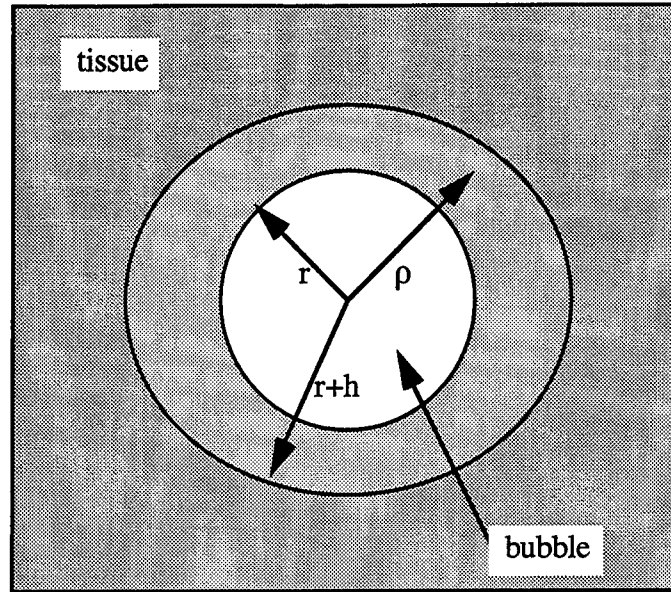


Figure 1. A bubble with a gradient shell.

If inside the bubble, $\rho \leq r$, the concentration of N_2 is C_b and $\rho \geq r+h$, C_t (equals to the concentration of N_2 in the incoming arterial blood C_a), then the concentration of N_2 in the shell is the solution Eqn (19) with the boundary conditions $C(r=r) = C_b$, $C(r=r+h) = C_t$:

$$(20) \quad C(\rho) = \frac{r C_b (r+h-\rho) + (r+h) C_t (\rho-r)}{\rho h}$$

and its derivative is

$$(21) \quad \frac{\partial C}{\partial \rho} = -\frac{(r+h)r}{h} (C_b - C_t) \frac{1}{\rho^2}.$$

From Eqn (10)

$$(22) \quad C_t = \alpha_t P_t \frac{P_s}{RT}$$

$$(23) \quad C_b = \alpha_t P_b \frac{P_s}{RT},$$

Eqn (21) for $r=r$ can be expressed by

$$(24) \quad \left. \frac{\partial C}{\partial \rho} \right|_{\rho=r} = -\frac{r+h}{rh} \frac{P_s}{RT} \alpha_t (P_b - P_t).$$

Replace $\partial C / \partial r$ in (18) by (24), then

$$(25) \quad \frac{dr}{dt} = \frac{\alpha_t D (P_b - P_t) P_s}{h (P_b - \frac{2\delta}{3r} + \frac{4}{3}\pi r^3 H)} \frac{r+h}{r}.$$

When r is large, the term $(r+h)/r$ is reduced to 1 approximately and (25) becomes:

$$(26) \quad \frac{dr}{dt} = \frac{\alpha_t D (P_b - P_t) P_s}{h (P_b - \frac{2\delta}{3r} + \frac{4}{3}\pi r^3 H)}.$$

When the radius gets larger, the curvature of the surface of the bubble gets smaller, hence it can be treated as a plane. Eqn (26) is the same as one given by Gernhardt in 1985 in which he assumed that the diffusing is planar. Furthermore, if one assumes that the pressure in a bubble does not change, Eqn(26) reduces down to Van Liew's equation in Van Liew (1967):

$$(27) \quad \frac{dr}{dt} = \frac{\alpha_t D (P_b - P_t) P_s}{h P_b},$$

(in Van Liew (1967), the shell thickness is L instead of h).

Case II

Consider a spherical bubble surrounded by tissue. The concentration of N_2 inside the bubble is constant C_b . Outside the bubble, in the tissue, the concentration of N_2 changes from C_b at the interface to the concentration of N_2 in the incoming arterial blood C_a (see Fig. 2).

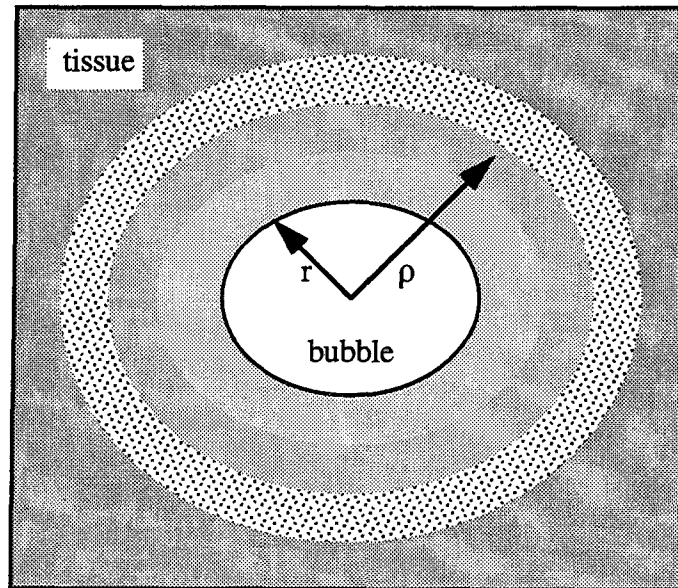


Figure 2. A bubble with an infinite gradient shell.

Here, the shell thickness is considered as infinity. With the given boundary condition

$$(28) \quad C(\rho=r) = C_b,$$

$$(29) \quad C(\rho=\infty) = C_a$$

and the assumption of no perfusion, the solution (19) can be written explicitly

$$(30) \quad C = C_a + (C_b - C_a) \frac{r}{\rho}, \quad \text{for } \rho \geq r,$$

and

$$(31) \quad \left. \frac{\partial C}{\partial \rho} \right|_{\rho=r} = - (C_b - C_a) \frac{1}{r} = \frac{1}{RT} \alpha_t (P_b - P_a) P_s \frac{1}{r}.$$

Replacing $\partial C / \partial r$ in Eqn (18) by (31) gives

$$(32) \quad \frac{dr}{dt} = \frac{\alpha_t D (P_b - P_a) P_s \frac{1}{r}}{P_b - \frac{2\delta}{3r} + \frac{4}{3}\pi r^3 H}.$$

Again Eqn (32) can be reduced to the equation in Van Liew and Hlastala (1969) with the assumption of no perfusion and $dP_b/dt=0$:

$$(33) \quad \frac{dr}{dt} = \alpha_t D \left(1 - \frac{P_a}{P_b}\right) P_s \frac{1}{r}.$$

If perfusion exists, the amount of gas absorbed by blood in the shell is (Van Liew and Hlastala (1969))

$$(C - C_a) k \dot{Q}$$

where $k\dot{Q}$ is the effective blood perfusion. With perfusion, Eqn (6) becomes (in steady-state)

$$(34) \quad D \nabla^2 C = (C - C_a) k \dot{Q}$$

or

$$(35) \quad D \nabla^2 \tilde{P} = \lambda^2 \tilde{P}$$

where $\tilde{P} = P - P_a$ and $\lambda^2 = \frac{\alpha_b k \dot{Q}}{\alpha_t D}$. The solution to (35) with the boundary conditions for Case II and the assumption $dP_b/dt=0$ is given by (Van Liew and Hlastala (1969)):

$$(36) \quad \frac{dr}{dt} = \alpha_t D P_s \left(1 - \frac{P_a}{P_b}\right) \left(\frac{1}{r} + \lambda\right).$$

If dP_b/dt is not zero, the growth equation becomes:

$$(37) \quad \frac{dr}{dt} = \frac{\alpha_t D (P_b - P_a) P_s}{P_b - \frac{2\delta}{3r} + \frac{4}{3}\pi r^3 H} \left(\frac{1}{r} + \lambda \right).$$

To extend the theory to transient-state, the following partial differential equation is considered

$$(38) \quad D \nabla^2 C = k \dot{Q} (C - C_a) + \frac{\partial C}{\partial t}$$

i.e., the perfusion term is added to Fick's law expression (6). Replace C in Eqn(38) by Eqn (10), one obtains

$$D \alpha_t P_s \frac{1}{RT} \nabla^2 P = \alpha_b k \dot{Q} (P - P_a) P_s \frac{1}{RT} + \alpha_t P_s \frac{1}{RT} \frac{\partial P}{\partial t}$$

$$\nabla^2 P = \frac{\alpha_b k \dot{Q}}{\alpha_t D} (P - P_a) + \frac{1}{D} \frac{\partial P}{\partial t}$$

or

or

$$(39) \quad \nabla^2 \tilde{P} = \lambda \tilde{P} + \frac{1}{D} \frac{\partial \tilde{P}}{\partial t}.$$

With boundary conditions for Case II, the solution to (39) is (Hlastala and Van Liew 1975).

$$(40) \quad \frac{P - P_a}{P_b - P_a} = \frac{r}{\rho} \left[\frac{1}{2} e^{-\lambda(\rho-r)} \operatorname{erfc} \left\{ \frac{\rho-r}{2\sqrt{Dt}} - \lambda\sqrt{Dt} \right\} + \frac{1}{2} e^{\lambda(\rho-r)} \operatorname{erfc} \left\{ \frac{\rho-r}{2\sqrt{Dt}} + \lambda\sqrt{Dt} \right\} \right]$$

where

$$(41) \quad \operatorname{erfc}(y) = 1 - \operatorname{erf}(y) = 1 - \frac{2}{\sqrt{\pi}} \int_0^y e^{-s^2} ds.$$

From (18),

$$(42) \quad \frac{1}{RT} \left(P_b - \frac{2\delta}{3r} + \frac{4}{3}\pi r^3 H \right) \frac{dr}{dt} = -D \frac{\partial C}{\partial r} = -D \alpha_t \frac{P_s}{RT} \frac{\partial P}{\partial t}$$

together with (40), then

$$(43) \quad \frac{dr}{dt} = \frac{\alpha_t D (P_b - P_a) P_s}{P_b - \frac{2\delta}{3r} + \frac{4}{3}\pi r^3 H} \left(\frac{1}{r} + \lambda \operatorname{erf}(\lambda\sqrt{Dt}) + \frac{1}{\sqrt{\pi Dt}} e^{-\lambda^2 Dt} \right).$$

If assuming $dP_b/dt = 0$, (43) becomes

$$(44) \quad \frac{dr}{dt} = \alpha_t D P_s \left(1 - \frac{P_a}{P_b}\right) \left(\frac{1}{r} + \lambda \operatorname{erf}(\lambda \sqrt{Dt})\right) + \frac{1}{\sqrt{\pi Dt}} e^{-\lambda^2 Dt}.$$

which is the same as the one in Hlastala and Van Liew (1975).

In applications, P_a is replaced by P_t , i.e. in tissue far away from the bubble, the partial pressure of N_2 is the same as the partial pressure of N_2 in the incoming arterial blood.

4. Summary

In summary, the equations which include reasonable assumptions will be considered in the altitude DCS prediction model and those are:

$$(25) \quad \frac{dr}{dt} = \frac{\alpha_t D (P_b - P_b) P_s}{h (P_b - \frac{2\delta}{3r} + \frac{4}{3}\pi r^3 H)} \frac{r+h}{r}.$$

$$(37) \quad \frac{dr}{dt} = \frac{\alpha_t D (P_b - P_a) P_s}{P_b - \frac{2\delta}{3r} + \frac{4}{3}\pi r^3 H} \left(\frac{1}{r} + \lambda\right).$$

and

$$(43) \quad \frac{dr}{dt} = \frac{\alpha_t D (P_b - P_a) P_s}{P_b - \frac{2\delta}{3r} + \frac{4}{3}\pi r^3 H} \left(\frac{1}{r} + \lambda \operatorname{erf}(\lambda \sqrt{Dt}) + \frac{1}{\sqrt{\pi Dt}} e^{-\lambda^2 Dt}\right).$$

The rest of the bubble growth equations won't be used since they did not include perfusion or surface tension or tissue elasticity. Studies need to be done to decide which of the equations, (25) or (37) should be used. If the infinite gradient shell is used, the bubble growth equation (43) is the one with the most reasonable assumptions and should be used in the altitude DCS prediction model. Meanwhile, a study should be conducted at various stages to determine if a simpler equation, Eqn (37), can be used to reduce computation time. The criterion is that if the initial transient state has little effect on the bubble growth time, Eqn (37) should be used.

Recently, in an *in vivo* study done by Dr. Olson, the finite gradient shell assumption seems to better describe the experimental data (bubble growth in water or water/acetone). If this is the case, Eqn (25) needs to be modified to include perfusion and transient state.